

REVISED STATIC MODELS OF THE THERMOSPHERE AND EXOSPHERE WITH EMPIRICAL TEMPERATURE PROFILES

L. G. Jacchia

1. INTRODUCTION

Only last year we published a set of static diffusion models with constant boundary conditions at 90 km and analytically defined temperature profiles (Jacchia, 1970a; hereafter referred to as J70). An effort had been made to increase the ratio $n(O)/n(O_2)$ above the value of 1.0 at 120 km adopted in previous models [Nicolet, 1961, 1963; CIRA, 1965; Jacchia, 1965a (hereafter referred to as J65)] to bring it in the direction indicated by mass-spectrometer (von Zahn, 1967) and EUV-absorption data (Hall, Chagnon, and Hinteregger, 1967). As soon as the new models appeared, in May 1970, new observational evidence was presented to the effect that the step toward a larger $n(O)/n(O_2)$ ratio had not been large enough. In a critical survey of all available density and composition data, von Zahn (1970) found that at 150 km the best value of $n(O_2)$ was only 0.64 that in J70, while $n(O)$ was larger by a factor 1.37; his proposed total density at 150 km was smaller by 7%. Von Zahn's proposed number densities, total densities, and mean molecular mass are compared below with the CIRA 1965 models, the J70 models, and the present models, in which we have striven, with considerable success, to approach von Zahn's parameters. We have not included a comparison with our J65 models, because their boundary conditions at 120 km were identical with those of CIRA 1965, so that the difference in composition between these two sets of models is minimal at 150 km. In the following, the average number densities are measured in cm^{-3} , the total mass density in g cm^{-3} , and the mean molecular mass \bar{M} in g mole^{-1} at 150 km:

This work was supported in part by grant NGR 09-015-002 from the National Aeronautics and Space Administration.

Parameter	von Zahn (1970)	CIRA 1965 (average)	J70 ($T_{\infty} = 950^{\circ}$) [*]	This paper ($T_{\infty} = 900^{\circ}$) [*]
$n(N_2)$	26×10^9	33.4×10^9	31.0×10^9	25.4×10^9
$n(O)$	23×10^9	14.2×10^9	16.8×10^9	23.6×10^9
$n(O_2)$	2.5×10^9	4.78×10^9	3.90×10^9	2.68×10^9
$n(Ar)$	0.05×10^9	0.18×10^9	0.08×10^9	0.04×10^9
ρ	1.96×10^{-12}	2.18×10^{-12}	2.10×10^{-12}	1.95×10^{-12}
\overline{M}	22.85	25.17	24.44	22.73

* Approximate average temperature for the interval 1961 to 1969 in the system of the models.

In Table 4 of his 1970 paper, von Zahn listed the number densities of N_2 , O_2 , and O, reduced to a height of 150 km, that were obtained in 44 experiments, both mass-spectrometric and EUV-absorption, from 1961 to 1969. While there is a large discrepancy among the mass-spectrometer data on $n(O)$, the same type of measurements show rather consistent values of $n(O_2)$ — all of them except one smaller than the corresponding value in J70; a similar result was obtained more recently by Reid and Withbroe (1970) from the absorption of $\lambda 1032$ (O VI), which requires an O_2 concentration at 120 km only two-thirds as large as that in J70. According to von Zahn, $n(N_2)$ at 150 km is also lower, by 16%, with respect to J70, while the total density is lower by only 7%. Clearly, if we have to decrease $n(N_2)$ and $n(O_2)$ by substantial amounts while leaving the total density almost unchanged, we have to increase $n(O)$. While mass-spectrometer measurements of $n(O)$ are too unreliable (Schaefer, 1966; von Zahn, 1967), it is significant that EUV-absorption measurements (Hall, Schweizer, and Hinteregger, 1965; Hall *et al.*, 1967) give, when reduced to a height of 150 km, values of $n(O)$ consistently about 25% higher than in J65. This value is not too different from the atomic-oxygen concentration that von Zahn derives by subtracting the density sum of all other constituents from the total density and assumes to be the best value under the circumstances.

We found that satisfactory models that would match von Zahn's parameters at 150 km and the observed densities from satellite drag at greater

heights could be obtained by maintaining intact the analytical structure of the J70 models and changing only the numerical parameters. The resulting models are given in detail in Table 6 and summarized in Table 7, at the end of this paper. Owing to the increased concentrations of atomic oxygen, the temperatures necessary to yield given densities at given heights in the satellite region are somewhat lower than in J70 — closer, therefore, to the temperatures obtained by the incoherent-scatter method (Carru and Waldteufel, 1969; McClure, 1969). Lower temperatures are also suggested by the absorption of the λ 304 (He II) line as measured by B. E. Woodgate (private communication, 1970).

Since the analytical structure of the basic models is, as we said, identical with that of the J70 models, many of the following descriptive pages will be almost a verbatim repetition of the corresponding pages of SAO Special Report No. 313, except for the numerical values reported in the text and for the correction of a few oversights. There are, however, substantial changes in the description of the individual types of atmospheric variations. While overhauling the basic models, we have also tried to reanalyze these variations. In so doing, we have found that for some of them — the geomagnetic effect, the semiannual variation, and the helium variation — the analytical formulation we had used was inadequate and had to be altered, or even drastically changed. In particular, the dissociation of the semiannual variation from temperature variations has cleared up many puzzling results in the helium-hydrogen region and eliminated the necessity of introducing ad hoc variations for these constituents.

2. COMPOSITION

We have assumed that the atmosphere is composed only of nitrogen, oxygen, argon, helium, and hydrogen, in a condition of mixing up to 100 km and in diffusion above this height. We have adopted the sea-level composition of the U. S. Standard Atmosphere 1962 (COESA, 1962) such as would obtain after elimination of the minor constituents and of hydrogen (which is introduced in our models at a height of 500 km). There is some evidence that for helium, gravitational separation starts at a lower height than for the other constituents. To eliminate the inconvenience of a separate homopause for helium, we have had recourse to the artifice of increasing the sea-level concentration of helium by an amount such that the atmospheric densities at heights where helium appears as a major constituent are in agreement with the observed densities. This results in an erroneous helium density below 100 km — a situation we are willing to tolerate in view of the entirely negligible contribution of helium to the total density at those heights. Thus, the assumed sea-level composition is as follows:

	Fraction by volume $q_0^{(i)}$	Molecular weight M_i
Nitrogen (N_2)	0. 78110	28. 0134
Oxygen (O_2)	0. 20955	31. 9988
Argon (Ar)	0. 0093432	39. 948
Helium (He)	<u>0. 0000061471</u>	4. 0026
Sum	1. 00000	

The resulting sea-level mean molecular mass is $\overline{M}_0 = 28.960$.

We have assumed that any change in the mean molecular mass \overline{M} in the mixing region below 100 km is caused only by oxygen dissociation. Therefore, the amount of atomic oxygen present in the atmosphere is uniquely determined by \overline{M} . From 90 to 100 km we have used an empirical \overline{M} profile that had to satisfy certain conditions. Starting from a value not too different from \overline{M}_0 at 90 km, we end at 100 km with a value that in diffusion must yield at 150 km the ratio $n(O)/n(O_2)$ of about 9.2 obtained by von Zahn for an exospheric temperature of 900° to 1000°K; the temperature profile from 90 to 150 km is adjusted to give the required total density at 150 km. The \overline{M} profile must end at the homopause with a gradient roughly equal to that given by diffusion conditions immediately above, so that there will be no sharp discontinuity in the \overline{M} profile across the homopause (in the belief that "natura non facit saltus").

The adopted \overline{M} profile can be found in the tables. For computer purposes, we have used a sixth-degree polynomial of the form

$$\overline{M}(z) = \sum_{n=0}^6 c_n (z - 90)^n \quad (90 < z < 100; z \text{ in km}) \quad (1)$$

to represent it. The coefficients c_n are given below:

$$\begin{aligned} c_0 &= 28.82678 \\ c_1 &= -7.40066 \times 10^{-2} \\ c_2 &= -1.19407 \times 10^{-2} \\ c_3 &= +4.51103 \times 10^{-4} \\ c_4 &= -8.21895 \times 10^{-6} \\ c_5 &= +1.07561 \times 10^{-5} \\ c_6 &= -6.97444 \times 10^{-7} . \end{aligned}$$

The number densities of the individual species i in the region from 90 to 100 km are obtained as follows. From the density ρ , the total number of particles N per unit volume is computed by

$$N = A \rho / \bar{M} , \quad (2)$$

where A is Avogadro's number.

For N_2 , Ar, and He, we have

$$n(i) = q_0(i) \frac{\bar{M}}{\bar{M}_0} N , \quad (3)$$

and for O and O_2 , respectively,

$$\begin{aligned} n(O) &= 2N \left(1 - \frac{\bar{M}}{\bar{M}_0} \right) \\ n(O_2) &= N \left\{ \frac{\bar{M}}{\bar{M}_0} \left[1 + q_0(O_2) \right] - 1 \right\} . \end{aligned} \quad (4)$$

For ρ in $g \text{ cm}^{-3}$, we have used $A = 6.02257 \times 10^{23}$.

3. COMPUTATION OF DENSITIES AND BOUNDARY CONDITIONS

From 90 to 100 km, for a given temperature profile $T(z)$, the density ρ was computed by integrating the barometric equation

$$d\ln\rho = d\ln\left(\frac{\bar{M}}{T}\right) - \frac{\bar{M}g^*}{RT} dz , \quad (5)$$

where g is the acceleration due to gravity, and $R^* = 8.31432$ joules $(^{\circ}\text{K})^{-1}$ mole $^{-1}$, the universal gas constant.

At the height $z = 90$ km, we have assumed the following boundary conditions:

$$\rho_0 = 3.46 \times 10^{-9} \text{ g cm}^{-3} ,$$

$$T_0 = 183^{\circ}\text{K} .$$

Above 100 km, the number density of each individual species $n(i)$ was computed by integrating the diffusion equation

$$\frac{dn(i)}{n(i)} = - \frac{M_i g^*}{RT} dz - \frac{dT}{T} (1 + \alpha_i) , \quad (6)$$

where α_i is the thermal diffusion coefficient. Following Nicolet (1961), we have used $\alpha = -0.38$ for helium, and $\alpha = 0$ for the other constituents.

For hydrogen, we have followed Kockarts and Nicolet (1962, 1963) and fitted the equation

$$\log_{10} n(H)_{500} = 73.13 - 39.40 \log_{10} T_{500} + 5.5 (\log_{10} T_{500})^2 \quad (7)$$

to their concentrations at 500 km. We have assumed hydrogen to be in diffusion equilibrium above 500 km; no hydrogen densities are given in the tables below this height.

The acceleration due to gravity was computed from the formula

$$g = 980.665 (1 + z/R_e)^{-2} \text{ cm sec}^{-2}, \quad (8)$$

with $R_e = 6.356766 \times 10^8$ cm. This equation (Harrison, 1951; Minzner and Ripley, 1956) is an excellent approximation to the actual value of g (centrifugal force included) for the latitude of $45^\circ 32' 40''$.

4. TEMPERATURE PROFILES

All temperature profiles start from a constant value $T_0 = 183^\circ\text{K}$ at the height $z_0 = 90 \text{ km}$, with a gradient $G_0 = (dT/dz)_{z=z_0} = 0$, rise to an inflection point at a fixed height $z_x = 125 \text{ km}$, and become asymptotic to a temperature T_∞ (often referred to as the "exospheric" temperature). Both the temperature T_x and the temperature gradient $G_x = (dT/dz)_{z=z_x}$ at the inflection point are functions of T_∞ ; for simplicity, we have made G_x a function of T_x .

The quantity T_x is defined by the equation

$$T_x = a + bT_\infty + c \exp(\bar{k} T_\infty) , \quad (z_x = 125 \text{ km}) , \quad (9)$$

with the constraint that $T_x = T_0$ when $T_\infty = T_0$ (i. e., for the hypothetical case in which the exospheric temperature is the same as the temperature at 90 km, namely 183° , there is no variation of temperature with height). The numerical values of the coefficients are as follows:

$$\begin{aligned} a &= 371.6678 , \\ b &= +0.0518806 , \\ c &= -294.3505 , \\ \bar{k} &= -0.00216222 . \end{aligned}$$

For $z_0 < z < z_x$ the temperature profiles are defined by a fourth-degree polynomial:

$$T = T_x + \sum_{n=1}^4 c_n (z - z_x)^n . \quad (10)$$

The coefficients c_1 , c_2 , c_3 , and c_4 are determined by the following conditions:

$$\text{when } z = z_0 \left\{ \begin{array}{l} T = T_0 \\ G_0 = \left(\frac{dT}{dz} \right)_{z=z_0} = 0 \end{array} ; \right.$$

$$\text{when } z = z_x \left\{ \begin{array}{l} G_x = \left(\frac{dT}{dz} \right)_{z=z_x} = 1.90 \frac{T_x - T_0}{z_x - z_0} \\ \left(\frac{d^2T}{dz^2} \right)_{z=z_x} = 0 \end{array} . \right. \quad (11)$$

These coefficients must be computed separately for every temperature profile, so their tabulation would be wasteful. The equation for G_x is justified in the following manner. The condition for having no inflections in the temperature profile in the interval $z_0 < z < z_x$ is given by

$$\frac{4}{3} < \frac{z_x - z_0}{T_x - T_0} G_x < 2 . \quad (12)$$

Experiments with gradients within this range have shown that it is quite feasible to keep the quantity $(z_x - z_0) G_x / (T_x - T_0)$ constant for all temperature profiles; the best value was found to be 1.90.

For $z > z_x$, the temperature profiles are determined by equations of the type

$$T = T_x + A \tan^{-1} \left\{ \frac{G_x}{A} (z - z_x) [1 + B(z - z_x)^\beta] \right\} , \quad (13)$$

where

$$A = \frac{2}{\pi} (T_\infty - T_x) ; \quad B = 4.5 \times 10^{-6} \quad (z \text{ in km}) ; \quad \beta = 2.5 .$$

As can be seen, continuity is provided in both dT/dz and d^2T/dz^2 when z crosses z_x . The inverse tangent was selected among several suitable asymptotic functions because of its ready availability in tabulated form and in computer libraries. The presence of the corrective term $[1 + B(z - z_x)^\beta]$ frees the temperature profiles from strict dependence on the selected type of asymptotic function.

The following shows the dependence of the maximum temperature gradient G_x on the exospheric temperature T_∞ :

T_∞ (°K)	G_x (deg km ⁻¹)	T_∞ (°K)	G_x (deg km ⁻¹)
500	6.23	1400	13.41
600	7.57	1600	14.24
800	9.66	1800	14.98
1000	11.22	2000	15.66
1200	12.43		

The family of temperature profiles originated by equations (9) to (14) is graphically illustrated in Figure 1. Figure 2 shows the composition of the atmosphere above 200 km for three representative exospheric temperatures — 600°, 1000°, and 1800°K. Figure 3 shows seven density profiles from 110 to 2000 km for various exospheric temperatures ranging from 500° to 1900°K, and Figure 4 shows how the density ρ varies with the exospheric temperature T_∞ at different height levels. Figure 4 is particularly instructive because it shows at a glance how, for heights below 500 km, $d\rho/dT_\infty$ generally increases with height but decreases with T_∞ . Above 500 km, hydrogen makes its appearance, causing the curves to have a dip at low temperatures; we thus have a situation in which at a given height a single density value corresponds to two distinct values of T_∞ .

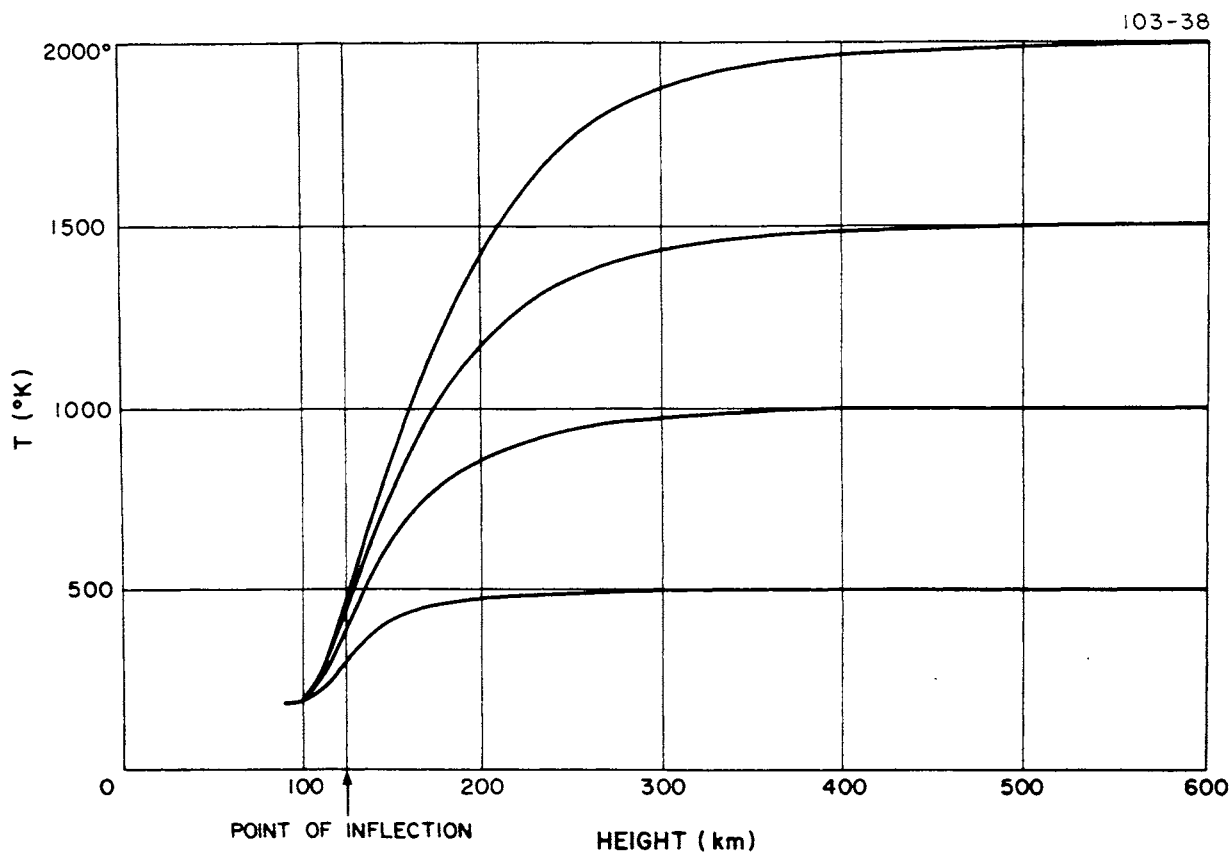


Figure 1. Four temperature profiles from the present models.

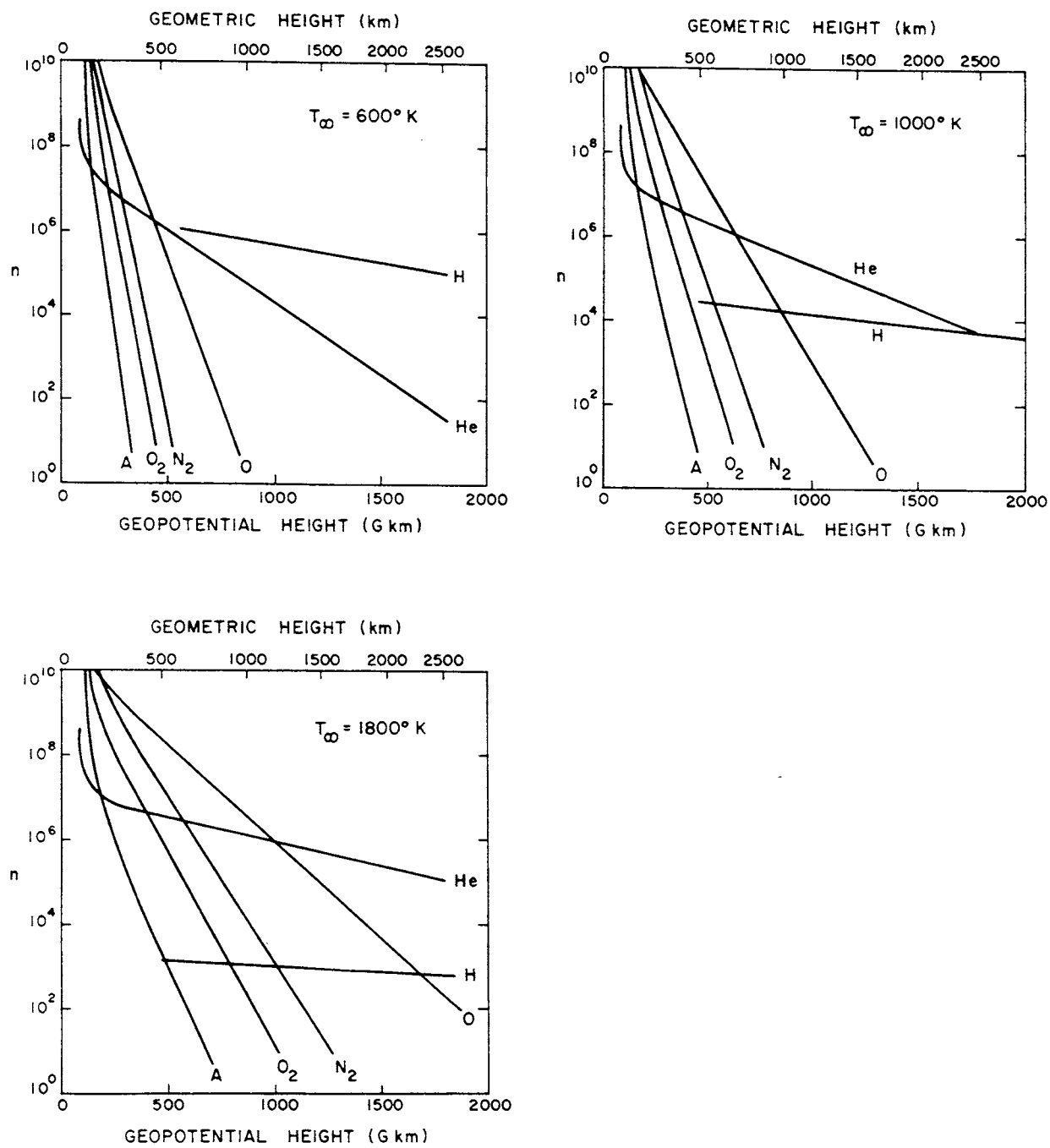


Figure 2. Atmospheric composition for three values of the exospheric temperature. Number densities (n) are plotted against geopotential height. The corresponding geometric heights are marked at the top of the diagrams.

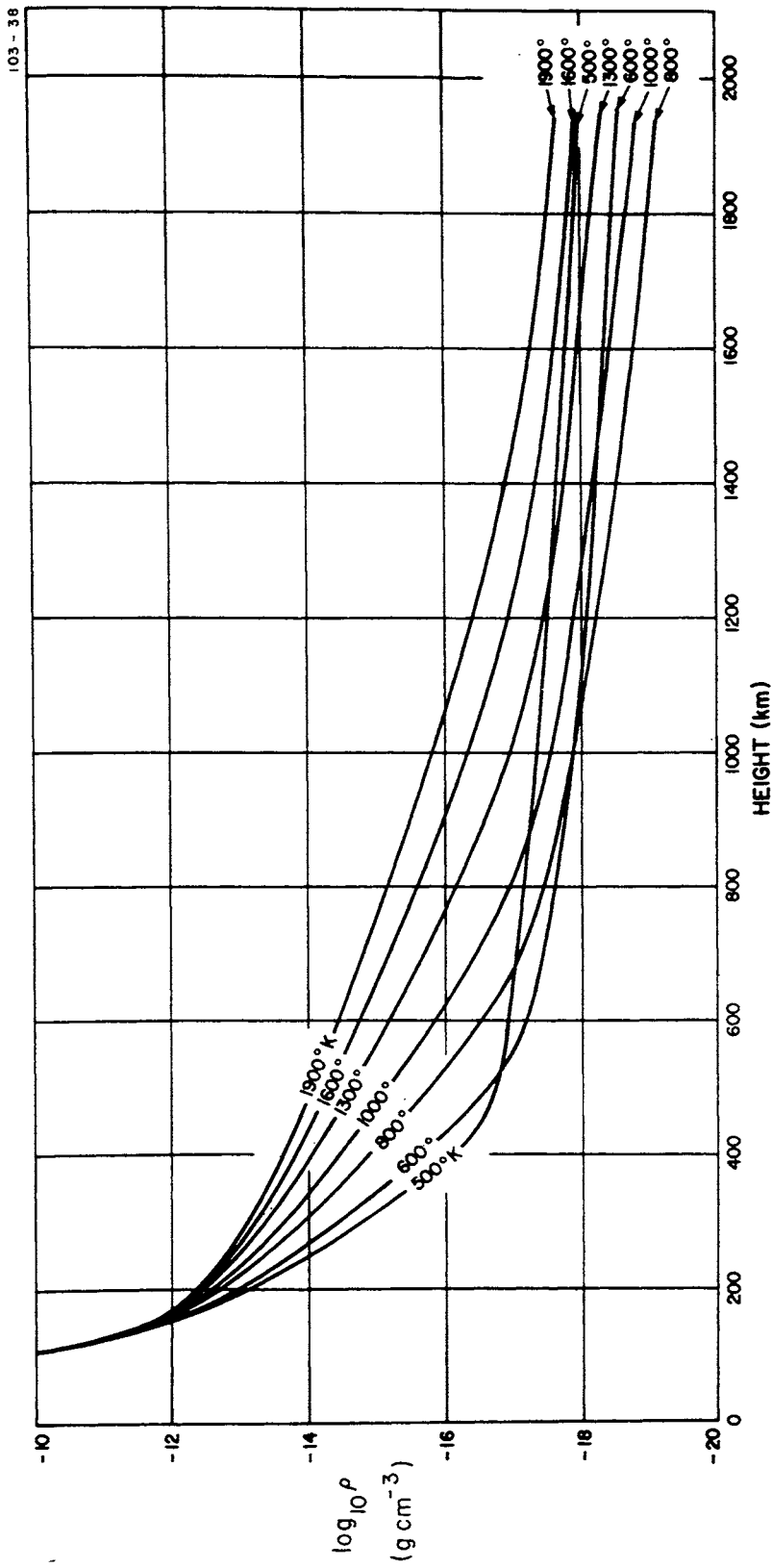


Figure 3. Density profiles for seven values of the exospheric temperature.

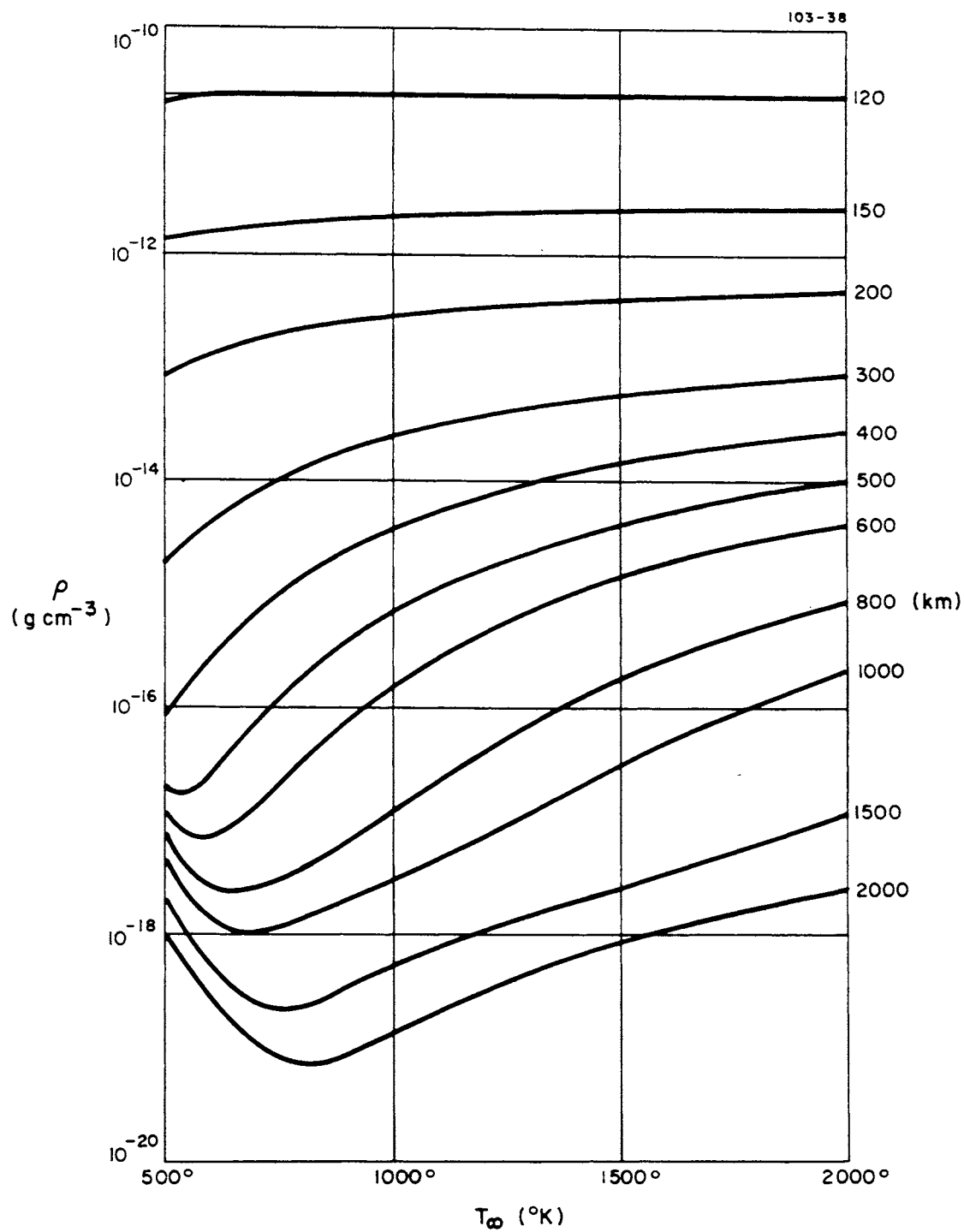


Figure 4. Dependence of atmospheric density on exospheric temperature at different heights.

5. VARIATIONS IN THE THERMOSPHERE AND EXOSPHERE

Several types of variation are recognized in the atmospheric regions covered by the present models. They can be classified as follows:

1. Variations with the solar cycle.
2. Variations with the daily change in activity on the solar disk.
3. The diurnal variation.
4. Variations with geomagnetic activity.
5. The semiannual variation.
6. Seasonal-latitudinal variations of the lower thermosphere.
7. Seasonal-latitudinal variations of helium.
8. Rapid density fluctuations probably connected with gravity waves.

All these variations, with the exception of the last type, are subject to some amount of regularity and can be predicted with varying degrees of accuracy on the basis of ground-based observations. It is obvious that static models cannot represent all the different types of variation equally well. They should be quite adequate when the characteristic time of the variation is much longer than the time involved in the conduction, convection, and diffusion processes; when, on the other hand, it is comparable or shorter — as in the diurnal variation and the geomagnetic effect — we must expect poorer results. By this we mean that if we try to represent the observed density variations, we may have to introduce temperature variations that are not entirely correct, or vice versa. Since, by far, the largest observational material consists of density measurements, it is the density variations that we have tried to keep correct. We have no direct evidence so far that the resulting temperature variations might actually be incorrect, although it would not be surprising if they turned out to be so, to a certain degree. Temperatures derived from nitrogen profiles at various times of the day (Spencer, Taeusch, and Carignan, 1966; Taeusch, Niemann, Carignan, Smith, and Ballance, 1968) actually are in relatively close agreement with the J65 static models.

An effort was made in the CIRA 1965 tables to treat the diurnal variation separately; unfortunately, the inadequacy of present-day theory does not justify the tremendous increase in the size of the tables if one were to cover the diurnal variation over the entire globe, instead of restricting it to one particular latitude as in CIRA 1965.

6. VARIATIONS WITH SOLAR ACTIVITY

The ultraviolet solar radiation that heats the earth's upper atmosphere actually consists of two components, one related to active regions on the solar disk and the other to the disk itself. The active-region component comes from areas of higher temperature and consists mainly of the spectral lines of highly ionized atoms, such as Fe XIV-XVI, Si IX-X, Mg X; the radiation from the clear disk comes from much less ionized atoms, such as He I-II and O IV, and the helium continuum. The active-region component varies rapidly from day to day in correspondence with the appearance and disappearance of active areas caused by the rotation of the sun and by spot formation; the disk component presumably varies more slowly in the course of the 11-year solar cycle. Since the radiation in the two components is different, we must expect the atmosphere to react in a different manner to each of them — and this is actually observed.

The 10.7-cm solar flux ($F_{10.7}$) is generally used as a readily available index of solar EUV radiation. It also consists of a disk component and of an active-area component, which can be separated by statistical methods by relating the observed values of the flux integrated over the whole solar disk to the corresponding sunspot numbers (Hachenberg, 1965) or, better, to sunspot areas. When the 10.7-cm flux increases, there is an increase in the temperature of the thermosphere and exosphere; for a given increase in the disk component, however, the temperature increases four times as much as for the same increase in the active-area component. Separate values of the two components of the solar flux are not readily available; fortunately, we have found (Jacchia and Slowey, unpublished) that the disk component is, for all practical purposes, linearly related to the flux averaged, or smoothed, over approximately three solar rotations ($\bar{F}_{10.7}$). We can, therefore, replace the relation between temperature and disk component with an equivalent relation between temperature and $\bar{F}_{10.7}$.

Since the temperature varies with the hour of the day, with geographic location, and with geomagnetic activity, we must specify the parameters of these variations to which the temperature is to be referred. The temperature T_c in the equation that follows is to be the nighttime minimum of the global exospheric temperature distribution when the planetary geomagnetic index K_p is zero. We find that

$$T_c = 379^\circ + 3.24 \bar{F}_{10.7} + 1.3(F_{10.7} - \bar{F}_{10.7}) \quad (\text{for } K_p = 0) ; \quad (14)$$

$F_{10.7}$ is expressed in units of 10^{-22} watt m^{-2} (cycle/sec) $^{-1}$ bandwidth. In this formula, the last numerical coefficient, 1.3, is considerably smaller than the value 1.8 used in all previous models. The change is the result of a new analysis, covering the years 1967 to 1969, which were characterized by a particularly large amplitude of the "27-day" fluctuations. It appears that in deriving the old coefficient (for the J65 models), we did not take the geomagnetic effect sufficiently into account: Most of the large geomagnetic perturbations occur near the maxima of the 27-day oscillations and contribute to increase the amplitude of the density variations.

According to Roemer (1968), the temperature variations occur with a time lag of 1.0 ± 0.12 days with respect to those of the solar flux.

If we want to compute the average exospheric temperature corresponding to a given phase of the solar cycle, i. e., to a given value of $\bar{F}_{10.7}$, we must drop the last term of equation (14), which corresponds to the day-to-day variations of solar activity, and add half the diurnal temperature range and the difference in temperature between average and quiet geomagnetic conditions.

Minimum nighttime and daytime maximum exospheric temperatures obtained, with the present models, from drag-derived densities for three long-lived satellites are plotted in Figure 5 against $\bar{F}_{10.7}$. To obtain the data points, all variations except the diurnal variation were suppressed. The straight line through the nighttime temperatures is represented by

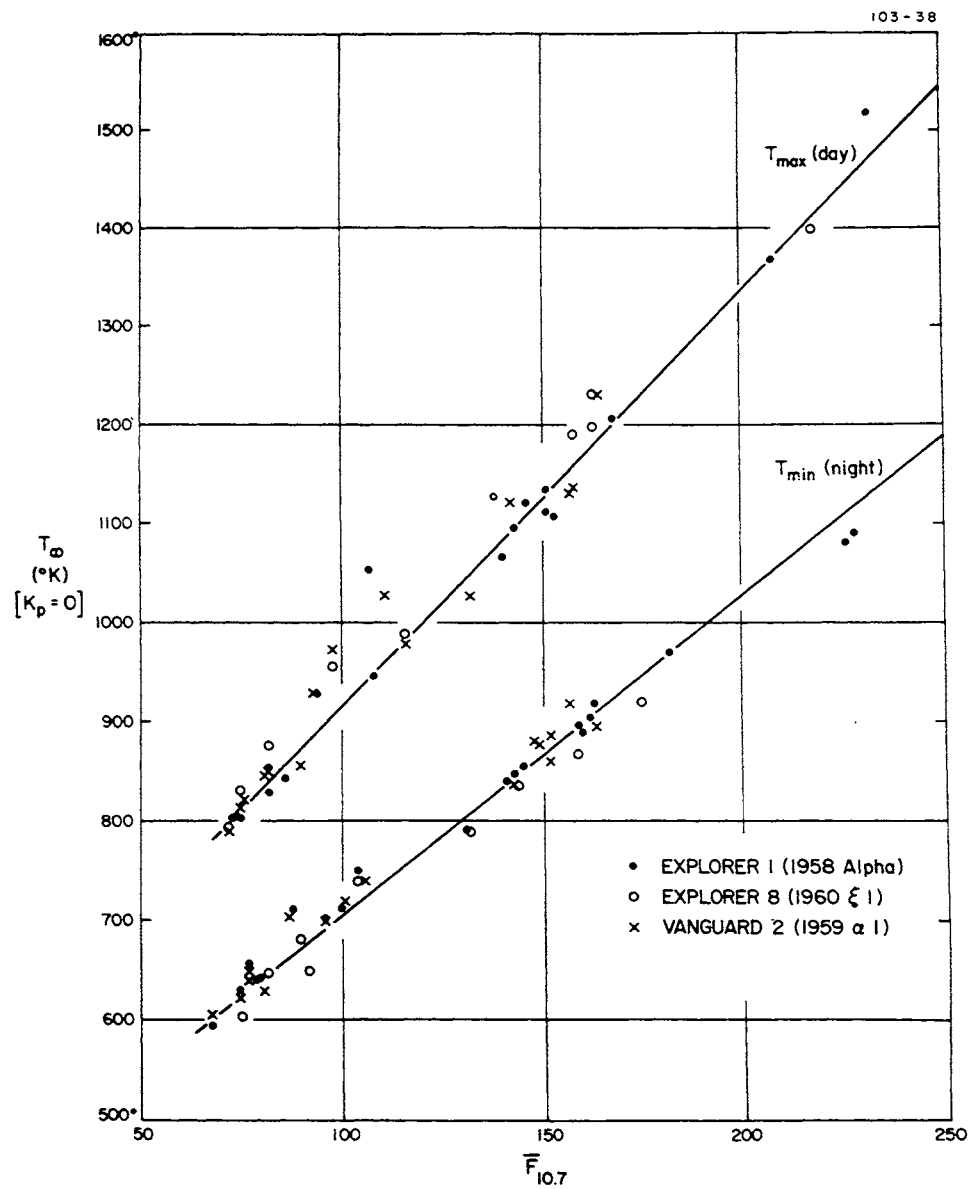


Figure 5. Global nighttime minimum and daytime maximum exospheric temperatures derived, through the use of the present models, from the densities obtained from the drag of three artificial satellites, plotted against the smoothed 10.7-cm solar flux $\bar{F}_{10.7}$. To obtain the data points, all variations except the diurnal variation were suppressed by using the equations associated with the models. The straight line through the minimum temperatures is represented by the equation $T_{\min} = 379 + 3.24 \bar{F}_{10.7}$ [see eq. (14)]; the one through the maxima, by $T_{\max} = 1.30 T_{\min}$.

$T_{\infty} = 379^{\circ} + 3.24 \bar{F}_{10.7}$ [the first part of eq. (14)]; the one through the day-time maxima is represented by $T_M = 1.30 T_{\infty}$.

The effect of solar activity on atmospheric density is illustrated in Figures 6 and 7, which both show results from the drag analysis of the Explorer 1 satellite (1958 Alpha). Ten-day means of the density, and of the temperature derived from it through the use of models, are shown in Figure 6. In this figure, the periodic oscillations, with a period of 300 days at the beginning and 200 days at the end, are caused by the diurnal variation, as the perigee of the satellite slowly moves from night into day and back again into night. When these oscillations are mentally removed, we remain essentially with an 11-year variation that parallels that of the smoothed 10.7-cm solar flux, shown at the bottom of the figure. A comparison of the temperature and density variations at sunspot maximum (1958 to 1959) and sunspot minimum (1963 to 1965) clearly shows the dependence of $d\rho/dT_{\infty}$ on T_{∞} illustrated in Figure 4.

Figure 7 shows an 800-day section of the curves of Figure 6 in greater detail, with individual observations rather than 10-day means. Here the 27-day oscillations caused by the sun's rotation are clearly visible in the density data, and the modulation caused by the semiannual variation can be discerned. The apparent irregularities in the normalized diurnal-variation curve, which was computed from the models, are caused by the rapid motion, back and forth in latitude, of the perigee of the satellite.

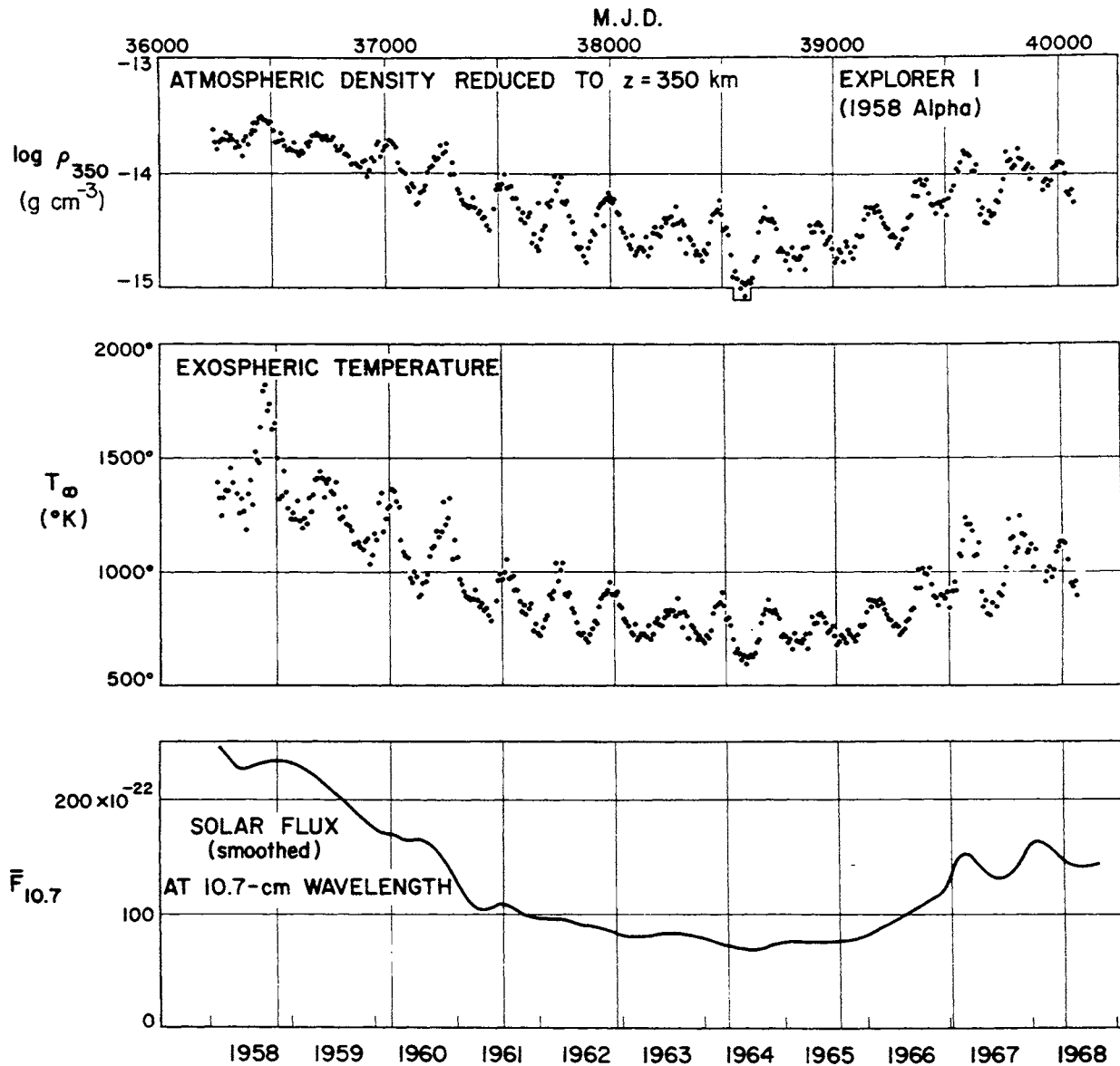


Figure 6. Ten-day means of the densities obtained from the drag of the Explorer I satellite and of the exospheric temperatures derived from them through the use of the J70 models. Since the purpose of this figure is to illustrate the variations of density and temperature with the solar cycle (see bottom curve), it was not deemed necessary to redo the temperature diagram by means of the present models; the difference would be hardly noticeable. M. J. D. is the Modified Julian Day (J. D. minus 2 400 000.5).

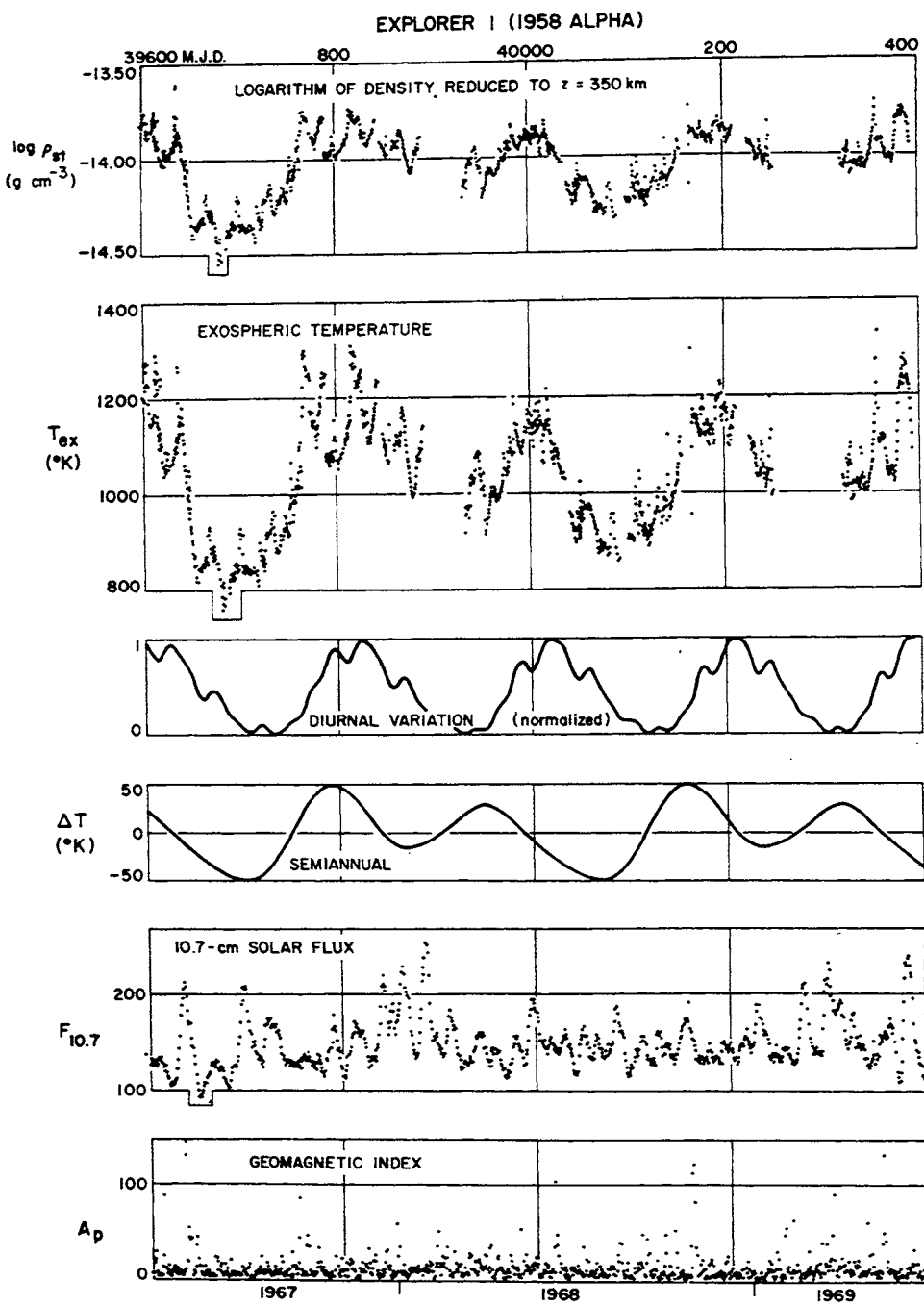


Figure 7. Densities obtained from the drag of the Explorer 1 satellite and exospheric temperatures derived from them by use of the J70 models. Since the purpose of this figure is to illustrate the 27-day oscillations and the geomagnetic effect superimposed on the diurnal variation, it was not deemed necessary to redo the temperature diagram by use of the present models; the difference would be hardly noticeable. The schematic diagrams of the diurnal and semiannual variations are also from J70.

7. THE DIURNAL VARIATION

Densities derived from satellite drag show a maximum around 2 p.m. local solar time (L.S.T.) at a latitude roughly equal to that of the subsolar point; the minimum occurs around 3 a.m. at about the same latitude with opposite sign. Thus, if we consider the atmosphere above a particular locality, the diurnal variation will undergo a seasonal change; this change, however, can be incorporated into a global description of the phenomenon by a set of suitable empirical equations (Jacchia, 1965b). The purpose of these equations is to represent the density variations by use of static atmospheric models. To this effect it appears necessary to use the temperature as an auxiliary parameter, but it must be understood that this "temperature" has no claim to accuracy, since consistency between temperature and density variation cannot be achieved, on a diurnal time scale, through static models.

We shall assume that the maximum daytime exospheric temperature T_M occurs at a latitude ϕ equal to the sun's declination δ_\odot , and the minimum temperature T_c [see eq. (14)] at latitude $-\delta_\odot$. At any other latitude ϕ , the daytime maximum temperature T_D will be smaller than T_M and the nighttime minimum temperature T_N larger than T_c . Figure I shows the relation between the 10.7-cm solar flux on the one hand, and T_c and T_M as determined on the basis of the present models from the drag of three low-inclination satellites over a complete solar cycle.

The maximum and minimum temperatures T_D and T_N can be conveniently represented by the following equations (Jacchia, 1965b):

$$\begin{aligned} T_D &= T_c(1 + R \cos^m \eta) , \\ T_N &= T_c(1 + R \sin^m \theta) , \end{aligned} \quad (15)$$

where

$$\eta = \frac{1}{2} |\phi - \delta_{\odot}| ,$$

$$\theta = \frac{1}{2} |\phi + \delta_{\odot}| .$$

The temperature T_{ℓ} at any given point can be expressed as a function of the hour angle H of the sun (the local solar time, counted from upper culmination). Let us write

$$T_{\ell} = T_N (1 + A \cos^n \frac{\tau}{2}) , \quad (16)$$

with

$$A = \frac{T_D - T_N}{T_N} = R \frac{\cos^m \eta - \sin^m \theta}{1 + R \sin^m \theta}$$

and

$$\tau = H + \beta + p \sin(H + \gamma) , \quad (-\pi < \tau < \pi) ,$$

where β , γ , and p are constants. It should be remembered that T_{ℓ} , which is derived from T_c , is referred to $K_p = 0$.

The constant β determines the lag of the temperature maximum with respect to the sun's culmination, while p introduces in the temperature curve an asymmetry, whose location is determined by γ . Replacing T_D and T_N from equation (15), we can write

$$T_{\ell} = T_c (1 + R \sin^m \theta) \left(1 + R \frac{\cos^m \eta - \sin^m \theta}{1 + R \sin^m \theta} \cos^n \frac{\tau}{2} \right) . \quad (17)$$

Densities derived from satellite drag are best represented by use of the following parameters:

$$\begin{aligned} m &= 2.2 , & \beta &= -37^\circ , \\ n &= 3.0 , & p &= +6^\circ , \\ R &= 0.3 , & \gamma &= +43^\circ . \end{aligned}$$

There is some evidence that the shape of the diurnal density curve changes with height (Jacchia, 1970b) and with solar activity; present data, however, are insufficient to establish the rules of this variation with assurance, and therefore we have assumed that the parameters that fix the shape of the curve are constant.

Concerning the parameter R , which fixes the relative amplitude of the temperature variation, there is no a priori reason why it should be a constant. In a first analysis (Jacchia and Slowey, 1968), it was found that R was somewhat larger in 1959 to 1963 and smaller in 1964 to 1966, without any obvious relation to the solar cycle. Subsequently (Jacchia, 1970c), the suspicion arose that the variation of R followed that of solar activity with a lag of 1 to 2 years, in phase with the yearly means of the geomagnetic index K_p — a rather disturbing finding, since it implied a strong contribution of the solar wind to the heating of the atmosphere. More recent data on R , from the years 1969 and 1970, have failed to confirm this finding, and a new analysis of R using the present atmospheric models as a basis seems to indicate that, if there is a variation of R , it is not related to the solar cycle (see Figure 5). Under these circumstances, it seems best to make R independent of time or solar activity.

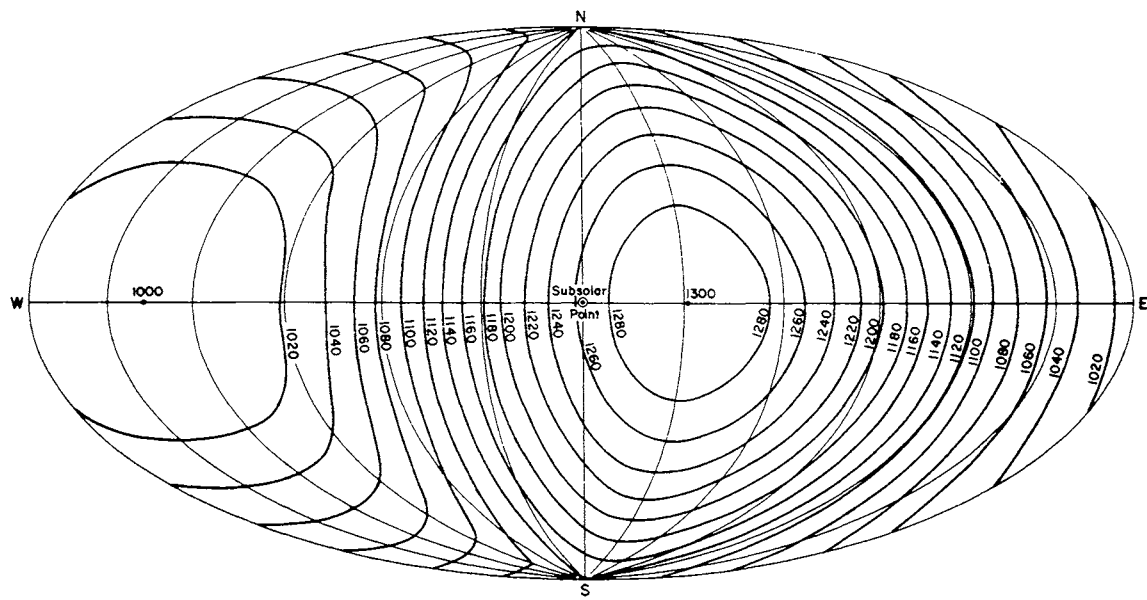
Recently, we found that there is a systematic change of R with height. The value $R = 0.3$ we have given refers to a height of about 400 km. At 600 km, however, we find that if we use this value of R , we are left with systematic density residuals, negative at night and positive in daytime, which can be corrected by using a larger value of R (0.35) and a lower value of T_c , such as to leave the mean daily temperature unchanged. The residuals are even larger at 900 km, always with the same characteristics, and require a value $R = 0.4$ with a correspondingly lower T_c for their correction. At 1100 to 1200 km, however, $R = 0.3$ again gives satisfactory results. We believe that this change of R is not a real variation of T_M/T_c with height but simply reflects the inadequacy of static models to represent the diurnal density variation throughout the whole atmosphere. If we consider the curve that represents the real diurnal temperature variation at a given height above

a given geographic location for a given day and if we select on it two points, one on the ascending branch (morning) and one on the descending branch (evening) such that they have the same ordinate (temperature), we shall find that in a truly dynamical model the two temperature profiles corresponding to the two instants are different, although they cross at our given point. In static models, however, the two profiles are identical. This difference in behavior is bound to result in discrepancies such as the one we have described. It is significant that in the CIRA 1965 models, which were constructed on a dynamical basis, the amplitude of the diurnal density variation increases with height faster than it does in the static models (Jacchia, 1968).

Table 1 gives the ratio T_{ℓ}/T_c , multiplied by the factor 1000, as a function of L.S.T. (counted from midnight) and latitude [computed from eqs. (15) and (16)]. According to this model, the hours of minimum and maximum of the daily density variation are independent of latitude and are 2.87^{h} and 14.08^{h} L.S.T., respectively. A graphical representation of the resulting temperature distribution is shown in Figure 8 for the equinoxes and the northern summer solstice.

A certain degree of smoothing must be expected in the daily density variation as determined from satellite drag. The smoothing occurs not only because the drag is experienced over a considerable arc of the orbit but also because the slow motion of the perigee with respect to the sun prevents the determination of individual diurnal density oscillations. It takes, on the average, 200 to 300 days for the perigee of a satellite orbit to move from night into daylight and into night again, so the diurnal oscillation as seen through satellite drag resembles an oscillatory phenomenon studied by stroboscopic means (Figures 6 and 7). During the average synodic cycle of 200 to 300 days, the perigee of a satellite moves back and forth in latitude (and therefore from summer to winter) several times, and there are all sorts of variations with solar and geomagnetic activity that must be suppressed if we want to have a clean picture of the diurnal variation.

Temperatures derived from nitrogen profiles obtained from six rocket firings from Cape Kennedy on January 24, 1967 (Taeusch et al., 1968),



EXOSPHERIC TEMPERATURE DISTRIBUTION AT NORTHERN SUMMER SOLSTICE

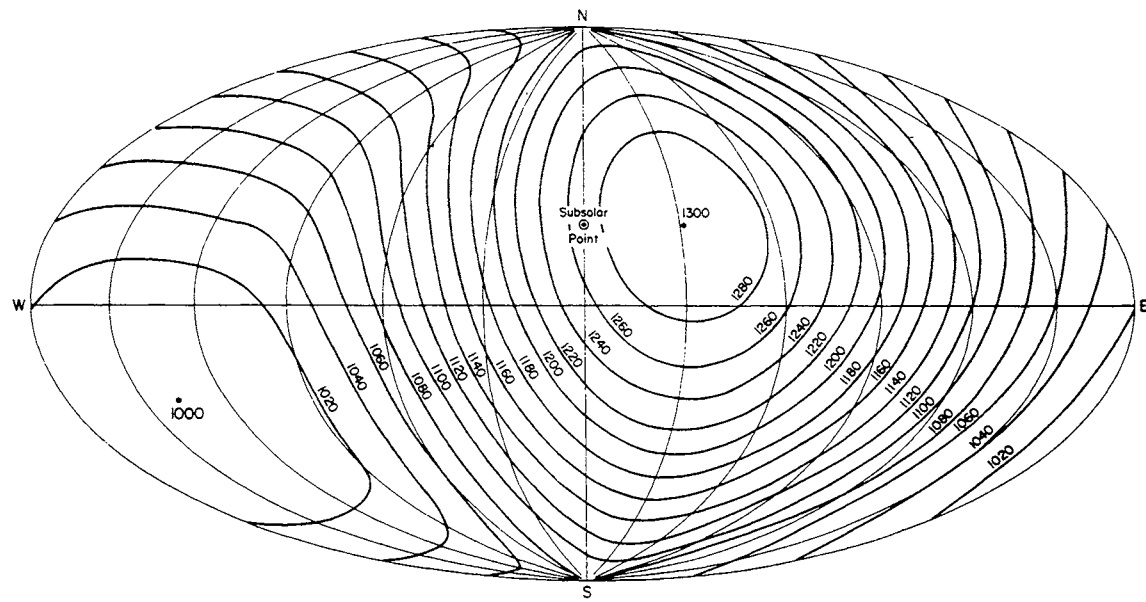


Figure 8. Exospheric isotherms ($^{\circ}\text{K}$) above the globe, computed from equations (15) and (16), for the case when the minimum temperature is 1000°K . Aitoff's equal-area projection; meridians of local solar time and parallels of latitude are drawn 30° apart. Top, equinoxes; bottom, northern summer solstice.

essentially agree in amplitude and phase with those of the present model. Also in good agreement with the model are the temperature ranges obtained from thermosphere probes (Spencer *et al.*, 1966), from mass-spectrometer data on Explorer 17 (Reber and Nicolet, 1965) and Explorer 32 (Newton, 1969), and from EUV absorption (Hall *et al.*, 1967).

Temperatures in the neutral atmosphere can be inferred from Thomson-scatter measurements (Carru, Petit, and Waldteufel, 1967; Carru and Waldteufel, 1969; McClure, 1969), and much has been written about the discrepancies between the diurnal temperature variations as derived by this method and those derived from densities by means of existing models. The Thomson-scatter temperatures are essentially ion temperatures and refer to a height of about 300 km. They generally show secondary oscillations that cannot entirely be accounted for by geomagnetic activity. Occasionally, however, the temperature curves are relatively smooth, and in such cases they seem to follow quite closely the temperatures predicted by the present models, as we can see from Figure 9. The data plotted in this figure are hourly running means, taken at 10-min intervals, of temperatures measured by Carru and Waldteufel (1969). The continuous curve represents the temperature predicted by the present models; the small irregularities in the curve are caused by the geomagnetic effect. As can be seen, the agreement, on the whole, is extraordinarily good. A systematic deviation from the predicted curve is generally present around the time of maximum, in the afternoon. The temperatures determined by Thomson-scatter techniques seem to linger at maximum a little longer, dropping only after 4 p.m., while the predicted maximum occurs shortly after 2 p.m. As can be seen from Figure 9, however, this particular discrepancy is not serious and can be explained by the smoothing, of which we spoke earlier, inherent in drag measurements, and therefore also in the equations that represent the diurnal variation in the models. Apart from this minor discrepancy, the temperature curve seems to lag about 30 min behind the density curve in the 12-hour interval from 6^h to 18^h. Although the lag is not so serious as it would appear if we simply compare the times of the maxima of the two curves, it is somewhat surprising because of its direction: Offhand, one would expect the density curve to lag

behind the temperature curve, as in the CIRA 1965 models. Speculations on the mechanism by which such a lag can be achieved have recently appeared in the literature (see, for example, Rishbeth, 1969). Although the diurnal temperature variations as obtained by incoherent-scatter techniques can be considered to be in fair agreement, generally speaking, with those given by the present models, there seems to be some discrepancy in the variation of the amplitude with the seasons (Waldteufel, 1970).

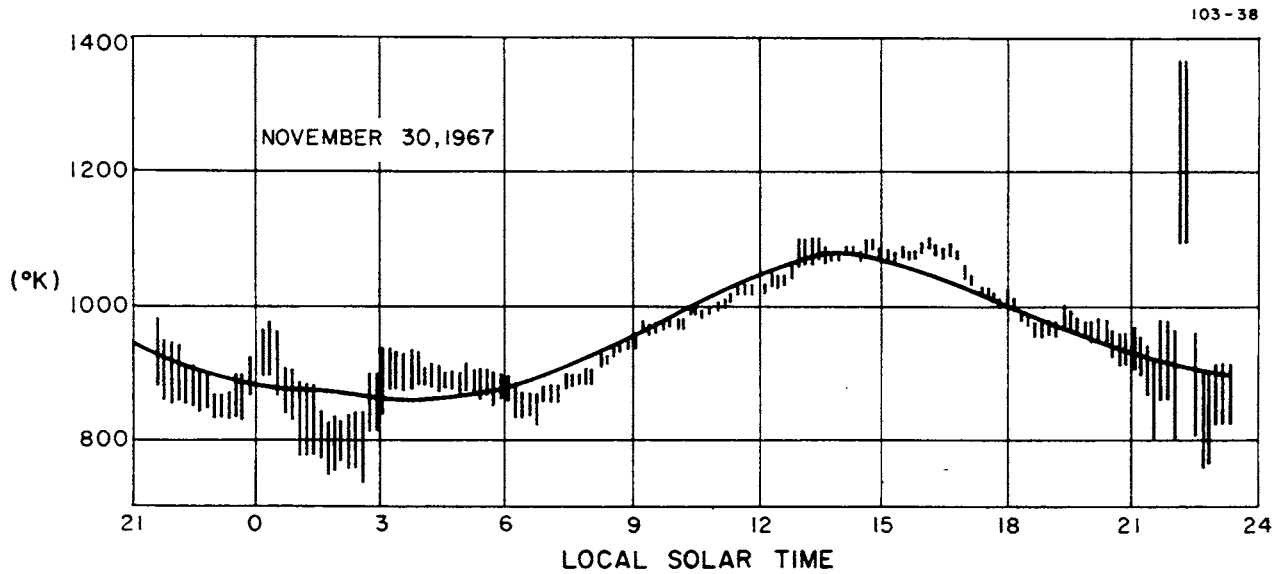


Figure 9. Atmospheric temperatures obtained on November 30, 1967, by Carru and Waldteufel (1969) by use of Thomson-scatter techniques, compared with temperatures predicted by the present models for a height of 300 km (solid line).

8. VARIATIONS WITH GEOMAGNETIC ACTIVITY

Recent high-resolution satellite measurements of temperatures with Doppler techniques applied to the λ 6300 oxygen line (Blamont and Luton, 1971) and of densities with accelerometers (DeVries, 1971) have made it increasingly clear that the geographic distribution of temperatures and densities at the onset of a geomagnetic disturbance and its variation in the course of the development of the disturbance follow a rather complex pattern, of which the orbital-drag method, with its limited resolution, can give only a very blurred picture. It would seem that at the start of a magnetic storm, there is an immediate increase of temperature and density in the thermosphere above part of the auroral belt and that the atmospheric perturbation propagates, reaching the equatorial regions, considerably weakened, some 7 hours later. The transport of energy from high to low latitudes during magnetic storms is corroborated by observations of winds (Smith, 1968) and gravity waves (Newton, Pelz, and Volland, 1969; Champion, Marcos, and McIsaac, 1970) in the thermosphere.

The highest time resolution that can be achieved by orbital-drag analysis of satellites is one density value per satellite revolution (90 to 120 min), and this value is not that of the density at a precise location, but rather a density averaged over a sizable orbital arc centered around the perigee point. Clearly, even under the most favorable conditions, a great deal of smoothing is introduced into the results. Yet, even satellite-drag data can establish, in broad outlines, the main features of the atmospheric perturbation that follows a magnetic disturbance: the greater intensity at high latitudes (Jacchia and Slowey, 1964; Jacchia, Slowey, and Verniani, 1967; Roemer, 1971) and the increase in the lag time from high to low latitudes [Jacchia et al. (1967); however, Roemer (1971) failed to detect this feature]. Since no workable model has been produced to date to give a quantitative representation of the high-resolution data, we shall have to be content with models based on orbital-drag measurements. Although they will not be adequate for comparisons with instantaneous data, they should be helpful in satellite-drag work.

Since the characteristic time of geomagnetic disturbances is hours rather than days, static models cannot be expected to represent correctly both temperature and density variations, so we must apply to the equations that describe the phenomenon the same reservations we applied to the equations for the diurnal variation (Section 7). The equations that have been most widely used (Jacchia, 1965a; Jacchia *et al.*, 1967) relate the exospheric temperature to the planetary geomagnetic index a_p or to its quasi-logarithmic equivalent K_p ; thus, implicitly, they make the assumption (*a priori* unlikely to be true) that in the process of atmospheric heating, the shape of the temperature profiles remains unchanged with respect to the basic models. Although these formulas seem to fit drag data reasonably well at heights greater than 200 km, we find that the density variations they predict at lower heights are too small (Zirm, 1964; King-Hele and Walker, 1969a,b; Schusterman, 1970). This means, in all probability, that the temperature profiles in the lower thermosphere are distorted by geomagnetic heating with respect to those of the basic models, in the direction of higher temperatures. Eventually it should be possible to determine this distortion on the basis of observations, but the task of computing densities from temperature profiles with shapes that change with geomagnetic activity presents practical problems of considerable difficulty. As a stopgap, we have recently resorted to using a hybrid formula, in which part of the density variation is obtained by altering the boundary density as a function of K_p and the rest by changing the exospheric temperature just as in the old formulas. The density part of the equation is intended to compensate roughly for the distortion in the temperature profile at lower heights. As a result of this artifice, the variations in the exospheric temperature become smaller — but this would also be true if we actually used the distorted temperature profile.

In view of this confused situation, we shall give here formulas based on changes in the exospheric temperature alone, as well as the hybrid formula. It must be remembered that if the former are used, the density variations below 200 km will be too small; on the other hand, if the hybrid formula is used, the density variations below 200 km will be represented somewhat better (except, perhaps, near the 90-km boundary), but the exospheric temperatures may be in error.

Jacchia et al. (1967) gave the following formula for the geomagnetic effect on the temperature:

$$\Delta T_{\infty} = 28^{\circ} K_p + 0.03 \exp(K_p) , \quad (18)$$

in which K_p is the 3-hour geomagnetic planetary index. The time lag Δt of the atmospheric variation behind the geomagnetic disturbance was given as 7.2 ± 0.3 hours at latitude 25° and 5.8 ± 0.5 hours at latitude 65° , with an overall mean of 6.7 ± 0.3 hours. It was also found that at 65° the amplitude of the variation was some 10 to 20% greater than at 25° .

Roemer (1971) modified equation (18) to incorporate a latitude dependence into the first coefficient:

$$\Delta T_{\infty} = (21.4 \sin \phi + 17.9) \bar{K}_p + 0.03 \exp(\bar{K}_p) , \quad (19)$$

where \bar{K}_p is the 0.4-day mean of the original 3-hourly planetary index K_p . This formula reduces to equation (18) when the latitude ϕ is 28° . Roemer found an average time lag $\Delta t = 5.5 \pm 0.3$ hours but could not find any variation of Δt with latitude. He did, on the other hand, find a sinusoidal variation of $\Delta T_{\infty}/K_p$ with local time, with a maximum at 3 a.m. larger by a factor 1.30 with respect to a 3 p.m. minimum.

The hybrid formula we find best to represent density variations below 200 km is as follows:

$$(a) \Delta \log_{10} \rho = 0.012 K_p + 1.2 \times 10^{-5} \exp(K_p) ;$$

$$(b) \Delta T_{\infty} = 14^{\circ} K_p + 0.02 \exp(K_p) . \quad (20)$$

To obtain the total density variation from the rest value $K_p = 0$ to that corresponding to a given value of K_p , the density variation given by equation (a) must be added to that resulting from equation (b).

As we said earlier in this section, all these equations give only a smoothed version of the real variations, for which no model exists, and should be valid only for comparisons with satellite-drag data. Even in this case, however, the formulas should not be used with the original 3-hourly K_p indexes but rather with a smoothed \bar{K}_p index, in which the smoothing is commensurate with the resolution of the observed data.

Corrections for the geomagnetic effect according to equation (18) are given in Table 2a; Table 2b gives corrections according to equations (20). As an illustration of the geomagnetic effect, we have plotted in Figure 10 the temperature residuals, obtained through the use of static models when all other variations are suppressed, from the drag-derived densities for six satellites with perigee heights from 338 to 1001 km, in a 3-week interval in May to June 1967 covering one of the greatest magnetic storms on record. The bottom diagram shows, for comparison, temperature residuals ΔT computed from equation (18).

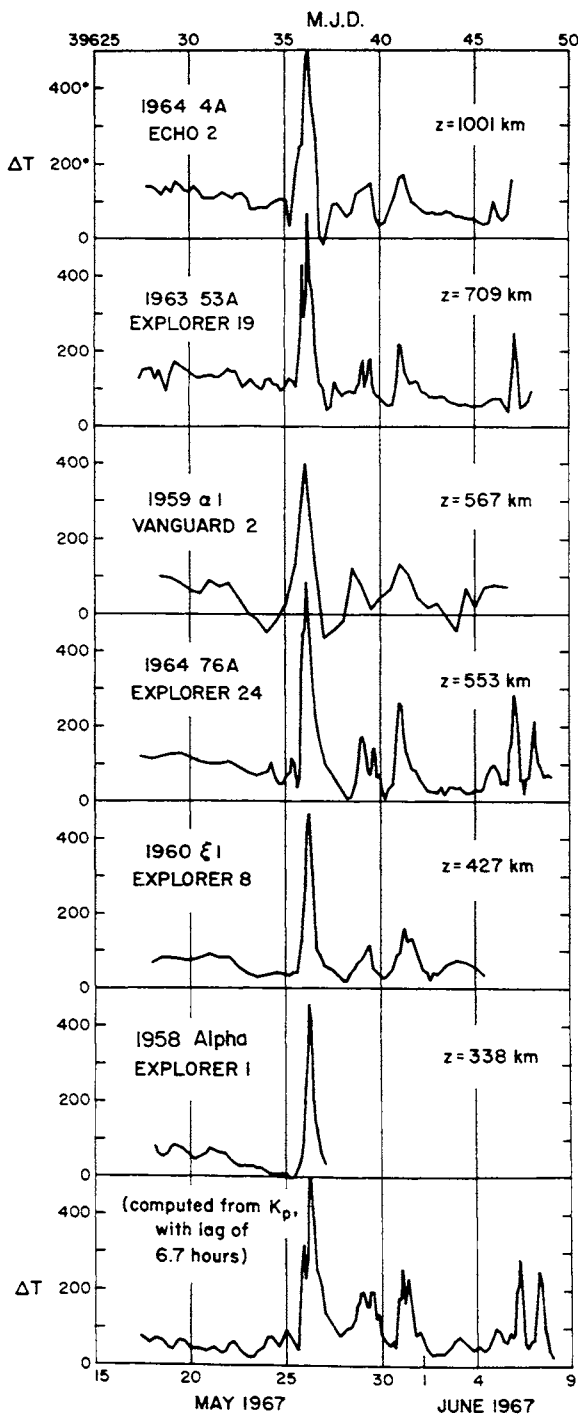


Figure 10. The geomagnetic effect as derived from the drag of six satellites in May and June 1967. The plotted ΔT 's are temperature residuals from the models when all variations except the geomagnetic effect have been taken into account. The diagram at the bottom shows ΔT as computed from equation (18). M.J.D. is the Modified Julian Day (J.D. minus 2 400 000.5).

9. THE SEMIANNUAL VARIATION

The semiannual density variation observed in the thermosphere and lower exosphere is a rather puzzling feature for which no satisfactory explanation has yet been found. Temperature variations are the immediate cause of the solar-activity effect, the diurnal variation, and the geomagnetic effect. While attempting to find a way of representing the semiannual variation in analytic form for the J65 models, we thought it rather logical to try to link it also to temperature variations, and the formula we found seemed to work for the data we had available at that time, i.e., densities from the drag of satellites with perigee heights between 250 and 650 km. The amplitude of the temperature variation seemed to be dependent on solar activity, and this seemed further to justify the assumed dependence on temperature variations.

Difficulties, however, soon became apparent. Cook and Scott (1966) and Cook (1967, 1969a) found that near sunspot minimum the amplitude of the semiannual density variation at 1100 km derived from the drag of the Echo 2 and the Calsphere satellites was much larger than that predicted on the basis of the J65 formula. At that height, according to the models, in 1964 to 1965 any temperature variation would have resulted in extremely small density variations, because of the near-balance of the helium variations in phase with the temperature and the hydrogen variations in antiphase. At the time the variation should have been no larger than 6%, the observed variations reached a factor of 2. In 1966, when solar activity rose toward its maximum (and hydrogen became a negligible constituent at that height), the discrepancy became smaller and almost disappeared.

With the launching of longer lived satellites with low perigee heights, another discrepancy became evident for heights below 200 km. Also here, at heights of 150 to 200 km, the observed variation was larger than that predicted by J65 (King-Hele and Hingston, 1967, 1968; King-Hele, 1967; King-Hele and Walker, 1970). Initially, we attributed this discrepancy to the fact

that in the J65 models constant boundary conditions were assumed at 120 km, where fairly large density variations with temperature actually occur: The reasoning was that, approaching 120 km, the computed density variations should have proved too small. More recent models, however (Jacchia, 1970a), in which the constant-boundary conditions were moved to 90 km, also proved inadequate to represent the observed semiannual density variation in the 150- to 180-km region. Cook (1969b) actually found that the semiannual variation, still in phase with that in the thermosphere and exosphere, can be discerned even at 90 km, which is a near-isopycnic level at which all other density variations nearly vanish (Groves, 1970). The range in density found by Cook at 90 km amounts to about 30%, but a reanalysis of his data by this writer, eliminating high-latitude measurements, which are affected by annual (seasonal) variations, reduces the range to 15%, which is still a respectable amount.

Decreasing the amount of hydrogen in the atmosphere would increase the computed amplitudes at 1100 km, but then the computed total density is too low at sunspot minimum. Besides, hydrogen densities from Balmer a observations (Tinsley, 1970) would indicate a larger, not a smaller, hydrogen concentration. Also, any tampering with the hydrogen concentration in the models would not cure the discrepancies observed at heights below 200 km.

An obvious way out of all these difficulties is to assume that the semiannual density variations are not caused by temperature variations. The main reason for clinging to a model based on temperature variations was the apparent dependence of the amplitude of the diurnal variation on solar activity. As it turns out, however, this is really a built-in variation, because at any given height in the heterosphere the change of density with temperature $d\rho/dT$ is strongly dependent on the temperature T itself (see Figure 4). Therefore, even a density variation with constant amplitude throughout the solar cycle, if interpreted as a thermal variation, would yield a temperature amplitude dependent on the phase of the solar cycle. Reanalyzing the density variations obtained from the orbital drag of six satellites in the interval 1958 to 1970, we find that this is precisely the case (Jacchia, 1971): The

amplitude of semiannual density variation, although strongly height dependent and variable from year to year (Figure 11), does not seem to be related to solar activity.

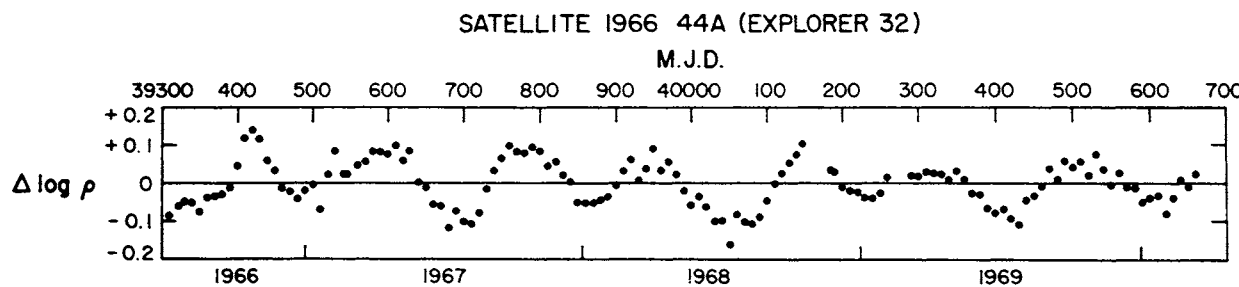


Figure 11. The semiannual density variation as derived from drag analysis on Satellite 1966 44 A (Explorer 32). All other variations have been suppressed by using the appropriate equations. M. J. D. is the Modified Julian Day (J. D. minus 2 400 000.5).

We deem it best, therefore, to express the semiannual density variation in the form

$$\Delta \log_{10} \rho_{\text{semiannual}} = f(z) g(t) , \quad (21)$$

where $g(t)$ represents the average density variation as a function of time in which the amplitude (i.e., the difference in $\log \rho$ between the principal minimum in July and the principal maximum in October) is normalized to 1, and $f(z)$ is the relation between the amplitude and the height z . We found the following equations to fit the data best:

$$f(z) = (5.876 \times 10^{-7} z^{2.331} + 0.06328) \exp(-2.868 \times 10^{-3} z) \quad (z \text{ in km}) ;$$

$$g(t) = 0.02835 + 0.3817 [1 + 0.4671 \sin(2\pi\tau + 4.137)] \sin(4\pi\tau + 4.259) , \quad (22)$$

with

$$\tau = \Phi + 0.09544 \left\{ \left[\frac{1}{2} + \frac{1}{2} \sin(2\pi\Phi + 6.035) \right]^{1.650} - \frac{1}{2} \right\} ,$$

where Φ is the phase of the semiannual variation, i.e., approximately the number of days elapsed since January 1 divided by the duration of the tropical year in days. A more rigorous expression, better suited for computer purposes, is

$$\Phi = (t - 36204)/365.2422 , \quad (23)$$

where t is time expressed in Modified Julian Days (M.J.D. = Julian Day minus 2 400 000.5). M.J.D. 36204 corresponds to January 1, 1958. The absolute term (0.02835) in the expression for $g(t)$ has the purpose of making $\int g(t) dt = 0$ over one cycle of the variation. The functions $f(z)$ and $g(t)$ are tabulated in Table 3.

It should be understood, of course, that even though temperature variations are apparently not the primary cause of the semiannual density variations, these must be accompanied by some temperature changes, however small. The determination of such temperature changes must wait, however, for better observations or, more likely, for dynamical models of the phenomenon.

10. SEASONAL-LATITUDINAL VARIATIONS OF THE LOWER THERMOSPHERE

In the present models we have assumed that temperature and density are constant at 90 km all over the globe. In reality, seasonal-latitudinal variations are observed at that height — fairly large in temperature, although relatively small in density. All the variations we have described so far could be taken into account with a fair degree of approximation by operating on the exospheric temperature; such a procedure is obviously impossible for the seasonal-latitudinal variations, for which it is necessary to operate on the lower boundary conditions. However reluctantly, the decision to keep the lower boundary conditions constant had to be taken to prevent the models' becoming unmanageable in their complexity.

An attempt was made in the U. S. Standard Atmosphere Supplements, 1966 (COESA, 1966) to effect a smooth junction between the densities of lower-thermosphere models with seasonal variations and the densities of upper-atmosphere models computed by use of constant boundary conditions at 120 km. The models were limited to a fixed, intermediate latitude and to three seasons (summer, winter, and spring/fall); any greater detail would have entailed a prohibitive proliferation of tables. If we wanted to have models for every month at 15° intervals in latitude, the number of models would increase by a factor of 84!

The amplitude of the seasonal-latitudinal density variations increases very rapidly between 90 and 100 km; the maximum amplitude is apparently reached between 105 and 120 km; above this height it must decrease quite rapidly because above 160 km there seem to be no appreciable seasonal-latitudinal variations other than those involved in the global pattern of the diurnal variation. This means that the temperature variations, which at 100 km are in phase with the density variations, must undergo a phase inversion around 110 km and reach a maximum amplitude, in opposite phase with respect to the densities, somewhere around 150 km. While it is relatively easy to represent the density variations in analytical, and even in tabular,

form, it would be prohibitively laborious to do the same thing for the temperatures. We thought the best that could be done was to give formulas for computing the seasonal-latitudinal variations in density, ignoring the temperature variations.

The equation we present here is an attempt to fit the seasonal variations as derived by Champion (1967) and Groves (1970). We find that the values of $\log \rho$ given by the models must be corrected by adding a quantity $\Delta \log \rho$ given by

$$\Delta \log_{10} \rho = 0.014(z - 90) \exp[-0.0013(z - 90)^2] \frac{\phi}{|\phi|} \sin(2\pi\Phi + 1.72) \sin^2 \phi , \quad (24)$$

where ϕ is the geographic latitude, z the height in kilometers, and Φ the phase as defined by equation (23). We can write this formula as

$$\Delta \log_{10} \rho = S \frac{\phi}{|\phi|} P \sin^2 \phi ,$$

with $S = 0.014(z - 90) \exp[-0.0013(z - 90)^2]$ and $P = \sin(2\pi\Phi + 1.72)$. Tabulations of S , P , and $\sin^2 \phi$ are given in Table 4.

There are no reliable data on the seasonal-latitudinal variation above 120 km. In the J70 models we adjusted the parameters of equation (24) in such a way that the logarithmic half-range S would reach a maximum of about 0.16 at 110 to 115 km and decline to one-tenth this value at 200 km. According to that formula, at 150 km we had $S = 0.08$, or half the maximum value. According to recent observations (Schusterman, 1970), this value is too large: At 150 km, hardly any seasonal-latitudinal variations can be discerned. Consequently, we have modified the equation so that S declines much faster for heights greater than 110 km; with the present equation, we have $S = 0.008$ at 150 km.

11. SEASONAL-LATITUDINAL VARIATIONS OF HELIUM

A strong increase of helium concentration above the winter pole has been revealed by mass-spectrometer measurements (Hartmann, Mauersberger, and Müller, 1968; Kasprzak, Krankowsky, and Nier, 1968; Krankowsky, Kasprzak, and Nier, 1968; Müller and Hartmann, 1969), by observations of the intensity of the λ 10830 resonance line of helium (Fedorova, 1967; Shefov, 1968; Tinsley, 1968), and by satellite-drag data (Jacchia and Slowey, 1968; Keating and Prior, 1968).

While the mechanism of the seasonal migration of helium is not yet clear, it is possible to establish empirical equations to describe the phenomenon. An equation we tentatively proposed in the J70 models appears to be rather unwieldy and does not respect the conservation of helium on a global scale; this resulted in a spurious semiannual variation of helium. Keating, Mullins, and Prior (1970) used, with considerable success, a formula of the type

$$\Delta \log_{10} n(\text{He}) = C \phi \delta_{\odot},$$

where ϕ is the latitude and δ_{\odot} the declination of the sun. For the constant C , they found the value -0.4 when ϕ and δ_{\odot} are expressed in radians; this would give a total range in $\log n(\text{He})$ of 0.514 at the poles, corresponding to a ratio of 3.3 in $n(\text{He})$. This formula has the disadvantage of having a cusp in the helium distribution at the poles. We find that the seasonal density variations derived from the drag of Explorer 19 and Explorer 24 can be satisfactorily represented using the following expression for the helium variation:

$$\Delta \log_{10} n(\text{He}) = 0.65 \left| \frac{\delta_{\odot}}{\epsilon} \right| \left[\sin^3 \left(\frac{\pi}{4} - \frac{\phi}{2} \frac{\delta_{\odot}}{|\delta_{\odot}|} \right) - \sin^3 \frac{\pi}{4} \right]. \quad (25)$$

Here ϵ is the obliquity of the ecliptic, $23^\circ 44$. According to this formula, the range of the helium variation at the poles corresponds to a factor of 4.5 in $n(\text{He})$. Table 5 gives $\Delta \log_{10} n(\text{He})$ as a function of ϕ and of the date of the year, according to equation (25). Figure 12 shows density residuals from the drag of the Explorer 19 satellite when all variations except the helium variation are suppressed. The curve through the data points represents equation (25).

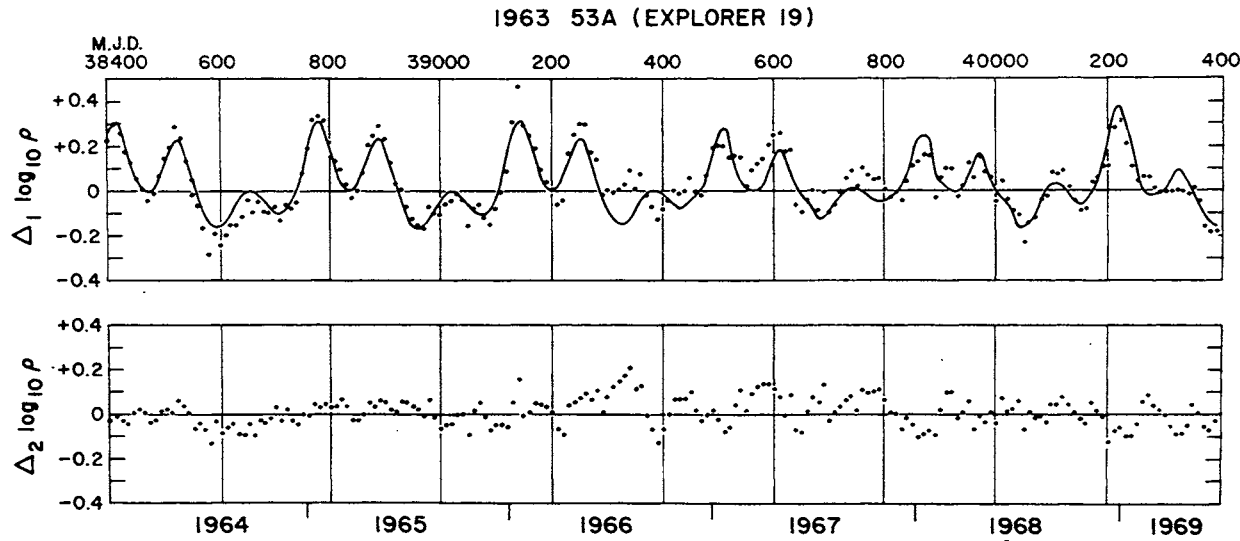


Figure 12. Observed and computed density variations caused by the helium migration, as derived from the drag on Satellite 1963 53A (Explorer 19). The data points in $\Delta_1 \log \rho$ are density residuals from the model when all variations except the helium variation are suppressed. The solid line represents the residuals computed by means of equation (25). $\Delta_2 \log \rho$ is the difference O-C in $\Delta_1 \log \rho$. M. J. D. is the Modified Julian Day (J. D. minus 2 400 000.5).

12. VARIATIONS IN HYDROGEN CONCENTRATION

As explained in Section 3, the hydrogen concentrations in the basic models are adopted from the theory of Kockarts and Nicolet (1962, 1963). Since the amount of neutral hydrogen in the atmosphere is primarily determined by its production and escape rates, there can be no diffusion equilibrium of hydrogen in the true sense. The computations made by Kockarts and Nicolet show, however, that above 500 km the hydrogen density profiles approximate those corresponding to diffusion equilibrium. For heights lower than 500 km, the departure from diffusion equilibrium becomes progressively larger, so we have not included hydrogen in our tables for $z < 500$ km; for data at those heights, we must refer the user of our models to the original papers by Kockarts and Nicolet. Although not given in the tables, hydrogen concentrations at heights below 500 km were actually computed in the same manner as above 500 km and taken into account in the computation of the total density, in order to avoid any discontinuity — no matter how small — in the density profiles across the 500-km level.

On the basis of theory, it could be expected that the variations in hydrogen concentration should mirror the variations of the exospheric temperature even on a relatively small time scale. Until recently, most of the observational evidence of a variation in $n(H)$ came from Lyman α airglow measurements, which showed the existence of a diurnal variation and a variation with the solar cycle (Donahue, 1966) in the expected direction (more hydrogen at lower temperatures). Quantitative conclusions from these observations are difficult because of the variable intensity of solar Lyman α (Meier, 1969). Recently, Brinton and Mayr (1971) derived the temporal variations of thermospheric $n(H)$ from $n(H^+)$ measured by an ion mass spectrometer on the Explorer 32 satellite in the altitude range 275 to 400 km between June 1966 and January 1967, during a period of rapid increase in solar activity accompanied by large 27-day fluctuations in the solar decimetric flux. Although assumptions had to be made regarding charge-exchange equilibrium, the results that were obtained

concerning the diurnal variation and the variation with solar activity look very reasonable and confirm a variation of $n(H)$ with temperature in essential agreement with the variations predicted by the present models when the temperature variations with solar activity are computed from equation (14) and the diurnal temperature variations from equations (16) and (17); the observed amplitude of $n(H)$ in the diurnal variation, however, is smaller than the predicted amplitude — a factor of 2 instead of 4.

Should the smaller amplitude of the diurnal $n(H)$ variation be confirmed, it may prove convenient to reduce it also in the models. This can be accomplished by using for hydrogen a fictitious temperature T' that in the diurnal variation oscillates around the average daily temperature with a smaller amplitude. If, for simplicity, we assume that the average daily temperature \bar{T} is the arithmetic mean between T_c and T_M (see Section 7) and we call c the reduction factor in the amplitude, we can write

$$\bar{T} = T_c \left(1 + \frac{R}{2}\right) ,$$

$$T' = \bar{T} + c(T_\ell - \bar{T}) . \quad (26)$$

Large seasonal-latitudinal asymmetries in the distribution of geocoronal hydrogen seem to be indicated by Lyman- α observations (Donahue, 1969) and may be expected also as a consequence of the so-called "polar wind" (Banks and Holzer, 1968). A quantitative evaluation of these variations seems out of the question for the time being.

13. DENSITY WAVES

Density gauges on the Explorer 32 satellite have detected the existence of waves throughout the upper atmosphere in the height range from 286 (satellite perigee) to at least 510 km (Newton *et al.*, 1969). An analysis of these waves indicates that they propagate in the neutral atmosphere. The waves are most prevalent at the higher latitudes near the auroral zone (the orbital inclination of the satellite is 65°) and were observed most frequently in the late evening and early morning hours, but they were not limited to those latitudes and times. The apparent vertical half-wavelengths of the waves increase with altitude from 1 km at 286-km altitude to 70 km at 510-km altitude; their half-amplitudes in density range from the limit of detectability to a maximum of about 50% of the mean density. It appears that some of the observed wavelengths are integrally related, indicating the existence of "fundamental" wavelengths and of second, third, and fourth harmonics.

These waves have been interpreted as free internal gravity waves propagating predominantly from north to south or from south to north, with maximum horizontal wavelengths between 130 and 520 km. The altitude dependence of the apparent vertical half-wavelengths results from the satellite moving with varying vertical velocity through a slowly propagating wave pattern with nearly vertical phase planes. It is tempting to visualize these waves as part of the mechanism by which energy deposited in the auroral zones is conveyed to lower latitudes (see Section 8). In the densities derived from satellite drag, these waves are entirely smoothed out; their existence, however, must be kept in mind when comparisons are made between densities from satellite drag and densities obtained from high-resolution gauges.

14. COMPARISON WITH OBSERVATIONS; DRAG COEFFICIENT

In Figures 13, 14, and 15, we have compared densities derived from the drag of several artificial satellites with those predicted by the present models.

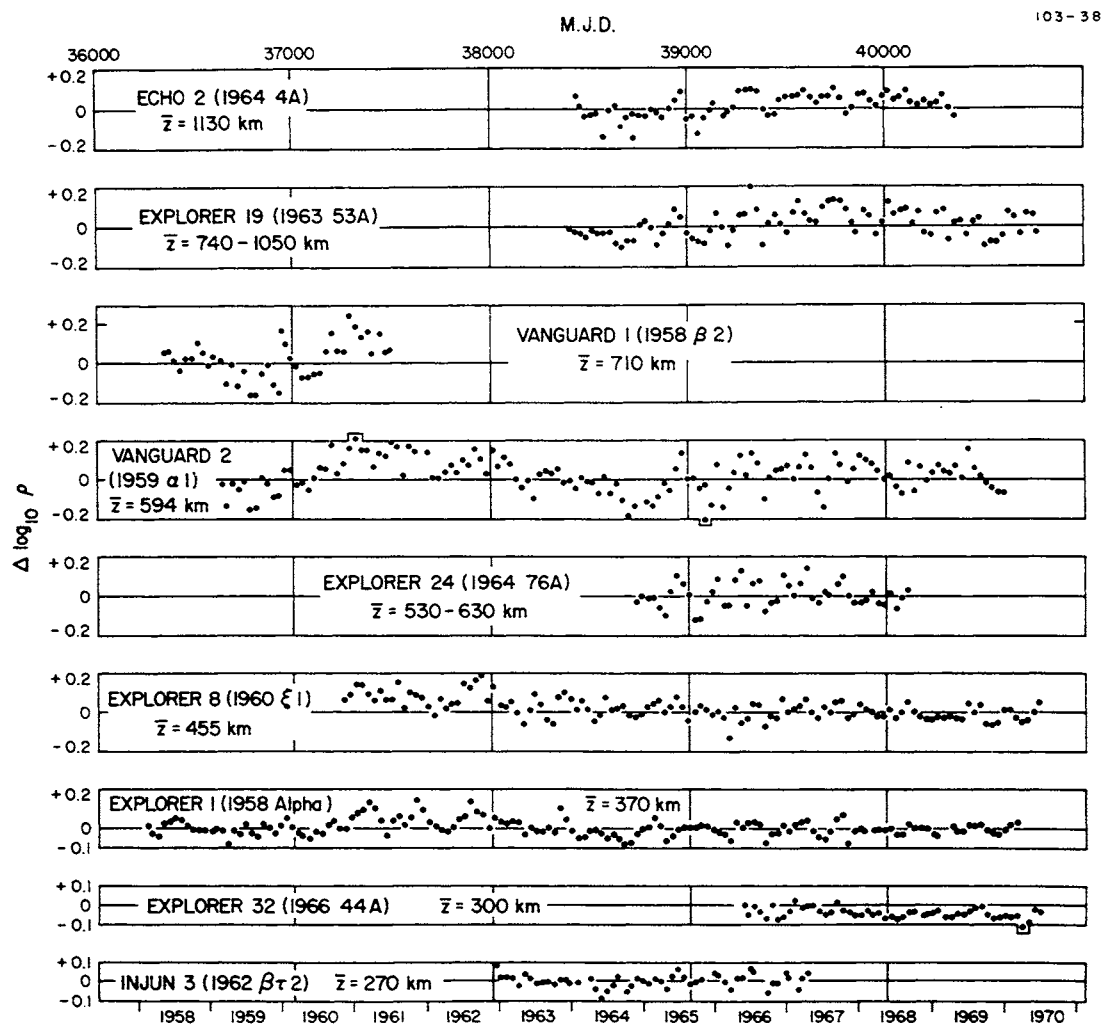


Figure 13. Thirty-day means of density residuals from the present models for nine satellites covering a wide range of heights. \bar{z} is the average effective height of the satellite (see text). The 12 years in the diagram cover a full sunspot cycle. The purpose of the figure is to show how effectively the models account for the density variation with height and with solar activity. M. J. D. is the Modified Julian Day (J. D. minus 2 400 000.5).

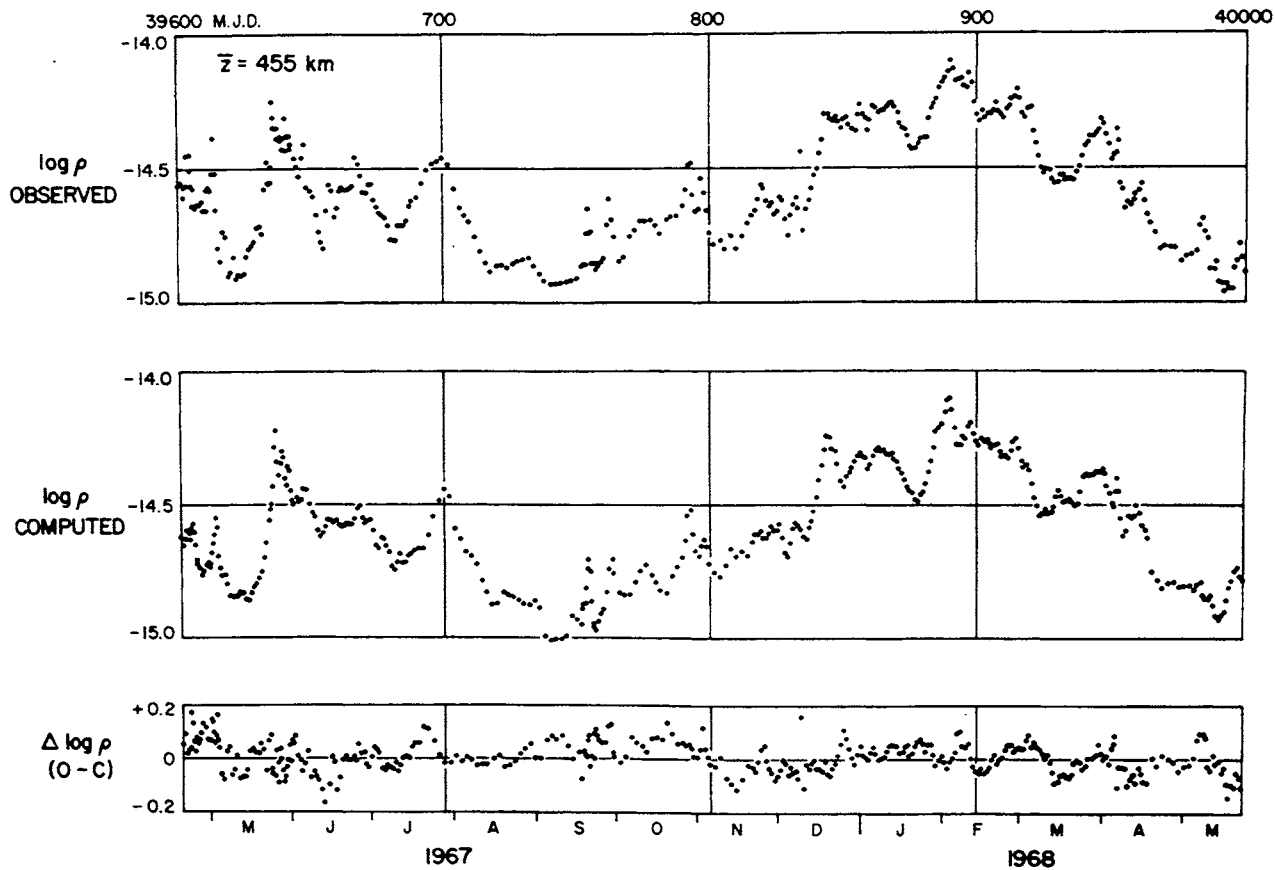


Figure 14. Observed and computed densities for Satellite 1960 §1 (Explorer 8) during 1967 and 1968. The observed densities (top) were derived from drag analysis; the middle strip shows densities computed from the present models; the difference (O-C) is plotted at the bottom. The purpose of this figure is to show how effectively the models account for the diurnal variation (slow, 230-day oscillation) and the 27-day fluctuations in apparent solar activity.
M. J. D. is the Modified Julian Day (J. D. minus 2 400 000.5).

In Figure 13, intended to show at a glance how closely the model represents the large, slow variations with the 11-year solar cycle, we have plotted 30-day means of the density residuals for nine satellites with effective heights ranging from 270 to 1130 km. The data cover the 12-year interval from 1958 to 1970, i.e., an entire solar cycle.

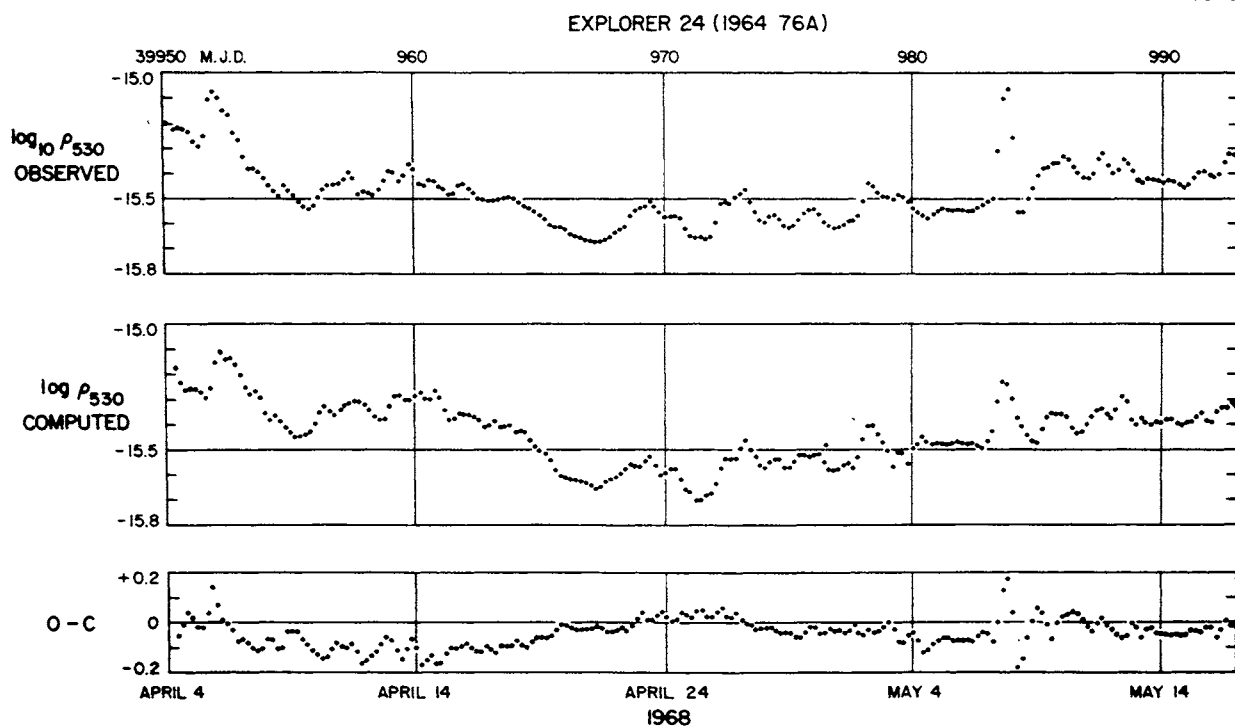


Figure 15. Observed and computed densities, reduced to a standard height of 530 km, for Satellite 1964 76A (Explorer 24) during 46 days in April and May 1968. The observed densities were derived from drag analysis by use of positions from precision-measured photographs taken with the Baker-Nunn cameras; the middle strip shows densities computed with the present models; the difference (O-C) is plotted at the bottom. The purpose of this figure is to show how effectively the models account for the geomagnetic effect. All the fluctuations with a characteristic time of 1 to 5 days are caused by the geomagnetic effect and are superimposed on a slower oscillation caused by the 27-day variation in solar activity. M. J. D. is the Modified Julian Day (J. D. minus 2 400 000.5).

Figure 14 compares observed and computed densities on a shorter time scale. The observed data are the densities derived from the drag analysis of field-reduced positions obtained from photographs taken by the Baker-Nunn cameras for Satellite 1960 §1 (Explorer 8). These positions have an accuracy of about 2 arcmin and permit a resolution of 1 to 2 days, except around

magnetic storms, where a resolution of 0.5 days or higher might be achieved. In the computed densities, a variable smoothing factor has been used in the geomagnetic effect to match the actual resolution. The large, slow fluctuation in the densities, with a period of 230 days, is caused by the diurnal variation (see also Figures 5 and 6); the superimposed fluctuations are caused by the 27-day variations in the apparent solar activity, by the variations in latitude of the satellite perigee, and by magnetic storms (such as the sharp peak in May 1967, near the beginning of the diagram, and the two peaks in the second half of September 1967). The entire time interval covered by the diagram was one of lively 27-day variations connected with solar rotation.

Figure 15 shows observed and computed densities on an even shorter time scale. The observed data are, this time, densities derived from the drag analysis of precise positions obtained, by photoreduction of Baker-Nunn films, for the 12-foot balloon satellite Explorer 24 (1964 76A). The accuracy of these positions is of the order of 3 arcsec. This accuracy, combined with the high drag of the satellite, allowed a resolution of 0.2 days throughout the interval covered by the diagram. Here the slow background variation is caused by the 27-day oscillations, while all the numerous irregular fluctuations seen throughout the diagram are caused by the geomagnetic effect.

The height \bar{z} marked on each diagram is the average effective height to which the data refer. The effective height, variable from revolution to revolution, is the weighted mean of the heights above the geoid in the course of one revolution, with the drag taken as the weight. For moderate and high orbital eccentricities, this "effective" height is approximately half a density-scale height higher than the perigee height; for zero eccentricity, of course, it is close to the perigee height itself.

In the computation of densities from satellite drag, we have used a drag coefficient C_D variable according to theory (Cook, 1965), in which the numerical parameters in the accommodation coefficient have been selected in such a way as to give $C_D = 2.2$ at heights between 200 and 400 km. The

actual value of the drag coefficient was computed point by point along the satellite orbit by means of the present atmospheric models, which are also used in the numerical-integration process leading from the observed drag to the corresponding density.

15. NUMERICAL EXAMPLES

Suppose we want to find the atmospheric density given by the models above a point with the following geographic coordinates:

longitude = 120° W of Greenwich, latitude = $+45^{\circ}$,

on January 20, 1969, at $19^{h}11^{m}$ U.T. = $11^{h}0^{m}$ L.S.T., for three heights:
 $z = 350, 140,$ and 800 km.

We shall first compute T_c from equation (14). For that purpose, we need the smoothed solar flux $\bar{F}_{10.7}$ for that date and the actual flux $F_{10.7}$ on the day before (to account for the lag of $1^d 0^h$). Consulting solar records, we find the following: $\bar{F}_{10.7} = 155$, $F_{10.7} = 136$, so $T_c = 856.5$. This is the minimum exospheric temperature anywhere on the globe at the desired instant, for quiet geomagnetic conditions ($K_p = 0$).

Next we shall use equation (16) or Table 1 to compute the exospheric temperature T_ℓ . The declination of the sun on January 20.8 was $-20^{\circ}0$. For $\phi = +45^{\circ}$ and L.S.T. = $11^{h}0^{m}$, Table 1 gives $T_\ell/T_c = 1.158$, so we obtain $T_\ell = 991.8$.

We must now add the effects of the semiannual variation and of geomagnetic heating. Let us start with the geomagnetic effect, because it involves a temperature change. We must first look up the value of K_p at a time 6.7 hours before the desired date; from geomagnetic records we find $K_p = 2_0$. If we use equation (18), we find (Table 2a) $\Delta T = 56^{\circ}$; adding this to T_ℓ , we find $T_\infty = 1048^{\circ}$. If we look up $\log \rho$ in the basic tables for $T_\infty = 1048^{\circ}$ and $z = 350$ km, we find, by interpolation, the value -13.976 (g cm^{-3}). To this value we must still add a correction for the semiannual variation. From Table 3 we obtain $f(z) = 0.207$, $g(t) = -0.183$, so $\Delta \log \rho = f(z) g(t) = -0.038$. Adding, we find $\log \rho = -14.014$. According to Table 5, seasonal-latitudinal

variations are negligible at 350 km, and since at this height the basic tables show helium to be a negligible constituent, we have no further corrections to make to the value of $\log \rho$ we just found. If we had decided to use the hybrid equations (20) to compute the geomagnetic effect, we would have had to add to T_ℓ , according to Table 2b, a correction $\Delta T = +28^\circ$ and to $\log \rho$ a correction $+0.024$. This would have led to $T_\infty = 1020^\circ$ and a final $\log \rho = -14.028$.

For $z = 140$ km, we can no longer neglect the seasonal-latitudinal variations, and we must use equations (20) to compute the geomagnetic effect. We shall thus have $T_\infty = 1020^\circ$, as in the previous example when we used equations (20); for this temperature and $z = 140$ km, the basic tables give $\log \rho = -11.413$. With a correction $\Delta \log \rho = +0.024$ for the geomagnetic effect, this becomes $\log \rho = -11.389$. For the seasonal-latitudinal variation, Table 4 gives $S = 0.027$, $P = +0.882$, $\sin^2 \phi = 0.500$, from which we obtain $\Delta \log \rho = SP \sin^2 \phi = +0.012$. So the final density is $\log \rho = -11.377$.

For $z = 800$ km, we can again neglect the seasonal-latitudinal variation of the lower thermosphere, but we find that helium is not negligible, so that a correction to the helium concentration must be computed from equation (25) or found in Table 5. Let us use equation (18) for the geomagnetic effect. We shall then have $T_\infty = 1048^\circ$; for this temperature and $z = 800$ km, the basic tables give $\log \rho = -16.795$. With the correction $\Delta \log \rho = -0.038$ for the semiannual variation, we obtain $\log \rho = -16.833$, i.e., $\rho = 1.60 \times 10^{-17}$. From the basic tables, we derive, for $T_\infty = 1048^\circ$, $\log n_0(\text{He}) = 5.958$; to this value we must apply, according to Table 5, a correction $\Delta \log n(\text{He}) = +0.243$. Converting to natural values: $n_0(\text{He}) = 9.08 \times 10^5$, $n(\text{He}) = n_0(\text{He}) + \Delta n(\text{He}) = 15.89 \times 10^5$, whence $\Delta n = 6.81 \times 10^5$. The correction to the total density can be computed from $\Delta \rho = [M(\text{He})/A] \Delta n(\text{He})$, where $M(\text{He})$ is the atomic mass of helium, 4.0026, and A is Avogadro's number, 6.02257×10^{23} . We obtain $\Delta \rho = 0.453 \times 10^{-17}$; the final density is $\rho = 1.60 \times 10^{-17} + 0.45 \times 10^{-17} = 2.05 \times 10^{-17}$.

16. ACKNOWLEDGMENT

It is a pleasure to acknowledge the constant cooperation of Mr. I. G. Campbell, who was responsible for most of the laborious programing and computing involved in the preparation of these models.

17. REFERENCES

BANKS, P. M., and HOLZER, T. E.

1968. The polar wind. *Journ. Geophys. Res.*, vol. 73, pp. 6846-6854.

BLAMONT, J. E., and LUTON, J. M.

1971. OGO-VI direct measurement of the temperature of the neutral atmosphere from 200 to 350 km of altitude. In Space Research XI, Akademie-Verlag, Berlin (in press).

BRINTON, H. C., and MAYR, H. G.

1971. Atomic hydrogen concentration in the thermosphere: Observed temporal variations. Prepared for presentation at AGU meeting, Washington, April.

CARRU, H., PETIT, M., and WALDTEUFEL, P.

1967. On the diurnal variation of the thermopause temperature. *Planet. Space Sci.*, vol. 15, pp. 944-945.

CARRU, H., and WALDTEUFEL, P.

1969. Étude par diffusion de Thomson des variations de la température exosphérique. *Ann. de Géophys.*, vol. 25, pp. 485-494.

CHAMPION, K. S. W.

1967. Variations with season and latitude of density, temperature, and composition in the lower thermosphere. In Space Research VII, ed. by R. L. Smith-Rose and J. W. King, pp. 1101-1118, North-Holland Publ. Co., Amsterdam.

CHAMPION, K. S. W., MARCOS, F. A., and MCISAAC, J. P.

1970. Atmospheric density measurements by research satellite OVI-15. In Space Research X, ed. by T. M. Donahue, P. A. Smith, and L. Thomas, pp. 450-458, North-Holland Publ. Co., Amsterdam.

CIRA 1965

1965. COSPAR International Reference Atmosphere 1965. Compiled by the members of COSPAR Working Group IV, North-Holland Publ. Co., Amsterdam, 313 pp.

COESA (U.S. Committee on the Extension of the Standard Atmosphere)

1962. U.S. Standard Atmosphere 1962. U.S. Government Printing Office, Washington, D.C., 278 pp.
1966. U.S. Standard Atmosphere Supplements, 1966. U.S. Government Printing Office, Washington, D.C., 289 pp.

COOK, G. E.

1965. Satellite drag coefficients. *Planet. Space Sci.*, vol. 12, pp. 929-946.
1967. The large semi-annual variation in exospheric density: A possible explanation. *Planet. Space Sci.*, vol. 15, pp. 627-632.
- 1969a. The semi-annual variation in the upper atmosphere: A review. *Ann. de Géophys.*, vol. 25, pp. 451-469.
- 1969b. Semi-annual variation in density at a height of 90 km. *Nature*, vol. 222, pp. 969-971.

COOK, G. E., and SCOTT, D. W.

1966. Exospheric densities near solar minimum derived from the orbit of Echo 2. *Planet. Space Sci.*, vol. 14, pp. 1149-1165.

DEVRIES, L. L.

1971. Analysis and interpretation of density data from the Low-G Accelerometer Calibration System (LOGACS). Prepared for presentation at COSPAR meeting, Seattle, Washington, June.

DONAHUE, T. M.

1966. The problem of atomic hydrogen. *Ann. de Géophys.*, vol. 22, pp. 175-188.
1969. A hydrogen bulge over the springtime pole. *Journ. Geophys. Res.*, vol. 74, pp. 3717-3719.

FEDEROVA, N. I.

1967. Aurorae and airglow. *Sov. Geophys. Comm. USSR Acad. Sci.*, vol. 13, p. 53.

GROVES, G. V.

1970. Seasonal and latitudinal models of atmospheric temperature, pressure, and density, 25 to 110 km. Air Force Surveys in *Geophys.*, No. 218 (AFCRL-70-0261), May.

HACHENBERG, O.

1965. Radio frequency emissions of the sun in the centimeter wavelength range: The slowly varying sunspot component. In Solar System Radio Astronomy, ed. by J. Aarons, pp. 95-108, Plenum Press, New York.

HALL, L. A., CHAGNON, C. W., and HINTEREGGER, H. E.

1967. Daytime variations in the composition of the upper atmosphere.

Journ. Geophys. Res., vol. 72, pp. 3425-3427.

HALL, L. A., SCHWEIZER, W., and HINTEREGGER, H. E.

1965. Improved extreme ultraviolet absorption measurements in the upper atmosphere. Journ. Geophys. Res., vol. 70, pp. 105-111.

HARRISON, L. P.

1951. Relation between geopotential and geometric height. In Smithsonian Meteorological Tables, sixth ed., pp. 217-219, Washington, D.C.

HARTMANN, G., MAUERSBERGER, K., and MÜLLER, D.

1968. Evaluation of the turbopause level from measurements of the helium and argon content of the lower thermosphere above Fort Churchill. In Space Research VIII, ed. by A. P. Mitra, L. G. Jacchia, and W. S. Newman, pp. 940-946, North-Holland Publ. Co., Amsterdam.

JACCHIA, L. G.

1965a. Static diffusion models of the upper atmosphere with empirical temperature profiles. Smithsonian Contr. Astrophys., vol. 8, no. 9, pp. 215-257.

1965b. The temperature above the thermopause. In Space Research V, ed. by P. Muller, pp. 1152-1174, North-Holland Publ. Co., Amsterdam.

1968. Recent results in the atmospheric region above 200 km and comparisons with CIRA 1965. In Space Research VIII, ed. by A. P. Mitra, L. G. Jacchia, and W. S. Newman, pp. 800-810, North-Holland Publ. Co., Amsterdam.

1970a. New static models of the thermosphere and exosphere with empirical temperature profiles. Smithsonian Astrophys. Obs. Spec. Rep. No. 313, 87 pp.

1970b. Recent advances in upper atmospheric structure. In Space Research X, ed. by T. M. Donahue, P. A. Smith, and L. Thomas, pp. 367-388, North-Holland Publ. Co., Amsterdam.

JACCHIA, L. G.

1970c. Solar-wind dependence of the diurnal temperature variation in the thermosphere. *Journ. Geophys. Res.*, vol. 75, pp. 4347-4349.

1971. The semiannual density variation in the heterosphere: A reappraisal. Prepared for presentation at COSPAR meeting, Seattle, Washington, June.

JACCHIA, L. G., and SLOWEY, J.

1964. Atmospheric heating in the auroral zones: A preliminary analysis of the atmospheric drag of the Injun 3 satellite. *Journ. Geophys. Res.*, vol. 69, pp. 905-910.

1968. Diurnal and seasonal-latitudinal variations in the upper atmosphere. *Planet. Space Sci.*, vol. 16, pp. 509-524.

JACCHIA, L. G., SLOWEY, J., and VERNIANI, F.

1967. Geomagnetic perturbations and upper-atmosphere heating. *Journ. Geophys. Res.*, vol. 72, pp. 1423-1434.

KASPRZAK, W. T., KRANKOWSKY, D., and NIER, A. O.

1968. A study of day-night variations in the neutral composition of the lower thermosphere. *Journ. Geophys. Res.*, vol. 73, pp. 6765-6782.

KEATING, G. M., MULLINS, J. A., and PRIOR, E. J.

1970. The polar exosphere near solar maximum. In Space Research X, ed. by T. M. Donahue, P. A. Smith, and L. Thomas, pp. 439-449, North-Holland Publ. Co., Amsterdam.

KEATING, G. M., and PRIOR, E. J.

1968. The winter helium bulge. In Space Research VIII, ed. by A. P. Mitra, L. G. Jacchia, and W. S. Newman, pp. 982-992, North-Holland Publ. Co., Amsterdam.

KING-HELE, D. G.

1967. Upper atmosphere density in 1966-67: The dominance of a semi-annual variation at heights near 200 km. *Nature*, vol. 216, p. 880.

KING-HELE, D. G., and HINGSTON, J.

1967. Variations in air density at heights near 150 km, from the orbit of the satellite 1966-101G. *Planet. Space Sci.*, vol. 15, pp. 1883-1893.

KING-HELE, D. G., and HINGSTON, J.

1968. Air density at heights near 190 km in 1966-67, from the orbit of Secor 6. *Planet. Space Sci.*, vol. 16, pp. 675-691.

KING-HELE, D. G., and WALKER, D. M. C.

- 1969a. Air density between 130 and 160 km, from analysis of the orbit of 1968-59B. *Planet. Space Sci.*, vol. 17, pp. 985-997.

- 1969b. Air density at heights of 140-180 km, from analysis of the orbit of 1968-59A. *Planet. Space Sci.*, vol. 17, pp. 1539-1556.

1970. Air density at heights near 180 km in 1968 and 1969, from the orbit of 1967-31A. Royal Aircraft Establishment, Tech. Rep. 70084, May.

KOCKARTS, G., and NICOLET, M.

1962. Le problème aéronomique de l'hélium et de l'hydrogène neutres. *Ann. de Géophys.*, vol. 18, pp. 269-290.

1963. L'hélium et l'hydrogène atomique au cours d'un minimum d'activité solaire. *Ann. de Géophys.*, vol. 19, pp. 370-385.

KRANKOWSKY, D., KASPRZAK, W. T., and NIER, A. O.

1968. Mass spectrometric studies of the composition of the lower thermosphere during summer 1967. *Journ. Geophys. Res.*, vol. 73, pp. 7291-7306.

McCLURE, J. P.

1969. Diurnal variation of neutral and charged particle temperatures in the equatorial F region. *Journ. Geophys. Res.*, vol. 74, pp. 279-291.

MEIER, R. R.

1969. Temporal variations of solar Lyman alpha. *Journ. Geophys. Res.*, vol. 74, pp. 6487-6490.

MINZNER, R. A., and RIPLEY, W. S.

1956. The ARDC model atmosphere, 1956. AFCRC TN-56-204; ASTIA Document 110233, 202 pp.

MÜLLER, D., and HARTMANN, G.

1969. A mass spectrometric investigation of the lower thermosphere above Fort Churchill with special emphasis on the helium content. *Journ. Geophys. Res.*, vol. 74, pp. 1287-1293.

NEWTON, G. P.

1969. Resolution of the difference between atmospheric density measurements from Explorer 17 density gage and drag technique. Journ. Geophys. Res., vol. 74, pp. 6409-6414.

NEWTON, G. P., PELZ, D. T., and VOLAND, H.

1969. Direct in situ measurements of wave propagation in the neutral thermosphere. Journ. Geophys. Res., vol. 74, pp. 183-196.

NICOLET, M.

1961. Density of the heterosphere related to temperature. Smithsonian Astrophys. Obs. Spec. Rep. No. 75, 30 pp.

1963. La constitution et la composition de l'atmosphère supérieure. In Geophysics, The Earth's Environment, ed. by C. DeWitt, J. Hieblot, and A. Lebeau, pp. 201-277, Gordon and Breach, Science Publishers, New York.

REBER, C. A., and NICOLET, M.

1965. Investigation of the major constituents of the April-May 1963 heterosphere by the Explorer XVII satellite. Planet. Space Sci., vol. 13, pp. 617-646.

REID, R. H. G., and WITHBROE, G. L.

1970. The density and vibrational distribution of molecular oxygen in the lower thermosphere. Planet. Space Sci., vol. 18, pp. 1255-1265.

RISHBETH, H.

1969. On the phase of the diurnal bulge in the thermosphere. Ann. de Géophys., vol. 25, pp. 495-498.

ROEMER, M.

1968. Reaction time of the upper atmosphere within the 27-day variation. Forschungsberichte der Astronomischen Institute, Bonn, 68-08, 29 pp.

1971. Dichteschwankungen der Hochatmosphäre während geomagnetischer Störungen im Höhenbereich 250 bis 800 km. Veröff Astr. Inst. Bonn (in press).

SCHAEFER, E. J.

1966. Neutral composition. Univ. of Michigan, High Altitude Engineering Lab., Sci. Rep. 05627-3-S, February.

SCHUSTERMAN, L.

1970. Evaluation of low-altitude satellite density data. Aerospace Corp., Aerospace Rep. No. TDR-0059(6755)-1, pp. 1-139, July.

SHEFOV, N. N.

1968. Twilight helium emission during low and high geomagnetic activity. Planet. Space Sci., vol. 16, pp. 1103-1107.

SMITH, L. B.

1968. An observation of strong thermospheric winds during a geomagnetic storm. Journ. Geophys. Res., vol. 73, pp. 4959-4963.

SPENCER, N. W., TAEUSCH, D. R., and CARIGNAN, G. R.

1966. N_2 temperature and density data for the 150 to 300 km region and their implications. Ann. de Géophys., vol. 22, pp. 151-160.

TAEUSCH, D. R., NIEMANN, H. B., CARIGNAN, G. R., SMITH, R. E., and BALLANCE, J. O.

1968. Diurnal survey of the thermosphere (1) neutral particle results. In Space Research VIII, ed. by A. P. Mitra, L. G. Jacchia, and W. S. Newman, pp. 930-939, North-Holland Publ. Co., Amsterdam.

TINSLEY, B. A.

1968. Measurements of twilight helium 10,830 Å emission. Planet. Space Sci., vol. 16, pp. 91-99.

1970. Variations of Balmer-a emission and related hydrogen distributions. In Space Research X, ed. by T. M. Donahue, P. A. Smith, and L. Thomas, pp. 582-601, North-Holland Publ. Co., Amsterdam.

VON ZAHN, U.

1967. Mass spectrometric measurements of atomic oxygen in the upper atmosphere: A critical review. Journ. Geophys. Res., vol. 72, pp. 5933-5937.

1970. Neutral air density and composition at 150 kilometers. Journ. Geophys. Res., vol. 75, pp. 5517-5527.

WALDTEUFEL, P.

1970. Une étude par diffusion incohérente de la haute atmosphère neutre. Faculté des Sciences de Paris; Thèse de doctorat d'état ès sciences physiques, 253 pp.

ZIRM, R. R.

1964. Variations in decay rate of satellite 1963-21. Journ. Geophys. Res., vol. 69, pp. 4696-4697.

Table 1. Ratio of the local temperature T_ℓ to the global minimum temperature T_c as a function of L.S.T. and of latitude (ϕ). All ratios have been multiplied by 1000 to eliminate the decimal point.

		$\delta_\odot = +23.44$																							
		L.S.T.																							
ϕ	0	1	2	3	4	5	6	7	8	9	10	11	12	13	14	15	16	17	18	19	20	21	22	23	
90	1202	1202	1202	1202	1202	1202	1202	1202	1202	1202	1202	1202	1202	1202	1202	1202	1202	1202	1202	1202	1202	1202	1202		
75	1166	1164	1163	1163	1163	1163	1163	1163	1163	1163	1163	1163	1163	1163	1163	1163	1163	1163	1163	1163	1163	1163	1163		
60	1129	1124	1123	1122	1123	1124	1123	1124	1123	1124	1123	1124	1123	1124	1123	1124	1123	1124	1123	1124	1123	1124	1123		
45	1093	1087	1085	1085	1085	1085	1089	1099	1116	1141	1172	1206	1238	1264	1282	1288	1284	1270	1248	1222	1194	1167	1142	1104	
30	1062	1055	1052	1052	1053	1057	1069	1120	1157	1198	1238	1270	1291	1299	1293	1276	1250	1219	1185	1151	1121	1096	1076	1056	
15	1038	1030	1026	1026	1027	1032	1045	1068	1101	1142	1188	1231	1266	1289	1298	1292	1273	1245	1210	1172	1136	1102	1074	1053	
0	1021	1013	1009	1009	1010	1015	1028	1052	1086	1128	1174	1218	1254	1277	1286	1280	1261	1232	1196	1158	1121	1087	1058	1036	
-15	1012	1004	1001	1001	1001	1002	1007	1019	1042	1074	1114	1157	1199	1233	1256	1264	1259	1240	1213	1179	1143	1107	1075	1048	1027
-30	1011	1004	1001	1001	1001	1006	1017	1036	1065	1100	1139	1176	1206	1226	1234	1229	1213	1188	1158	1126	1095	1066	1042	1023	
-45	1016	1010	1008	1008	1008	1012	1021	1037	1060	1089	1120	1150	1175	1191	1197	1193	1180	1160	1136	1110	1084	1061	1041	1026	
-60	1029	1025	1024	1023	1024	1026	1033	1044	1060	1081	1103	1124	1142	1153	1158	1153	1151	1145	1131	1114	1096	1078	1061	1047	
-75	1051	1049	1048	1048	1048	1050	1053	1059	1067	1078	1089	1100	1109	1115	1118	1116	1111	1104	1095	1076	1068	1060	1057	1055	
-90	1080	1080	1080	1080	1080	1080	1080	1080	1080	1080	1080	1080	1080	1080	1080	1080	1080	1080	1080	1080	1080	1080	1080		

		$\delta_\odot = +20^\circ$																							
		L.S.T.																							
ϕ	0	1	2	3	4	5	6	7	8	9	10	11	12	13	14	15	16	17	18	19	20	21	22	23	
90	1193	1193	1193	1193	1193	1193	1193	1193	1193	1193	1193	1193	1193	1193	1193	1193	1193	1193	1193	1193	1193	1193	1193		
75	1157	1154	1154	1153	1154	1155	1155	1159	1165	1175	1186	1199	1211	1221	1228	1230	1229	1223	1215	1205	1195	1184	1175	1161	
60	1120	1115	1114	1113	1114	1114	1117	1124	1136	1154	1177	1201	1225	1244	1257	1262	1258	1248	1232	1213	1193	1173	1155	1128	
45	1085	1079	1077	1076	1077	1077	1081	1091	1109	1134	1166	1200	1233	1260	1281	1278	1285	1280	1266	1244	1217	1188	1160	1135	1097
30	1056	1048	1045	1045	1046	1051	1063	1084	1115	1153	1195	1235	1268	1289	1297	1292	1274	1248	1215	1181	1147	1116	1090	1070	1070
15	1033	1025	1022	1021	1022	1028	1041	1064	1098	1140	1186	1230	1267	1290	1299	1293	1274	1245	1209	1177	1133	1099	1071	1048	1048
0	1019	1010	1007	1006	1013	1026	1050	1085	1128	1175	1220	1257	1281	1290	1284	1264	1234	1198	1159	1121	1086	1057	1034	1034	1034
-15	1012	1004	1001	1000	1001	1006	1019	1042	1075	1116	1161	1203	1238	1262	1270	1264	1246	1217	1183	1146	1109	1076	1048	1027	1027
-30	1012	1004	1002	1001	1002	1007	1018	1048	1068	1104	1144	1182	1213	1234	1262	1220	1194	1164	1131	1098	1069	1044	1025	1025	1025
-45	1019	1013	1011	1010	1011	1015	1024	1041	1064	1094	1127	1158	1193	1200	1206	1202	1188	1168	1143	1116	1089	1065	1045	1029	1029
-60	1034	1030	1029	1028	1029	1031	1038	1050	1067	1088	1111	1133	1151	1162	1164	1154	1140	1122	1103	1084	1067	1053	1042	1042	1042
-75	1058	1056	1055	1055	1056	1056	1066	1075	1086	1097	1109	1118	1124	1127	1125	1120	1112	1103	1093	1084	1075	1068	1062	1062	1062
-90	1088	1088	1088	1088	1088	1088	1088	1088	1088	1088	1088	1088	1088	1088	1088	1088	1088	1088	1088	1088	1088	1088	1088	1088	

Table 1 (Cont.)

		$\delta_{\odot} = +10^\circ$		$\delta_{\odot} = 0^\circ$		$\delta_{\odot} = -10^\circ$																		
		L.S.T.		L.S.T.		L.S.T.																		
ϕ	0	1	2	3	4	5	6	7	8	9	10	11	12	13	14	15	16	17	18	19	20	21	22	23
90	1167	1167	1167	1167	1167	1167	1167	1167	1167	1167	1167	1167	1167	1167	1167	1167	1167	1167	1167	1167	1167	1167	1167	1167
75	1130	1128	1127	1127	1128	1132	1139	1149	1161	1174	1186	1197	1204	1206	1204	1199	1191	1180	1169	1159	1149	1141	1134	1130
60	1095	1090	1089	1088	1089	1092	1099	1112	1131	1154	1204	1224	1238	1228	1242	1234	1192	1171	1150	1131	1115	1103	1101	1076
45	1064	1058	1055	1055	1056	1060	1070	1088	1114	1147	1163	1217	1245	1270	1266	1251	1228	1200	1171	1142	1115	1093	1076	1075
30	1040	1032	1029	1028	1029	1034	1047	1069	1101	1140	1184	1225	1259	1292	1290	1284	1246	1238	1205	1169	1134	1102	1075	1054
15	1023	1014	1011	1010	1011	1031	1055	1090	1134	1162	1228	1265	1290	1293	1273	1242	1202	1177	1137	1109	1101	1062	1039	1030
0	1014	1005	1002	1001	1002	1008	1022	1028	1129	1177	1224	1264	1288	1297	1291	1279	1239	1201	1161	1121	1084	1054	1030	1028
-15	1013	1004	1001	1000	1001	1007	1020	1044	1079	1122	1169	1214	1251	1275	1285	1278	1259	1229	1192	1153	1115	1080	1051	1028
-30	1017	1010	1007	1006	1007	1012	1024	1046	1077	1116	1158	1198	1232	1262	1256	1278	1252	1221	1179	1144	1109	1078	1052	1031
-45	1030	1024	1022	1021	1022	1045	1048	1079	1111	1145	1179	1202	1224	1230	1226	1211	1189	1162	1134	1106	1080	1058	1039	1028
-60	1052	1047	1045	1046	1048	1055	1068	1086	1109	1133	1157	1176	1189	1193	1190	1180	1164	1125	1105	1087	1071	1060	1049	1038
-75	1080	1077	1077	1076	1077	1078	1082	1088	1109	1122	1134	1144	1151	1153	1152	1146	1138	1128	1118	1108	1098	1084	1073	1063
-90	1113	1113	1113	1113	1113	1113	1113	1113	1113	1113	1113	1113	1113	1113	1113	1113	1113	1113	1113	1113	1113	1113	1113	1113

Table 1 (Cont.)

		$\delta_{\odot} = -20^{\circ}$																							
		L.S.T.																							
ϕ	0	1	2	3	4	5	6	7	8	9	10	11	12	13	14	15	16	17	18	19	20	21	22	23	
90	1088	1088	1088	1088	1088	1088	1088	1088	1088	1088	1088	1088	1088	1088	1088	1088	1088	1088	1088	1088	1088	1088	1088		
75	1058	1056	1055	1055	1055	1055	1056	1060	1066	1075	1086	1097	1109	1118	1124	1127	1125	1120	1112	1103	1093	1084	1075	1068	
60	1034	1030	1029	1028	1029	1031	1038	1050	1067	1088	1111	1133	1151	1162	1167	1164	1154	1140	1122	1103	1084	1067	1053	1042	
45	1019	1013	1011	1010	1011	1015	1024	1041	1064	1094	1127	1158	1183	1200	1206	1202	1188	1168	1143	1116	1089	1065	1045	1029	
30	1012	1004	1002	1001	1002	1001	1007	1018	1038	1068	1104	1144	1182	1213	1234	1242	1236	1220	1194	1164	1131	1098	1069	1044	
15	1012	1004	1001	1000	1001	1006	1019	1042	1075	1116	1161	1203	1238	1262	1270	1264	1246	1217	1183	1146	1109	1076	1046	1027	
0	1019	1010	1007	1006	1007	1013	1026	1050	1085	1128	1175	1220	1257	1281	1290	1284	1264	1234	1198	1159	1121	1086	1057	1034	
-15	1033	1025	1021	1022	1028	1041	1064	1098	1140	1186	1230	1267	1290	1299	1293	1274	1245	1209	1171	1133	1099	1071	1048		
-30	1056	1048	1045	1045	1046	1051	1063	1084	1115	1153	1195	1235	1268	1289	1292	1274	1248	1215	1181	1147	1116	1090	1070		
-45	1085	1079	1077	1077	1076	1081	1091	1109	1134	1166	1200	1233	1260	1276	1285	1280	1266	1244	1217	1188	1160	1135	1113	1097	
-60	1120	1115	1114	1113	1114	1117	1124	1136	1154	1177	1201	1225	1244	1257	1262	1258	1248	1232	1213	1193	1173	1155	1140	1128	
-75	1157	1154	1154	1153	1154	1155	1159	1165	1175	1186	1199	1211	1221	1228	1230	1229	1223	1215	1205	1195	1195	1184	1175	1161	
-90	1193	1193	1193	1193	1193	1193	1193	1193	1193	1193	1193	1193	1193	1193	1193	1193	1193	1193	1193	1193	1193	1193	1193		
		$\delta_{\odot} = -23^{\circ}44'$																							
		L.S.T.																							
ϕ	0	1	2	3	4	5	6	7	8	9	10	11	12	13	14	15	16	17	18	19	20	21	22	23	
90	1080	1080	1080	1080	1080	1080	1080	1080	1080	1080	1080	1080	1080	1080	1080	1080	1080	1080	1080	1080	1080	1080	1080		
75	1051	1049	1048	1048	1048	1048	1049	1053	1059	1067	1076	1089	1100	1109	1115	1115	1118	1118	1111	1104	1093	1085	1076	1060	
60	1029	1025	1024	1023	1023	1024	1024	1026	1033	1044	1060	1081	1103	1124	1142	1153	1156	1156	1145	1131	1114	1096	1081	1067	
45	1016	1010	1008	1008	1008	1008	1008	1008	1012	1021	1037	1060	1089	1100	1115	1115	1117	1117	1109	1106	1103	1091	1077		
30	1011	1004	1001	1001	1001	1001	1001	1006	1017	1036	1065	1100	1139	1176	1206	1226	1234	1229	1213	1188	1158	1126	1095	1066	
15	1012	1004	1001	1001	1002	1007	1019	1042	1074	1114	1157	1199	1233	1256	1264	1259	1240	1213	1179	1143	1107	1075	1048	1027	
0	1021	1013	1009	1009	1010	1015	1028	1052	1086	1128	1174	1218	1254	1277	1286	1280	1261	1232	1196	1158	1121	1087	1058	1036	
-15	1039	1030	1026	1026	1027	1032	1045	1068	1101	1142	1188	1231	1266	1289	1298	1299	1292	1273	1245	1210	1172	1136	1102	1074	1053
-30	1062	1055	1052	1052	1053	1057	1069	1120	1157	1198	1238	1270	1291	1293	1276	1250	1219	1185	1151	1121	1096	1076			
-45	1093	1087	1085	1085	1085	1089	1099	1116	1141	1172	1206	1238	1264	1282	1290	1270	1248	1222	1194	1167	1142	1121	1104		
-60	1129	1124	1123	1122	1123	1126	1133	1145	1163	1185	1209	1232	1251	1263	1268	1254	1239	1220	1201	1181	1163	1148	1137		
-75	1166	1164	1163	1163	1164	1164	1168	1174	1184	1195	1208	1219	1229	1236	1238	1237	1231	1223	1214	1203	1193	1184	1176	1170	
-90	1202	1202	1202	1202	1202	1202	1202	1202	1202	1202	1202	1202	1202	1202	1202	1202	1202	1202	1202	1202	1202	1202	1202		

Table 2a. Temperature increment ΔT as a function of the geomagnetic index K_p when equation (18) is used (ΔT lags behind K_p by 6.7 hours).

K_p	ΔT	K_p	ΔT	K_p	ΔT
0_0	0°	3_0	85°	6_0	180°
$0+$	9	$3+$	94	$6+$	194
$1-$	19	$4-$	104	$7-$	210
1_0	28	4_0	114	7_0	229
$1+$	37	$4+$	124	$7+$	251
$2-$	47	$5-$	134	$8-$	279
2_0	56	5_0	145	8_0	313
$2+$	66	$5+$	156	$8+$	358
$3-$	75	$6-$	167	$9-$	417
				9_0	495

Table 2b. Temperature increment ΔT and simultaneous density increment $\Delta \log_{10} \rho$ when equations (20) are used (ΔT and $\Delta \log_{10} \rho$ lag behind K_p by 6.7 hours).

K_p	ΔT	$\Delta \log_{10} \rho$	K_p	ΔT	$\Delta \log_{10} \rho$	K_p	ΔT	$\Delta \log_{10} \rho$
0_0	0°	0.000	3_0	42°	0.036	6_0	92°	0.077
$0+$	5	0.004	$3+$	47	0.040	$6+$	100	0.083
$1-$	9	0.008	$4-$	52	0.044	$7-$	109	0.089
1_0	14	0.012	4_0	57	0.049	7_0	120	0.097
$1+$	19	0.016	$4+$	62	0.053	$7+$	133	0.106
$2-$	23	0.020	$5-$	67	0.057	$8-$	150	0.118
2_0	28	0.024	5_0	73	0.062	8_0	172	0.132
$2+$	33	0.028	$5+$	79	0.066	$8+$	200	0.150
$3-$	38	0.032	$6-$	85	0.071	$9-$	237	0.174
						9_0	288	0.205

Table 3. Tables for the computation of the semiannual density variation
 $\Delta \log_{10} \rho = f(z) g(t)$.

a) Table of $f(z)$

z (km)	$f(z)$	z (km)	$f(z)$	z (km)	$f(z)$
100	0.068	500	0.289	900	0.347
150	0.086	550	0.309	950	0.341
200	0.112	600	0.326	1000	0.332
250	0.142	650	0.338	1050	0.322
300	0.174	700	0.347	1100	0.311
350	0.207	750	0.351	1150	0.298
400	0.237	800	0.353	1200	0.285
450	0.265	850	0.351		

b) Table of $g(t)$

Date	$g(t)$	Date	$g(t)$	Date	$g(t)$	Date	$g(t)$
Jan. 11	-0.145	Apr. 1	+0.354	June 30	-0.417	Sept. 28	+0.226
11	-0.184	11	+0.353	July 10	-0.478	Oct. 8	+0.365
21	-0.183	21	+0.303	20	-0.515	18	+0.452
31	-0.146	May 1	+0.216	30	-0.519	28	+0.478
Feb. 10	-0.081	11	+0.106	Aug. 9	-0.485	Nov. 7	+0.447
20	+0.008	21	-0.013	19	-0.405	17	+0.365
Mar. 2	+0.113	31	-0.130	29	-0.281	27	+0.249
12	+0.219	June 10	-0.239	Sept. 8	-0.122	Dec. 7	+0.118
22	+0.306	20	-0.336	18	+0.056	17	-0.007
						27	-0.107

Table 4. Tables for the seasonal-latitudinal density variation
 $\Delta \log_{10} \rho = SP \sin^2 \phi$.

a) Table of the maximum half-range $S = 0.014(z - 90) \exp [-0.0013(z - 90)^2]$

z (km)	S	z (km)	S	z (km)	S
90	0.000	120	0.130	150	0.008
95	0.068	125	0.100	155	0.004
100	0.123	130	0.070	160	0.002
105	0.157	135	0.045	165	0.001
110	0.166	140	0.027	170	0.000
115	0.155	145	0.015		

b) Table of the phase $P = \sin(2\pi\Phi + 1.72)^*$

Day	P	Day	P	Day	P	Day	P
Jan. 1	± 0.989	Apr. 1	∓ 0.129	June 30	∓ 0.994	Sept. 28	± 0.086
11	± 0.948	11	∓ 0.297	July 10	∓ 0.961	Oct. 8	± 0.255
21	± 0.880	21	∓ 0.456	20	∓ 0.900	18	± 0.417
31	± 0.786	May 1	∓ 0.602	30	∓ 0.812	20	± 0.567
Feb. 10	± 0.668	11	∓ 0.730	Aug. 9	∓ 0.699	Nov. 7	± 0.699
20	± 0.531	21	∓ 0.836	19	∓ 0.567	17	± 0.812
Mar. 2	± 0.378	31	∓ 0.918	29	∓ 0.417	27	± 0.900
12	± 0.214	June 10	∓ 0.972	Sept. 8	∓ 0.255	Dec. 7	± 0.961
22	± 0.043	20	∓ 0.998	18	∓ 0.086	17	± 0.994
						27	± 0.998

*Take the upper sign for the Northern Hemisphere, the lower for the Southern Hemisphere.

c) Table of $\sin^2 \phi$

ϕ	$\sin^2 \phi$	ϕ	$\sin^2 \phi$	ϕ	$\sin^2 \phi$
0°	0.000	30°	0.250	60°	0.750
5	0.008	35	0.329	65	0.821
10	0.030	40	0.413	70	0.883
15	0.067	45	0.500	75	0.933
20	0.117	50	0.587	80	0.970
25	0.179	55	0.671	85	0.992
				90	1.000

Table 5. Seasonal-latitudinal variations of helium (correction to tabular helium concentrations
 $\Delta \log_{10} n(\text{He})$ according to equation (25)).

Date		Latitude										
		-90	-80	-70	-60	-50	-40	-30	-20	-10	0	10
JAN 1	*.226	-.223	-.215	-.200	-.178	-.146	-.105	-.056	.000	.061	.125	.189
JAN 11	-.215	-.214	-.212	-.204	-.191	-.169	-.139	-.100	-.053	.000	.058	.119
JAN 21	-.197	-.196	-.194	-.174	-.155	-.127	-.092	-.049	-.043	.000	.053	.109
JAN 31	-.172	-.172	-.170	-.164	-.153	-.136	-.111	-.080	-.043	.000	.047	.096
FEB 10	-.143	-.143	-.141	-.141	-.136	-.127	-.112	-.092	-.067	-.036	.000	.039
FEB 20	-.110	-.109	-.108	-.104	-.097	-.086	-.071	-.051	-.027	-.000	.030	.061
MAR 2	-.073	-.073	-.072	-.070	-.065	-.058	-.047	-.034	-.018	-.000	.020	.041
MAR 12	-.035	-.035	-.034	-.034	-.028	-.028	-.023	-.016	-.009	.000	.010	.020
MAR 22	-.006	-.006	-.006	-.005	-.005	-.004	-.003	-.002	-.001	.000	-.001	-.002
APR 1	.076	.075	.071	.065	.056	.046	.035	.023	.011	.000	-.010	-.019
APR 11	.144	.142	.134	.122	.106	.087	.066	.044	.021	.000	-.020	-.037
APR 21	.208	.204	.194	.176	.153	.126	.095	.063	.031	.000	-.028	-.053
MAY 1	.266	.262	.248	.226	.196	.161	.122	.081	.040	.000	-.036	-.068
MAY 11	.317	.312	.295	.269	.234	.192	.145	.096	.047	.000	-.043	-.081
MAY 21	.359	.353	.334	.304	.265	.217	.164	.109	.053	.000	-.049	-.092
MAY 31	.391	.384	.364	.331	.288	.236	.179	.119	.058	.000	-.053	-.100
JUN 10	.411	.404	.383	.349	.303	.249	.188	.125	.061	.000	-.056	-.105
JUN 20	.420	.413	.391	.356	.309	.254	.192	.127	.062	.000	-.057	-.107
JUN 30	.416	.409	.387	.353	.307	.252	.191	.126	.062	.000	-.057	-.106
JUL 10	.400	.393	.372	.339	.295	.242	.183	.121	.059	.000	-.054	-.102
JUL 20	.373	.366	.347	.316	.275	.225	.171	.113	.055	.000	-.051	-.102
JUL 30	.335	.329	.312	.284	.247	.203	.153	.102	.050	.000	-.046	-.095
AUG 9	.288	.283	.268	.244	.212	.174	.132	.087	.043	.000	-.039	-.073
AUG 19	.233	.229	.217	.198	.172	.141	.107	.071	.035	.000	-.032	-.060
AUG 29	.172	.169	.161	.146	.127	.104	.079	.052	.026	.000	-.023	-.044
SEP 8	.107	.105	.100	.091	.079	.065	.049	.032	.016	.000	-.015	-.027
SEP 18	.039	.038	.036	.033	.028	.023	.018	.012	.006	.000	-.005	-.010
SEP 28	-.017	-.017	-.017	-.016	-.015	-.013	-.011	-.008	-.004	.000	-.005	-.014
OCT 8	-.055	-.055	-.054	-.052	-.049	-.043	-.035	-.026	-.014	.000	-.015	-.030
OCT 18	-.092	-.091	-.090	-.087	-.081	-.072	-.059	-.043	-.023	.000	-.025	-.051
OCT 28	-.126	-.126	-.124	-.120	-.112	-.099	-.082	-.059	-.031	.000	-.034	-.070
NOV 7	-.157	-.157	-.155	-.150	-.140	-.124	-.102	-.073	-.039	.000	-.043	-.087
NOV 17	-.184	-.184	-.182	-.175	-.164	-.145	-.119	-.086	-.046	.000	-.050	-.102
NOV 27	-.205	-.205	-.203	-.196	-.183	-.162	-.133	-.096	-.051	.000	-.056	-.114
DEC 7	-.221	-.221	-.218	-.210	-.196	-.174	-.143	-.103	-.055	.000	-.060	-.122
DEC 17	-.229	-.229	-.228	-.225	-.217	-.203	-.180	-.148	-.057	.000	-.062	-.127
DEC 27	-.229	-.229	-.226	-.223	-.218	-.203	-.180	-.148	-.057	.000	-.062	-.127

Table 6. Atmospheric temperature, density, and composition as functions of height and exospheric temperature.
EXOSPHERIC TEMPERATURE = 500 DEGREES

HEIGHT KM	TEMP DEG K	LOG N(ν2) /CM ³	LOG N(O) /CM ³	LOG N(A) /CM ³	LOG N(He) /CM ³	MEAN MOL WT	DENSITY HT KM	DENSITY GM/CM ³	LOG DEN GM/CM ³
90.0	183.0	13.7498	13.1687	11.8225	8.6457	28.83	5.46	3.460E-09	-8.461
92.0	183.1	13.5902	12.9446	12.0536	11.6680	8.4861	28.63	2.396E-09	-8.621
94.0	183.7	13.4302	12.8138	12.1530	11.5080	8.3262	28.37	1.658E-09	-8.780
96.0	184.8	13.2708	12.6300	12.1696	11.1668	8.1668	28.09	5.47	-8.940
98.0	186.6	13.1129	12.4487	12.1268	11.1907	8.0089	27.84	5.54	-9.098
100.0	189.2	12.9571	12.2734	12.0446	11.0349	7.8531	27.64	5.60	-9.254
102.0	192.7	12.8035	12.0990	11.9534	10.8192	7.8274	27.43	5.65	-9.408
104.0	197.2	12.6509	11.9261	11.8620	10.6059	7.8008	27.21	5.74	-9.561
106.0	202.6	12.5001	11.7555	11.7707	10.3958	7.7736	26.97	5.85	-9.711
108.0	209.1	12.3515	11.5878	11.6891	10.1898	7.7459	26.73	5.98	-9.858
110.0	216.6	12.2059	11.4236	11.5903	9.9886	7.7178	26.47	6.15	-10.001
115.0	239.4	11.8576	11.0319	11.3728	9.5105	7.6473	25.79	6.70	-10.440
120.0	267.1	11.5363	10.6716	11.1688	9.0725	7.5786	25.10	7.44	-10.648
125.0	297.8	11.2443	10.3448	10.9818	8.6762	7.5144	24.41	8.37	-10.924
130.0	328.3	10.9815	10.0507	10.8135	8.3195	7.4566	23.74	9.49	-11.168
135.0	355.9	10.7453	9.7859	10.6637	7.9976	7.4062	23.11	10.75	-11.383
140.0	378.8	10.5311	9.5297	10.5297	7.7038	7.3626	22.51	12.02	-11.574
145.0	397.3	10.3337	9.3225	10.4081	7.4311	7.3224	21.94	13.23	-11.746
150.0	411.9	10.1487	9.1134	10.2956	7.1739	7.2906	21.39	14.34	-11.903
155.0	423.6	9.9728	8.9142	10.1900	6.9283	7.2597	20.88	15.36	-12.049
160.0	433.1	9.8037	8.7225	10.0893	6.6913	7.2310	20.40	16.29	-12.187
170.0	447.4	9.4802	8.3550	8.0022	9.7172	7.1780	19.53	17.97	-12.440
180.0	457.7	9.1702	8.0022	5.9980	7.1290	18.78	19.47	2.128E-13	-12.672
190.0	465.4	8.8694	7.6597	5.5423	5.3722	7.0826	18.15	20.83	-12.887
200.0	471.4	8.5755	7.3247	9.3720	4.9554	7.0379	17.62	22.06	-13.090
210.0	476.2	8.2868	6.9956	9.2053	4.5456	6.9946	17.17	23.16	-13.282
220.0	480.1	8.0025	6.6713	9.0414	4.1417	6.9522	16.79	24.14	-13.466
230.0	483.3	7.7421	6.3510	8.8798	3.7425	6.9108	16.44	25.00	-13.794
240.0	485.9	7.4439	6.0241	3.3474	6.8699	16.12	25.75	1.537E-14	-13.813
250.0	488.1	7.1688	5.7201	8.5621	2.9559	6.8297	15.79	26.40	-13.980
260.0	489.9	6.8959	5.4086	8.4056	2.5675	6.7899	15.43	26.98	-14.143
270.0	491.4	6.6251	5.0994	8.2563	2.1818	6.7500	15.03	27.49	-14.302
280.0	492.7	6.3560	4.7922	8.0962	1.7986	6.7116	14.55	27.96	-14.459
290.0	493.7	6.0885	4.4868	7.9430	1.4175	6.6730	13.98	28.41	-14.613
300.0	494.6	5.8225	4.1831	7.7908	1.0386	6.6346	13.29	28.86	-14.764
310.0	495.4	5.5579	3.8809	7.6294	•6614	6.5965	12.49	29.33	1.220E-15
320.0	496.0	5.2945	3.5801	7.4887	•2861	6.5586	11.57	29.84	-14.914
330.0	496.5	5.0323	3.2807	7.3388	6.5209	6.4834	10.54	30.44	-15.061
340.0	496.9	4.7712	2.9825	7.1895	6.4461	6.4834	9.45	31.15	-15.346
350.0	497.3	4.5111	2.6855	7.0408	6.4461	8.33	8.33	32.03	-15.483
360.0	497.6	4.2521	2.3896	6.8927	6.4089	7.23	33.14	2.417E-16	-15.617
370.0	497.9	3.9940	2.0948	6.7452	6.3720	6.20	34.55	1.798E-16	-15.745
380.0	498.2	3.7369	1.8011	6.5912	6.3351	5.28	36.36	1.256E-16	-15.868
390.0	498.4	3.4806	1.5084	6.4518	6.2984	4.48	38.69	1.038E-16	-15.984
400.0	498.5	3.2252	1.2168	6.3059	6.2619	3.81	41.68	8.090E-17	-16.092

Table 6 (Cont.)

EXOSPHERIC TEMPERATURE = 500 DEGREES

HEIGHT KM	TEMP DEG K	LOG N(N2) /CM3	LOG N(O2) /CM3	LOG N(O) /CM3	LOG N(A) /CM3	LOG N(H) /CM3	LOG N(H) /CM3	MEAN MOL WT	DENSITY HT KM	SCALE HT KM	DENSITY GM/CM3	LOG DEN GM/CM3
420.0	498.8	2.7170	.6363	6.0155	6.1891	2.82	5.215E-17	-16.283				
440.0	499.1	2.2222	.0596	5.7271	6.1169	2.19	64.17	3.661E-17	-16.436			
460.0	499.2	1.7105		5.4405	6.0451	1.81	84.64	2.787E-17	-16.555			
480.0	499.4	1.2119		5.1557	5.9739	1.58	112.51	2.269E-17	-16.644			
500.0	499.5	.7164		5.2119	5.9030	1.44	146.52	1.942E-17	-16.712			
520.0	499.5	.2239		4.8727	5.8326	1.35	183.33	1.719E-17	-16.765			
540.0	499.6	4.3117		4.5914	5.8420	1.29	219.04	1.556E-17	-16.808			
560.0	499.7	4.0337		4.3117	5.7626	1.25	250.92	1.429E-17	-16.845			
580.0	499.7	3.7574		4.3117	6.0243	1.21	278.14	1.325E-17	-16.878			
600.0	499.8	3.4827		4.3117	6.7893	1.19	301.08	1.237E-17	-16.908			
620.0												
640.0												
660.0												
680.0												
700.0												
720.0												
740.0												
760.0												
780.0												
800.0												
820.0												
840.0												
860.0												
880.0												
900.0												
920.0												
940.0												
960.0												
980.0												
1000.0												
1050.0												
1100.0												
1150.0												
1200.0												
1250.0												
1300.0												
1350.0												
1400.0												
1450.0												
1500.0												
1600.0												
1700.0												
1800.0												
1900.0												
2000.0												
2100.0												
2200.0												
2300.0												
2400.0												
2500.0												

Table 6 (Cont.)

EXOSPHERIC TEMPERATURE = 600 DEGREES

HEIGHT KM	TEMP DEG K	LOG N(N2) /CM3	LOG N(O2) /CM3	LOG N(O) /CM3	LOG N(A) /CM3	LOG N(He) /CM3	MEAN MOL WT	DENSITY SCALE HT KM	DENSITY GM/CM3	LOG DEN GM/CM3
90.0	183.0	13.7498	13.1687	11.8225	11.8276	8.6457	28.83	5.46	3.460E-09	-8.461
92.0	183.0	13.5901	12.9945	12.0536	11.6679	8.4861	28.63	5.43	2.396E-09	-8.821
94.0	183.0	13.6299	12.8135	12.1527	11.5077	8.3259	28.37	5.42	1.657E-09	-8.781
96.0	185.2	13.2702	12.6294	12.1690	11.3480	8.1661	28.09	5.46	1.17E-09	-8.441
98.0	187.4	13.1119	12.4477	12.1257	11.1897	8.0079	27.84	5.52	7.965E-10	-9.099
100.0	190.5	12.9556	12.2719	12.0431	11.0334	7.8516	27.64	5.58	5.558E-10	-9.555
102.0	194.8	12.8017	12.0973	11.9510	10.8179	7.8250	27.43	5.64	3.892E-10	-9.410
104.0	200.2	12.6489	11.9246	11.8587	10.6052	7.7975	27.21	5.74	2.738E-10	-9.563
106.0	206.8	12.4983	11.7665	10.3964	7.7694	26.98	5.86	1.939E-10	-9.713	
108.0	214.7	12.3503	11.5878	11.6751	10.1923	7.7404	26.74	6.01	1.388E-10	-9.859
110.0	223.8	12.2057	11.4252	11.5848	9.9937	7.7111	26.49	6.20	9.970E-11	-10.001
115.0	251.5	11.8624	11.0403	11.3670	9.5258	7.6379	6.82	4.612E-11	-10.336	
120.0	285.2	11.5493	10.6904	11.1648	9.1026	7.5671	7.65	2.305E-11	-10.637	
125.0	322.4	11.2683	10.3770	10.9815	8.7246	7.5016	24.58	8.70	1.248E-11	-10.904
130.0	359.6	11.0185	10.0984	10.8184	8.3885	7.4432	23.98	9.95	7.285E-12	-11.138
135.0	393.9	10.7962	9.9501	10.6745	8.0884	7.3926	23.41	11.34	4.549E-12	-11.342
140.0	423.6	10.5967	9.6266	10.5470	7.8172	7.3477	22.87	12.77	3.003E-12	-11.522
145.0	448.2	10.4147	9.4223	10.4325	7.5683	7.3113	22.37	14.16	2.071E-12	-11.604
150.0	468.4	10.2461	9.2325	10.3281	7.3360	7.2781	21.89	15.46	1.478E-12	-11.830
155.0	484.9	10.0876	9.0535	10.2310	7.1163	7.2483	21.43	16.67	1.088E-12	-11.966
160.0	498.6	9.9367	8.8828	10.1397	6.9062	7.2209	20.99	17.77	8.097E-13	-12.092
170.0	519.6	9.6512	8.5593	9.9690	6.5068	7.1716	20.20	19.76	4.753E-13	-12.323
180.0	534.9	9.3810	8.2524	9.8092	6.1268	7.1270	19.49	21.50	2.927E-13	-12.334
190.0	546.6	9.1211	7.9569	9.6568	5.7603	7.0854	18.88	23.09	1.869E-13	-12.728
200.0	555.8	8.8689	7.6698	9.5096	5.4037	7.0459	18.35	24.56	1.229E-13	-12.911
210.0	563.2	8.6225	7.3892	9.3664	5.0547	7.0079	17.90	25.89	8.265E-14	-13.083
220.0	569.2	8.3808	7.1138	9.2264	4.7120	6.9712	17.51	27.12	5.668E-14	-13.247
230.0	574.1	8.1429	6.9426	9.0889	4.3744	6.9354	17.19	28.24	3.950E-14	-13.403
240.0	578.2	7.9083	6.5750	8.9536	4.0411	6.9004	16.91	29.25	2.789E-14	-13.554
250.0	581.6	7.6763	6.3104	8.8200	3.7114	6.8661	16.67	30.15	1.992E-14	-13.701
260.0	584.4	7.4467	6.0484	8.6880	3.3849	6.8323	16.46	30.95	1.436E-14	-13.843
270.0	586.7	7.2192	5.7888	8.5573	3.0611	6.7989	16.26	31.65	1.043E-14	-13.982
280.0	588.7	6.9934	5.5311	8.4277	2.7398	6.7660	16.08	32.28	7.631E-15	-14.117
290.0	590.3	6.7692	5.2752	8.2992	2.4206	6.7334	15.90	32.83	5.613E-15	-14.251
300.0	591.6	6.54465	5.0209	8.1715	2.1034	6.7011	15.72	33.33	4.149E-15	-14.382
310.0	592.8	6.3250	4.7680	8.0447	1.7879	6.6690	15.51	33.79	3.080E-15	-14.511
320.0	593.8	6.1047	4.5165	7.9186	1.4741	6.6372	15.29	34.21	2.295E-15	-14.639
330.0	594.6	5.8856	4.2662	7.7931	1.1618	6.6056	15.04	34.61	1.716E-15	-14.765
340.0	595.3	5.6674	4.0171	7.6683	0.8509	6.5742	14.75	35.01	1.288E-15	-14.890
350.0	595.8	5.4502	3.7691	7.5441	0.5414	6.5430	14.41	35.40	9.694E-16	-15.013
360.0	596.3	5.2339	3.5221	7.4204	0.2331	6.5119	14.01	35.81	7.320E-16	-15.135
370.0	596.8	5.0185	3.2760	7.2972	0.04810	6.4810	13.55	36.24	5.546E-16	-15.256
380.0	597.1	4.8039	3.0309	7.1745	0.4502	6.4502	13.03	36.72	4.216E-16	-15.375
390.0	597.5	4.5900	2.7867	7.0523	0.4195	6.4195	12.44	37.25	3.217E-16	-15.493
400.0	597.7	4.3770	2.5434	6.9306	0.3890	6.3890	11.79	37.86	2.465E-16	-15.608

Table 6 (Cont.)

EXOSPHERIC TEMPERATURE = 600 DEGREES

HEIGHT KM	TEMP DEG K	LOG N(N ₂) /CM ³	LOG N(CO) /CM ³	LOG N(O) /CM ³	LOG N(A) /CM ³	LOG N(H) /CM ³	MEAN MOL WT	DENSITY HT KM	DENSITY GM/CM ³	LOG DEN GM/CM ³	
420.0	598.2	3.9531	2.0593	6.6883	6.3283	10.33	39.39	1.0468E-16	-15.833		
440.0	598.5	3.5321	1.5784	6.4478	6.2280	8.77	41.54	8.945E-17	-16.048		
460.0	598.8	3.1138	1.1006	6.2088	6.2081	7.25	44.60	5.666E-17	-16.251		
480.0	599.0	2.6982	•6259	5.9714	6.1487	5.91	48.97	3.655E-17	-16.437		
500.0	599.2	2.2851	•1541	5.7354	6.0896	6.1258	4.82	55.14	2.466E-17	-16.605	
520.0	599.3	1.8746	5.5009	5.5009	6.0309	6.1109	3.98	63.62	1.772E-17	-16.752	
540.0	599.4	1.4666	5.2678	5.9726	6.0962	3.36	74.84	1.025E-17	-16.878		
560.0	599.5	1.0610	5.0361	5.9146	6.0815	2.92	88.96	1.037E-17	-16.984		
580.0	599.6	•6578	4.8058	5.8569	6.0670	2.60	105.66	8.433E-18	-17.074		
600.0	599.6	•2569	4.5769	5.7996	6.0525	2.37	124.14	7.082E-18	-17.150		
620.0	599.7	4.3493	4.1230	5.7427	6.0381	2.20	143.24	6.096E-18	-17.215		
640.0	599.7	3.8980	3.8980	5.6861	6.0239	2.07	161.88	5.346E-18	-17.272		
660.0	599.7	3.6743	3.6743	5.6298	6.0097	1.97	179.29	4.555E-18	-17.323		
680.0	599.8	3.4519	3.2308	5.5738	5.9956	1.88	195.06	4.273E-18	-17.369		
700.0	599.8	3.2308	3.0109	5.5182	5.9815	1.81	209.19	3.811E-18	-17.412		
720.0	599.8	2.7923	2.7923	5.4628	5.9676	1.74	222.02	3.528E-18	-17.452		
740.0	599.8	2.5749	2.3587	5.4078	5.9537	1.68	233.86	3.231E-18	-17.491		
760.0	599.9	2.3587	2.1438	5.3531	5.9399	1.63	245.04	2.973E-18	-17.527		
780.0	599.9	2.1438	1.9300	5.2987	5.9262	1.58	255.86	2.644E-18	-17.562		
800.0	599.9	1.9300	1.7174	5.1909	5.8990	1.50	266.44	2.542E-18	-17.595		
820.0	599.9	1.5060	1.5060	5.1374	5.8856	1.46	287.80	2.362E-18	-17.627		
840.0	599.9	1.2957	1.0867	5.0842	5.8722	1.43	298.76	2.055E-18	-17.658		
860.0	599.9	1.0867	•8787	5.0313	5.8588	1.40	309.98	1.924E-18	-17.687		
880.0	599.9	•8787	4.9264	4.9877	5.8456	1.37	321.49	1.806E-18	-17.716		
900.0	599.9	4.9264	4.9264	5.8324	5.8324	1.34	333.29	1.699E-18	-17.743		
920.0	599.9	4.8744	4.8744	5.8193	5.8193	1.31	345.40	1.602E-18	-17.770		
940.0	599.9	4.8226	4.6719	5.8063	5.8063	1.29	357.78	1.513E-18	-17.795		
960.0	599.9	4.6663	4.7112	5.7933	5.7933	1.27	370.42	1.432E-18	-17.820		
980.0	600.0	4.6663	4.7200	5.7804	5.7804	1.25	383.29	1.358E-18	-17.844		
1000.0	600.0	4.7200	4.7200	5.7485	5.7485	1.20	416.19	1.199E-18	-17.921		
1050.0	600.0	4.5933	4.5933	5.7170	5.7170	1.17	449.82	1.068E-18	-17.972		
1100.0	600.0	4.4683	4.4683	5.6860	5.6860	1.14	483.51	9.592E-19	-18.018		
1150.0	600.0	4.3450	4.2322	5.6553	5.6553	1.11	516.55	8.980E-19	-18.062		
1200.0	600.0	4.2322	4.1031	5.6251	5.6251	1.10	548.68	7.902E-19	-18.102		
1250.0	600.0	4.1031	3.9846	5.5952	5.5952	1.08	579.42	7.231E-19	-18.141		
1300.0	600.0	3.9846	3.8676	5.5658	5.5658	1.07	608.49	6.648E-19	-18.177		
1350.0	600.0	3.8676	3.7521	5.5367	5.5367	1.06	635.73	6.334E-19	-18.212		
1400.0	600.0	3.7521	3.6381	5.5079	5.5079	1.05	661.23	5.679E-19	-18.246		
1450.0	600.0	3.6381	3.5255	5.4796	5.4796	1.04	684.96	5.273E-19	-18.278		
1500.0	600.0	3.5255	3.3046	5.4240	5.4240	1.03	727.35	4.577E-19	-18.339		
1600.0	600.0	3.0892	3.0892	5.3697	5.3697	1.02	764.43	4.003E-19	-18.398		
1700.0	600.0	2.8791	2.8791	5.3168	5.3168	1.02	797.02	3.522E-19	-18.453		
1800.0	600.0	2.6741	2.6741	5.2652	5.2652	1.02	826.69	3.113E-19	-18.507		
1900.0	600.0	2.4740	2.4740	5.2148	5.2148	1.01	854.12	2.764E-19	-18.558		
2000.0	600.0	2.2786	2.2786	5.1656	5.1656	1.01	879.80	2.463E-19	-18.609		
2100.0	600.0	2.0877	2.0877	5.1175	5.1175	1.01	904.61	2.202E-19	-18.657		
2200.0	600.0	1.9013	1.9013	5.0706	5.0706	1.01	928.71	1.974E-19	-18.705		
2300.0	600.0	1.7192	1.7192	5.0247	5.0247	1.01	952.07	1.775E-19	-18.751		
2400.0	600.0	1.5411	1.5411	4.9799	4.9799	1.01	975.51	1.600E-19	-18.796		

Table 6 (Cont.)

EXOSPHERIC TEMPERATURE = 700 DEGREES

HEIGHT KM	TEMP DEG K	LOG N(N2) /CM3	LOG N(O2) /CM3	LOG N(O) /CM3	LOG N(A) /CM3	LOG N(HE) /CM3	MEAN MOL WT	DENSITY SCALE HT KM	DENSITY GM/CM3	LOG DEN GM/CM3
90.0	183.0	13.7498	13.1687	11.8225	8.6457	28.83	5.46	3.460E-09	-8.461	
92.0	183.2	13.5901	12.9945	12.0535	8.4860	28.63	5.42	2.395E-09	-8.621	
94.0	184.0	13.4297	12.8133	12.1525	8.3257	28.37	5.41	1.656E-09	-8.781	
96.0	185.5	13.2697	12.6288	12.1685	8.1656	28.09	5.45	1.145E-09	-8.941	
98.0	188.0	13.1110	12.4468	12.1248	8.0070	27.84	5.51	7.949E-10	-9.100	
100.0	191.7	12.9564	12.2706	12.0418	11.0322	27.64	5.57	5.542E-10	-9.256	
102.0	196.6	12.8001	12.0959	11.9490	10.8168	27.43	5.64	3.878E-10	-9.411	
104.0	202.8	12.6473	11.9233	11.8559	10.6047	27.22	5.74	2.72E-10	-9.564	
106.0	210.4	12.4967	11.7536	11.7631	10.3968	26.99	5.87	1.932E-10	-9.714	
108.0	219.4	12.3493	11.5877	11.6710	10.1943	26.76	6.04	1.380E-10	-9.860	
110.0	229.9	12.2055	11.4264	11.5802	9.9979	7.7057	26.52	9.961E-11	-10.002	
115.0	261.7	11.8661	11.0468	11.3622	9.5379	7.6303	6.92	4.644E-11	-10.333	
120.0	300.5	11.5593	10.7048	11.1613	9.1259	7.5579	25.29	7.92	2.349E-11	-10.629
125.0	343.2	11.2865	10.4015	10.9807	8.7615	7.4913	24.70	8.96	1.292E-11	-10.889
130.0	386.2	11.0461	10.1341	10.8214	8.4404	7.4325	24.15	10.31	7.675E-12	-11.115
135.0	426.3	10.8336	9.8975	10.6816	8.1557	7.3817	23.63	11.79	4.876E-12	-11.312
140.0	462.0	10.6440	9.6836	10.5584	7.9003	7.3377	23.14	13.34	3.273E-12	-11.485
145.0	492.5	10.4725	9.4939	10.4485	7.6675	7.3002	22.68	14.87	2.296E-12	-11.639
150.0	518.2	10.3149	9.3170	10.3490	7.4521	7.2671	22.24	16.33	1.666E-12	-11.778
155.0	539.7	10.1679	9.1516	10.2575	7.2501	7.2377	21.83	17.71	1.242E-12	-11.906
160.0	557.8	10.0291	8.9952	10.1721	7.0583	7.2110	21.43	18.98	9.456E-13	-12.024
170.0	586.3	9.7695	8.7016	10.0145	6.6972	7.1636	20.70	21.27	5.754E-13	-12.240
180.0	607.5	9.5265	8.4263	9.8692	6.3573	7.1215	20.03	23.28	3.673E-13	-12.435
190.0	623.8	9.2950	8.1635	9.7320	6.0321	7.0830	19.44	25.10	2.430E-13	-12.614
200.0	636.8	9.0718	7.9099	9.6007	5.7177	7.0468	18.92	26.79	1.652E-13	-12.782
210.0	647.3	8.8551	7.6633	9.4739	5.4116	7.0125	18.46	28.33	1.150E-13	-12.939
220.0	655.8	8.6433	7.4222	9.3505	5.1120	6.9795	18.06	29.78	8.148E-14	-13.089
230.0	662.9	8.4357	7.1857	9.2299	4.8180	6.9476	17.71	31.12	5.867E-14	-13.232
240.0	668.7	8.2315	6.9530	9.1117	4.5284	6.9166	17.41	32.36	4.281E-14	-13.368
250.0	673.5	8.0301	6.7234	8.9953	4.2426	6.8863	17.15	33.48	3.160E-14	-13.500
260.0	677.6	7.8312	6.4966	8.8806	3.9600	6.8567	16.92	34.51	2.355E-14	-13.628
270.0	680.9	7.6344	6.2721	8.7673	3.6803	6.8275	16.72	35.45	1.769E-14	-13.752
280.0	683.7	7.4394	6.0496	8.6551	3.4030	6.7988	16.54	36.28	1.339E-14	-13.873
290.0	686.0	7.2460	5.8289	8.5441	3.1278	6.7705	16.38	37.03	1.019E-14	-13.992
300.0	688.0	7.0560	5.6098	8.4339	2.8546	6.7425	16.24	37.71	7.801E-15	-14.108
310.0	689.6	6.8633	5.3921	8.3245	2.5831	6.7147	16.10	38.32	5.996E-15	-14.222
320.0	691.0	6.6738	5.1757	8.2159	2.3131	6.6872	15.96	38.87	4.628E-15	-14.335
330.0	692.2	6.4853	4.9605	8.1079	2.0446	6.6599	15.83	39.37	3.584E-15	-14.446
340.0	693.2	6.2977	4.7463	8.0005	1.7774	6.6329	15.68	39.84	2.784E-15	-14.555
350.0	694.0	6.1111	4.5332	7.8937	1.5114	6.6059	15.53	40.27	2.169E-15	-14.664
360.0	694.8	5.9253	4.3210	7.7874	1.2467	6.5792	15.37	40.68	1.694E-15	-14.771
370.0	695.4	5.7402	4.1097	7.6815	0.9830	6.5526	15.19	41.08	1.322E-15	-14.877
380.0	695.9	5.5560	3.8993	7.5761	0.7204	6.5261	14.99	41.47	1.041E-15	-14.982
390.0	696.4	5.3724	3.6887	7.4712	0.4587	6.4973	14.76	41.87	8.191E-16	-15.087
400.0	696.8	5.1896	3.4809	7.3667	0.1981	6.4735	14.50	42.27	6.458E-16	-15.190

Table 6 (Cont.)

EXOSPHERIC TEMPERATURE = 700 DEGREES

HEIGHT KM	TEMP DEG K	LOG N(N2)		LOG N(O2)		LOG N(A)		LOG N(HE)		LOG N(H)		MEAN MOL WT	DENSITY HT KM	DENSITY GM/CM3	LOG DEN GM/CM3
		/CM3	/CM3	/CM3	/CM3	/CM3	/CM3	/CM3	/CM3	/CM3	/CM3				
420.0	697.4	4.8238	3.0654	7.1588	6.4213	13.89	43.15	4.043E-16	-15.393						
440.0	697.9	4.4647	2.6529	6.9523	6.3695	13.13	44.17	2.557E-16	-15.592						
460.0	698.3	4.1059	2.2431	6.7473	6.3182	12.21	45.43	1.635E-16	-15.786						
480.0	698.6	3.7494	1.8360	6.5437	6.2671	11.16	47.04	1.061E-16	-15.974						
500.0	698.8	3.3952	1.4314	6.3413	6.2165	5.5593	10.02	49.16	6.996E-17	-16.155					
520.0	699.0	3.0432	1.0293	6.1402	6.1661	5.5465	8.86	51.95	4.707E-17	-16.327					
540.0	699.1	2.6933	.6297	5.9403	6.1161	5.5339	7.75	55.65	3.243E-17	-16.489					
560.0	699.3	2.3456	.2325	5.7417	6.0663	5.5213	6.75	60.50	2.966E-17	-16.639					
580.0	699.4	1.9999		5.5442	6.0169	5.5088	5.89	66.76	1.676E-17	-16.776					
600.0	699.5	1.6562		5.3479	5.9678	5.4963	5.19	74.66	1.262E-17	-16.899					
620.0	699.5	1.3146		5.1528	5.9190	5.4840	4.62	84.31	9.803E-18	-17.009					
640.0	699.6	.9750		4.9588	5.8704	5.4718	4.8	95.66	7.844E-18	-17.105					
660.0	699.6	.6373		4.7659	5.8222	5.4596	3.84	108.42	6.445E-18	-17.191					
680.0	699.7			4.5742	5.7742	5.4475	3.58	122.12	5.417E-18	-17.266					
700.0	699.7			4.3836	5.7265	5.4354	3.37	136.11	4.639E-18	-17.334					
720.0	699.7			4.1940	5.6791	5.4235	3.20	149.77	4.033E-18	-17.394					
740.0	699.8			4.0055	5.6319	5.4116	3.07	162.57	3.548E-18	-17.450					
760.0	699.8			3.8181	5.5850	5.3998	2.95	174.19	3.151E-18	-17.502					
780.0	699.8			3.6318	5.5384	5.3880	2.86	184.52	2.819E-18	-17.550					
800.0	699.8			3.4464	5.4920	5.3763	2.77	193.65	2.536E-18	-17.596					
820.0	699.9			3.2622	5.3647	5.3647	2.69	201.64	2.292E-18	-17.640					
840.0	699.9			3.0790	5.4001	5.3532	2.62	208.75	2.079E-18	-17.682					
860.0	699.9			2.8967	5.3545	5.3417	2.55	215.18	1.892E-18	-17.723					
880.0	699.9			2.7155	5.3091	5.303	2.49	221.12	1.726E-18	-17.763					
900.0	699.9			2.5353	5.2641	5.3189	2.42	226.73	1.579E-18	-17.802					
920.0	699.9			2.3561	5.2192	5.3076	2.36	232.14	1.447E-18	-17.840					
940.0	699.9			2.1779	5.1746	5.2964	2.30	237.46	1.329E-18	-17.877					
960.0	699.9			2.0006	5.1303	5.2852	2.25	242.77	1.23E-18	-17.913					
980.0	699.9			1.8243	5.0862	5.2741	2.19	248.15	1.127E-18	-17.948					
1000.0	699.9			1.6490	5.0423	5.2630	2.13	253.64	1.041E-18	-17.983					
1050.0	699.9			1.2149	4.9337	5.2357	2.01	268.11	8.589E-19	-18.066					
1100.0	700.0			0.7865	4.8266	5.2087	1.89	284.09	7.165E-19	-18.145					
1150.0	700.0			0.3639	4.7208	5.1821	1.78	301.83	6.040E-19	-18.219					
1200.0	700.0				4.6165	5.1558	1.68	321.48	5.144E-19	-18.289					
1250.0	700.0				4.5135	5.1299	1.59	343.26	4.425E-19	-18.354					
1300.0	700.0				4.4119	5.1043	1.51	367.18	3.844E-19	-18.415					
1350.0	700.0				4.3117	5.0790	1.44	393.20	3.370E-19	-18.472					
1400.0	700.0				4.2126	5.0541	1.39	421.21	2.980E-19	-18.526					
1450.0	700.0				4.1149	5.0295	1.33	451.18	2.657E-19	-18.576					
1500.0	700.0				4.0184	5.0052	1.29	482.81	2.387E-19	-18.622					
1600.0	700.0				3.8291	4.9575	1.22	549.83	1.966E-19	-18.706					
1700.0	700.0				3.6445	4.9110	1.16	619.95	1.657E-19	-18.781					
1800.0	700.0				3.4644	4.8656	1.12	690.12	1.422E-19	-18.847					
1900.0	700.0				3.2886	4.8214	1.09	758.32	1.238E-19	-18.907					
2000.0	700.0				3.1171	4.7782	1.07	822.72	1.091E-19	-18.962					
2100.0	700.0				2.9496	4.7360	1.06	882.24	9.705E-20	-19.013					
2200.0	700.0				2.7861	4.6948	1.04	936.98	9.695E-20	-19.061					
2300.0	700.0				2.6263	4.6546	1.04	986.99	7.836E-20	-19.106					
2400.0	700.0				2.4702	4.6153	1.03	1032.46	7.098E-20	-19.149					
2500.0	700.0				2.3176	4.5768	1.02	1074.71	6.455E-20	-19.190					

Table 6 (Cont.)

EXOSPHERIC TEMPERATURE = 800 DEGREES

HEIGHT KM	TEMP DEG K	LOG N(N ₂) /CM ³	LOG N(O ₂) /CM ³	LOG N(O) /CM ³	LOG N(A) /CM ³	LOG N(He) /CM ³	MEAN MOL WT	DENSITY SCALE HT KM	DENSITY GM/CM ³	LOG DEN GM/CM ³
90.0	183.0	13.7498	13.1687	11.8225	11.8276	8.6457	28.83	5.446	3.460E-09	-8.461
92.0	183.2	13.5900	12.9944	12.0335	11.6678	8.4860	28.63	5.42	2.395E-09	-8.621
94.0	184.1	13.4295	12.8131	12.1523	11.5073	8.3255	28.37	5.41	1.655E-09	-8.781
96.0	185.8	13.2692	12.6284	12.1680	11.3470	8.1652	28.09	5.44	1.144E-09	-8.941
98.0	188.6	13.1102	12.4460	12.1241	11.1880	8.0062	27.84	5.50	7.935E-10	-9.100
100.0	192.6	12.9533	12.2695	12.0407	11.0311	7.8493	27.64	5.56	5.528E-10	-9.257
102.0	198.1	12.7988	12.0947	11.9473	10.8159	7.8214	27.44	5.63	3.866E-10	-9.413
104.0	205.0	12.6459	11.9222	11.8536	10.6042	7.7925	27.22	5.73	2.718E-10	-9.566
106.0	213.4	12.4955	11.7529	11.7601	10.3971	7.7626	27.00	5.88	1.926E-10	-9.715
108.0	223.5	12.3484	11.5877	11.6675	10.1959	7.7321	26.77	6.05	1.377E-10	-9.861
110.0	235.1	12.2053	11.4274	11.5764	10.0012	7.7011	26.53	6.27	9.952E-11	-10.002
115.0	270.5	11.8691	11.0220	11.3583	9.5477	7.6240	25.94	6.99	4.669E-11	-10.331
120.0	313.5	11.5672	10.7163	11.1584	9.1445	7.5503	25.35	7.95	2.385E-11	-10.622
125.0	361.0	11.3007	10.206	10.9799	8.7906	7.4830	24.80	9.17	1.327E-11	-10.877
130.0	408.8	11.0673	10.1617	10.8234	8.4808	7.4239	24.28	10.60	7.991E-12	-11.097
135.0	454.1	10.8621	9.3337	10.6866	8.2076	7.3728	23.80	12.15	5.144E-12	-11.289
140.0	495.1	10.6797	9.7308	10.5664	7.9635	7.3288	23.35	13.78	3.496E-12	-11.456
145.0	531.1	10.5155	9.5476	10.4595	7.7424	7.2908	22.92	15.42	2.481E-12	-11.605
150.0	562.1	10.3656	9.3798	10.3633	7.5390	7.2576	22.52	17.01	1.822E-12	-11.739
155.0	588.6	10.2267	9.2240	10.2754	7.3495	7.2282	22.13	18.53	1.375E-12	-11.862
160.0	611.3	10.0964	9.0775	10.1939	7.1707	7.2018	21.77	19.95	1.061E-12	-11.974
170.0	647.8	9.8550	8.0053	10.0453	6.8371	7.1553	21.09	22.54	6.624E-13	-12.179
180.0	675.4	9.6315	8.5527	9.9099	6.5262	7.1147	20.46	24.82	4.343E-13	-12.362
190.0	697.1	9.4205	8.3136	9.7835	6.2311	7.0780	19.90	26.88	2.950E-13	-12.530
200.0	714.4	9.2185	8.0844	9.6635	5.9476	7.0041	19.39	28.79	2.059E-13	-12.686
210.0	728.4	9.0234	7.8628	9.5485	5.6731	7.0122	18.94	30.53	1.470E-13	-12.833
220.0	740.0	8.8338	7.6471	9.4372	5.4056	6.9818	18.53	32.18	1.069E-13	-12.971
230.0	749.5	8.6485	7.4362	9.3291	5.1437	6.9527	18.17	33.72	7.890E-14	-13.103
240.0	757.4	8.4669	7.2294	9.2234	4.8866	6.9245	17.85	35.17	5.902E-14	-13.229
250.0	764.0	8.2882	7.0259	9.1197	4.6335	6.8972	17.57	36.50	4.465E-14	-13.350
260.0	769.5	8.1122	6.8252	9.0178	4.3837	6.8706	17.32	37.74	3.411E-14	-13.467
270.0	774.0	7.9383	6.6269	8.9174	4.1368	6.8445	17.11	38.88	2.627E-14	-13.580
280.0	777.8	7.7662	6.4307	8.8183	3.8924	6.8189	16.91	39.92	2.038E-14	-13.691
290.0	781.0	7.5958	6.2363	8.7202	3.6504	6.7937	16.74	40.87	1.591E-14	-13.798
300.0	783.7	7.4268	6.0435	8.6230	3.4098	6.7689	16.59	41.73	1.294E-14	-13.903
310.0	785.9	7.2591	5.8521	8.5267	3.1711	6.7443	16.44	42.52	9.853E-15	-14.006
320.0	787.8	7.0925	5.6620	8.4311	2.9349	6.7200	16.31	43.23	7.804E-15	-14.108
330.0	789.4	6.9270	5.4730	8.3362	2.6983	6.6960	16.19	43.88	6.203E-15	-14.207
340.0	790.7	6.7623	5.2850	8.248	2.4638	6.6721	16.07	44.48	4.947E-15	-14.306
350.0	791.9	6.5985	5.0980	8.1480	2.2305	6.6484	15.96	45.03	3.956E-15	-14.403
360.0	792.8	6.4356	4.9119	8.0547	1.9983	6.6248	15.84	45.54	3.172E-15	-14.499
370.0	793.7	6.2733	4.7267	7.9618	1.7672	6.6014	15.72	46.02	2.550E-15	-14.593
380.0	794.4	6.1118	4.5422	7.8674	1.5370	6.5782	15.60	46.47	2.054E-15	-14.687
390.0	795.0	5.9509	4.3585	7.7774	1.3077	6.5550	15.47	46.90	1.658E-15	-14.780
400.0	795.6	5.7907	4.1755	7.6858	1.0794	6.5320	15.33	47.31	1.341E-15	-14.873

EXOSPHERIC TEMPERATURE = 800 DEGREES

Table 6 (Cont.)

HEIGHT KM	TEMP DEG K	LOG N(N2) /CM3	LOG N(O2) /CM3	LOG N(O) /CM3	LOG N(A) /CM3	LOG N(HE) /CM3	LOG N(H) /CM3	MEAN MOL WT	DENSITY HT KM	DENSITY SCALE	DENSITY GM/CM3	LOG DEN GM/CM3
420.0	796.5	5.4721	3.8116	7.5036	6.6252	6.4862	6.4408	15.00	48.12	8.817E-16	-15.055	
440.0	797.1	5.1557	3.4503	7.3227	6.1742	6.4408	6.4408	14.61	48.94	5.839E-16	-15.234	
460.0	797.6	4.8415	3.0915	7.1432	6.3958	6.3958	6.3958	14.13	49.84	3.894E-16	-15.410	
480.0	798.1	4.5294	2.7350	6.9648	6.3511	6.3511	6.3511	13.55	50.84	2.617E-16	-15.582	
500.0	798.4	4.2193	2.3808	6.876	6.3067	5.1084	5.0972	12.08	52.03	0.774E-16	-15.751	
520.0	798.6	3.9112	2.0289	6.6116	6.2626	5.0972	5.0972	11.20	53.47	1.214E-16	-15.916	
540.0	798.8	3.6049	1.6791	6.4366	6.2188	5.0861	5.0861	11.21	55.26	8.400E-17	-16.076	
560.0	799.0	3.3006	1.3314	6.2628	6.1753	5.0751	5.0751	10.28	57.50	5.889E-17	-16.230	
580.0	799.1	2.9980	•9858	6.0899	6.1320	5.0641	5.0641	9.34	60.34	4.193E-17	-16.378	
600.0	799.3	2.6973	•6423	6.0890	6.0532	5.0532	8.43	63.92	3.037E-17	-16.518		
620.0	799.4	2.3983	•3008	5.7474	6.0463	5.0424	5.0424	7.58	68.41	2.244E-17	-16.649	
640.0	799.4	2.1011	5.5776	6.0038	5.0317	6.82	7.39	73.99	1.633E-17	-16.771		
660.0	799.5	1.8056	5.4088	5.9616	5.0210	6.17	80.81	8.307E-17	-16.884			
680.0	799.6	1.5118	5.2410	5.9196	5.0104	5.61	88.98	1.032E-17	-16.986			
700.0	799.6	1.2197	5.0741	5.8778	4.9999	5.16	98.50	8.335E-18	-17.079			
720.0	799.7	•9293	4.9083	5.8363	4.9894	4.79	109.29	6.873E-18	-17.163			
740.0	799.7	•6405	4.7433	5.7950	4.9790	4.49	121.11	5.776E-18	-17.238			
760.0	799.7	•3533	4.5793	5.7540	4.9686	4.26	133.61	4.936E-18	-17.307			
780.0	799.8	•0678	4.4162	5.7132	4.9584	4.07	146.36	4.279E-18	-17.369			
800.0	799.8	4.2541	4.6726	4.9481	3.92	158.91	3.753E-18	-17.426				
820.0	799.8	4.0929	4.9380	5.6323	4.9380	3.79	170.82	3.324E-18	-17.478			
840.0	799.8	3.8325	5.5922	5.5922	4.9278	3.69	181.85	2.988E-18	-17.528			
860.0	799.8	3.7731	5.5523	5.5523	4.9178	3.61	191.81	2.667E-18	-17.574			
880.0	799.8	3.6145	5.5126	5.5126	4.9078	3.53	200.67	2.08E-18	-17.618			
900.0	799.9	3.4568	5.4731	4.8979	3.47	208.46	2.184E-18	-17.661				
920.0	799.9	3.3000	5.4339	4.8880	3.41	215.27	1.987E-18	-17.702				
940.0	799.9	3.1440	5.3949	4.8781	3.36	221.23	1.813E-18	-17.742				
960.0	799.9	2.9889	5.3561	4.8684	3.31	226.49	1.558E-18	-17.780				
980.0	799.9	2.8347	5.3175	4.8586	3.26	231.18	1.520E-18	-17.818				
1000.0	799.9	2.6813	5.2791	4.8490	3.22	235.41	1.395E-18	-17.855				
1050.0	799.9	2.3014	5.1841	4.8250	3.10	244.64	1.133E-18	-17.946				
1100.0	799.9	1.9266	5.0903	4.8014	2.99	252.94	9.264E-19	-18.033				
1150.0	799.9	1.5568	4.9978	4.7781	2.88	261.02	7.626E-19	-18.118				
1200.0	800.0	1.1919	4.9065	4.7551	2.77	269.30	6.315E-19	-18.200				
1250.0	800.0	•8318	4.8164	4.7324	2.65	278.10	5.261E-19	-18.279				
1300.0	800.0	•4764	4.7275	4.7100	2.54	287.61	4.408E-19	-18.356				
1350.0	800.0	•1256	4.6398	4.6879	2.42	297.94	3.716E-19	-18.430				
1400.0	800.0	1400.0	4.5531	4.6661	2.31	309.19	3.051E-19	-18.502				
1450.0	800.0	1450.0	4.4676	4.6446	2.20	321.60	2.689E-19	-18.570				
1500.0	800.0	1500.0	4.3832	4.6233	2.10	335.21	2.309E-19	-18.637				
1600.0	800.0	1600.0	4.2175	4.5816	1.91	366.34	1.735E-19	-18.761				
1700.0	800.0	1700.0	4.0560	4.5409	1.75	403.46	1.338E-19	-18.874				
1800.0	800.0	1800.0	3.8984	4.5012	1.61	446.93	1.057E-19	-18.976				
1900.0	800.0	1900.0	3.7446	4.4625	1.49	497.23	8.546E-20	-19.068				
2000.0	800.0	2000.0	3.5945	4.4247	1.39	554.10	7.063E-20	-19.151				
2100.0	800.0	2100.0	3.4480	4.3878	1.32	616.80	5.952E-20	-19.225				
2200.0	800.0	2200.0	3.3049	4.3518	1.25	684.69	5.03E-20	-19.353				
2300.0	800.0	2300.0	3.1651	4.3165	1.21	756.28	4.441E-20	-19.407				
2400.0	800.0	2400.0	3.0284	4.2821	1.17	829.87	3.914E-20	-19.457				
2500.0	800.0	2500.0	2.8949	4.2485	1.14	904.35	3.488E-20					

Table 6 (Cont.)

EXOSPHERIC TEMPERATURE = 900 DEGREES							MEAN MOL WT	DENSITY HT KM	LOG DEN GM/CM ³
HEIGHT KM	TEMP DEG K	LOG N(N ₂) /CM ³	LOG N(O ₂) /CM ³	LOG N(O) /CM ³	LOG N(H) /CM ³	DENSITY SCALE			
90.0	183.0	13.7498	13.1687	11.8225	8.6457	28.83	5.46	3.460E-09	-8.461
92.0	183.2	13.5900	12.9944	12.0534	8.4859	28.63	5.42	2.395E-09	-8.621
94.0	184.2	13.4293	12.8129	12.1521	8.3253	28.37	5.40	1.654E-09	-8.781
96.0	186.0	13.2688	12.6280	12.1677	8.1648	28.09	5.43	1.143E-09	-8.942
98.0	189.1	13.1096	12.4453	12.1234	8.0055	27.84	5.49	7.923E-10	-9.101
100.0	193.5	12.9524	12.2686	12.0398	7.8483	27.64	5.55	5.517E-10	-9.258
102.0	199.4	12.7977	12.0937	11.9458	7.8200	27.44	5.62	3.856E-10	-9.414
104.0	206.9	12.6446	11.9212	11.8516	10.6037	27.22	5.73	2.711E-10	-9.567
106.0	216.1	12.4943	11.7522	11.7576	10.3974	27.00	5.88	1.921E-10	-9.717
108.0	227.0	12.3476	11.5876	11.6646	10.1972	26.78	6.07	1.374E-10	-9.862
110.0	239.6	12.2051	11.4282	11.5732	10.0040	7.6973	6.30	9.944E-11	-10.002
115.0	278.0	11.8714	11.0563	11.3549	9.5557	7.6188	7.06	4.690E-11	-10.329
122.0	324.7	11.5735	10.7256	11.1558	9.1597	7.5440	25.41	8.07	2.415E-11
125.0	376.3	11.3120	10.4360	10.9790	8.8140	7.4761	24.88	9.35	1.357E-11
130.0	428.4	11.0841	10.1837	10.8247	8.5131	7.4167	24.39	10.84	8.253E-12
135.0	478.1	10.8845	9.9624	10.6902	8.2486	7.3654	23.94	12.45	5.366E-12
140.0	523.9	10.7076	9.7660	10.5722	8.0133	7.3212	23.51	14.13	3.681E-12
145.0	564.8	10.5488	9.5893	10.4675	7.8008	7.2829	23.11	15.85	2.636E-12
150.0	600.9	10.4044	9.4282	10.3735	7.6064	7.2495	22.73	17.54	1.953E-12
155.0	632.3	10.2714	9.2793	10.2880	7.4261	7.2199	22.38	19.17	1.487E-12
160.0	659.6	10.1473	9.1402	10.2092	7.2569	7.1934	22.03	20.73	1.158E-12
170.0	704.3	9.9191	8.8836	10.0667	6.9437	7.1472	21.40	23.59	7.372E-13
180.0	738.9	9.7100	8.6478	9.9384	6.6544	7.1074	20.81	26.14	4.931E-13
190.0	766.4	9.5143	8.4264	9.8198	6.3820	7.0719	20.28	28.45	3.419E-13
200.0	788.5	9.3282	8.2156	9.7082	6.1219	7.0394	19.79	30.59	2.436E-13
210.0	806.6	9.1495	8.0130	9.6019	5.8714	7.0091	19.35	32.54	1.775E-13
220.0	821.6	8.9767	7.8166	9.4998	5.6283	6.9806	18.95	34.39	1.316E-13
230.0	834.0	8.8085	7.6255	9.4010	5.3912	6.9535	18.58	36.13	9.913E-14
240.0	844.3	8.6442	7.4385	9.3048	5.1592	6.9275	18.26	37.76	7.562E-14
250.0	852.9	8.4830	7.2551	9.2109	4.9312	6.9024	17.97	39.29	5.833E-14
260.0	860.0	8.3246	7.0746	9.1188	4.7068	6.8780	17.71	40.71	4.543E-14
270.0	866.0	8.1683	6.8966	9.0283	4.4853	6.8542	17.47	42.04	3.568E-14
280.0	870.9	8.0141	6.7207	8.9391	4.2663	6.8310	17.26	43.27	2.822E-14
290.0	875.1	7.8614	6.5466	8.8511	4.0496	6.8082	17.07	44.40	2.247E-14
300.0	878.6	7.7103	6.3742	8.7640	3.8347	6.7858	16.91	45.45	1.798E-14
310.0	881.5	7.5604	6.2032	8.6778	3.6216	6.7637	16.75	46.40	1.446E-14
320.0	884.0	7.4116	6.0334	8.5923	3.4099	6.7418	16.61	47.28	1.168E-14
330.0	886.1	7.2638	5.8648	8.5074	3.1996	6.7202	16.49	48.09	9.474E-15
340.0	887.8	7.1170	5.6971	8.4232	2.9906	6.6988	16.37	48.84	7.708E-15
350.0	889.3	6.9709	5.5304	8.3395	2.7827	6.6776	16.26	49.53	6.290E-15
360.0	890.6	6.8257	5.3646	8.2563	2.5758	6.6566	16.15	50.17	5.147E-15
370.0	891.7	6.6811	5.1996	8.1735	2.3699	6.6357	16.05	50.76	4.221E-15
380.0	892.7	6.5373	5.0353	8.0911	2.1649	6.6149	15.94	51.30	3.470E-15
390.0	893.5	6.3940	4.8717	8.0911	1.9608	6.5942	15.84	51.81	2.858E-15
400.0	894.2	6.2514	4.7089	7.9275	1.7576	6.5737	15.74	52.30	2.359E-15

Table 6 (Cont.)

EXOSPHERIC TEMPERATURE = 900 DEGREES

HEIGHT KM	TEMP DEG K	LOG N(N2) /CM3	LOG N(O2) /CM3	LOG N(O) /CM3	LOG N(A) /CM3	LOG N(HE) /CM3	LOG N(H) /CM3	MEAN MOL WT	DENSITY HT KM	DENSITY SCALE	DENSITY GM/CM3	LOG DEN GM/CM3
420.0	895.4	5.9678	4.3850	7.7653	1.3534	6.5329	15.52	15.52	53.22	1.615E-15	-14.792	
440.0	896.2	5.68863	4.0635	7.6043	0.9521	6.4925	15.27	15.27	54.07	1.112E-15	-14.954	
460.0	896.9	5.4068	3.7443	7.4446	0.5537	6.4524	14.98	14.98	54.92	7.705E-16	-15.113	
480.0	897.4	5.1292	3.4272	7.2859	0.1579	6.4126	14.63	14.63	55.78	5.368E-16	-15.270	
500.0	897.9	4.8534	3.1122	7.1283	4.7415	6.3731	14.22	14.22	56.69	3.761E-16	-15.425	
520.0	898.2	4.5794	2.7992	6.9717	6.3339	4.7315	13.74	13.74	57.71	2.651E-16	-15.577	
540.0	898.5	4.3070	2.4882	6.8161	6.2949	4.7215	13.18	13.18	58.87	1.881E-16	-15.726	
560.0	898.7	4.0364	2.1790	6.6615	6.2562	4.7117	12.55	12.55	60.24	1.344E-16	-15.871	
580.0	898.9	3.7674	1.8718	6.5078	6.2177	4.7019	11.84	11.84	61.86	9.687E-17	-16.014	
600.0	899.0	3.5000	1.5663	6.3551	6.1795	4.6922	11.08	11.08	63.83	7.045E-17	-16.152	
620.0	899.2	3.2342	1.2627	6.2032	6.1414	4.6826	10.29	10.29	66.22	5.178E-17	-16.286	
640.0	899.3	2.9699	0.9609	6.0523	6.1037	4.6731	9.49	9.49	69.14	3.853E-17	-16.414	
660.0	899.4	2.7072	0.6608	5.9022	6.0661	4.6636	8.71	8.71	72.71	2.905E-17	-16.537	
680.0	899.4	2.4460	0.3625	5.7530	6.0288	4.6541	7.97	7.97	77.05	2.223E-17	-16.653	
700.0	899.5	2.1863	0.0659	5.6047	5.9916	4.6448	7.29	7.29	82.30	1.729E-17	-16.762	
720.0	899.6	1.9282	5.4573	5.9547	4.6354	6.69	6.69	6.69	88.56	1.368E-17	-16.864	
740.0	899.6	1.6714	5.3106	5.9181	4.6262	6.17	6.17	6.17	95.93	1.101E-17	-16.953	
760.0	899.6	1.4162	5.1648	5.8116	4.6170	5.72	10.45	10.45	9.013E-18	-17.045		
780.0	899.7	1.1624	5.0199	5.8453	4.6078	5.34	11.11	11.11	7.504E-18	-17.125		
800.0	899.7	0.9100	4.8757	5.8092	4.5987	5.03	12.84	12.84	6.346E-18	-17.198		
820.0	899.7	0.6591	4.7324	5.7334	4.5897	4.78	13.63	13.63	5.444E-18	-17.264		
840.0	899.8	4.0959	4.5899	5.7377	4.5807	4.57	14.850	14.850	4.730E-18	-17.325		
860.0	899.8	0.1613	4.4481	5.7022	4.5718	4.40	16.090	16.090	4.156E-18	-17.381		
880.0	899.8	0.0000	4.3072	5.6670	4.5629	4.26	17.323	17.323	3.687E-18	-17.433		
900.0	899.8	0.0000	4.1670	5.6319	4.5540	4.15	18.518	18.518	3.298E-18	-17.482		
920.0	899.8	0.0000	4.0276	5.5970	4.5452	4.05	19.649	19.649	2.970E-18	-17.527		
940.0	899.8	0.0000	3.8889	5.5623	4.5365	3.98	20.697	20.697	2.689E-18	-17.570		
960.0	899.9	0.0000	3.7510	5.5278	4.5278	3.91	21.551	21.551	2.442E-18	-17.611		
980.0	899.9	0.0000	3.6139	5.4935	4.5192	3.86	22.509	22.509	2.235E-18	-17.651		
1000.0	899.9	0.0000	3.4776	5.4594	4.5106	3.81	23.272	23.272	2.048E-18	-17.689		
1050.0	899.9	0.0000	3.1399	5.3749	4.4893	3.72	24.813	24.813	1.664E-18	-17.779		
1100.0	899.9	0.0000	2.8067	5.2916	4.4683	3.65	25.958	25.958	1.367E-18	-17.864		
1150.0	899.9	0.0000	2.4780	5.2093	4.4476	3.58	26.848	26.848	1.131E-18	-17.946		
1200.0	899.9	0.0000	2.1536	5.1282	4.4271	3.52	27.585	27.585	9.413E-19	-18.026		
1250.0	900.0	0.0000	1.8335	5.0481	4.4070	3.45	28.249	28.249	7.870E-19	-18.104		
1300.0	900.0	0.0000	1.5176	4.9691	4.3871	3.38	28.878	28.878	6.606E-19	-18.180		
1350.0	900.0	0.0000	1.2058	4.8911	4.3674	3.31	29.499	29.499	5.566E-19	-18.254		
1400.0	900.0	0.0000	0.8980	4.8141	4.3480	3.24	30.128	30.128	4.707E-19	-18.327		
1450.0	900.0	0.0000	0.5942	4.7381	4.3289	3.16	30.785	30.785	3.994E-19	-18.399		
1500.0	900.0	0.0000	0.2942	4.6630	4.3100	3.08	31.474	31.474	3.401E-19	-18.468		
1600.0	900.0	0.0000	0.0000	4.5158	4.2729	2.91	32.963	32.963	2.493E-19	-18.603		
1700.0	900.0	0.0000	0.0000	4.3722	4.2367	2.74	34.659	34.659	1.854E-19	-18.732		
1800.0	900.0	0.0000	0.0000	4.2321	4.2014	2.56	36.587	36.587	1.400E-19	-18.854		
1900.0	900.0	0.0000	0.0000	4.0954	4.1670	2.38	38.811	38.811	1.074E-19	-18.969		
2000.0	900.0	0.0000	0.0000	3.9620	4.1334	2.21	41.370	41.370	8.364E-20	-19.078		
2100.0	900.0	0.0000	0.0000	3.8317	4.1006	2.06	44.298	44.298	6.621E-20	-19.179		
2200.0	900.0	0.0000	0.0000	3.7045	4.0686	1.91	47.668	47.668	4.325E-20	-19.274		
2300.0	900.0	0.0000	0.0000	3.5802	4.0373	1.78	51.508	51.508	4.352E-20	-19.361		
2400.0	900.0	0.0000	0.0000	3.4588	4.0067	1.67	55.840	55.840	3.611E-20	-19.442		
2500.0	900.0	0.0000	0.0000	3.3401	3.9768	1.57	60.709	60.709	3.041E-20	-19.517		

Table 6 (Cont.)

EXOSPHERIC TEMPERATURE = 1000 DEGREES

HEIGHT KM	TEMP DEG K	LOG N(N2) /CM3	LOG N(O2) /CM3	LOG N(O) /CM3	LOG N(A) /CM3	LOG N(HE) /CM3	MEAN MOL WT	DENSITY SCALE HT KM	DENSITY GM/CM3	LOG DEN GM/CM3
90.0	183.0	13.7498	13.1687	11.8225	11.8276	8.6457	28.83	5.46	3.460E-09	-8.461
92.0	183.3	13.5900	12.9943	12.0534	11.6677	8.8559	28.63	5.41	2.395E-09	-8.621
94.0	184.2	13.4292	12.8128	12.1519	11.5070	8.3251	28.37	5.40	1.654E-09	-8.782
96.0	186.2	13.2685	12.6277	12.1673	11.3463	8.6645	28.09	5.42	1.142E-09	-8.942
98.0	189.5	13.1090	12.4448	12.1229	11.1868	8.0050	27.84	5.48	7.913E-10	-9.102
100.0	194.2	12.9516	12.2678	12.0390	11.0294	7.84515	27.64	5.54	5.507E-10	-9.259
102.0	200.5	12.7967	12.0928	11.9446	10.8144	7.8188	27.44	5.62	3.847E-10	-9.415
104.0	208.5	12.6436	11.9204	11.8498	10.6034	7.7888	27.23	5.73	2.04E-10	-9.568
106.0	218.4	12.4934	11.7517	11.7554	10.3976	7.7518	27.01	5.89	1.916E-10	-9.718
108.0	230.0	12.3469	11.5875	11.6621	10.1984	7.7261	26.79	6.09	1.372E-10	-9.863
110.0	243.5	12.2049	11.4289	11.5704	10.0064	7.6940	26.56	6.33	9.937E-11	-10.003
115.0	284.6	11.8734	11.0598	11.3520	9.3625	7.6143	25.99	7.12	4.707E-11	-10.327
120.0	334.5	11.5787	10.7332	11.1536	9.1723	7.5387	25.45	8.17	2.439E-11	-10.613
125.0	389.7	11.3213	10.4486	10.9781	8.9333	7.403	24.95	9.49	1.381E-11	-10.860
130.0	445.4	11.0978	10.2016	10.8256	8.5394	7.4107	24.48	11.04	8.473E-12	-11.072
135.0	499.1	10.9026	10.9856	10.6929	8.2831	7.352	24.04	12.69	5.553E-12	-11.255
140.0	549.0	10.7299	9.7943	10.5765	8.0535	7.3147	23.64	14.42	3.838E-12	-11.416
145.0	594.5	10.5753	9.6226	10.4734	7.8478	7.2762	23.26	16.19	2.767E-12	-11.558
150.0	635.2	10.4352	9.4666	10.3811	7.6601	7.2424	22.91	17.96	2.064E-12	-11.685
155.0	671.3	10.3065	9.3230	10.2973	7.4868	7.2126	22.57	19.68	1.593E-12	-11.801
160.0	703.1	10.1869	9.1893	10.2204	7.3250	7.1859	22.25	21.35	1.240E-12	-11.906
170.0	756.2	9.9687	8.9445	10.0822	7.0272	7.1396	21.65	24.45	8.013E-13	-12.096
180.0	798.1	9.7705	8.7215	9.9589	6.7545	7.1001	21.10	27.27	5.443E-13	-12.264
190.0	831.9	9.5864	8.5137	9.8460	6.4997	6.0653	20.59	29.82	3.844E-13	-12.416
200.0	859.3	9.4126	8.3172	9.7407	6.2578	7.0337	20.13	32.20	2.777E-13	-12.556
210.0	882.0	9.2467	8.1293	9.6411	6.0260	7.0046	19.70	34.37	2.056E-13	-12.687
220.0	900.7	9.0869	7.9481	9.5460	5.8021	6.9774	19.31	36.42	1.550E-13	-12.810
230.0	916.4	8.9322	7.7724	9.4544	5.5787	6.9517	18.95	38.36	1.187E-13	-12.926
240.0	929.4	8.7815	7.6012	9.3657	5.3724	6.9273	18.62	40.18	9.198E-14	-13.036
250.0	940.2	8.6334	7.4336	9.2794	5.1644	6.9038	18.33	41.89	7.208E-14	-13.142
260.0	949.3	8.4896	7.2691	9.1951	4.9600	6.88112	18.06	43.49	5.703E-14	-13.244
270.0	956.8	8.3474	7.1072	9.1124	4.7587	6.8592	17.82	44.99	4.549E-14	-13.342
280.0	963.1	8.2072	6.9474	9.0311	4.5601	6.8378	17.59	46.39	3.655E-14	-13.437
290.0	968.4	8.0688	6.7896	8.9510	4.3636	6.8169	17.39	47.69	2.955E-14	-13.529
300.0	972.8	7.9318	6.6334	8.8719	4.1691	6.7964	17.21	48.90	2.030E-14	-13.619
310.0	976.5	7.7961	6.4786	8.7937	3.9763	6.7762	17.05	50.02	1.963E-14	-13.707
320.0	979.7	7.6615	6.3251	8.7162	3.7850	6.7563	16.90	51.07	1.611E-14	-13.793
330.0	982.3	7.5279	6.1727	8.6394	3.5950	6.7367	16.76	52.03	1.327E-14	-13.877
340.0	984.6	7.3953	6.0213	8.5632	3.4063	6.7173	16.64	52.92	1.096E-14	-13.960
350.0	986.5	7.2634	5.8709	8.4876	3.2186	6.6980	16.52	53.76	9.090E-15	-14.041
360.0	988.1	7.1323	5.7212	8.4124	3.0320	6.6790	16.41	54.53	7.557E-15	-14.122
370.0	989.5	7.0019	5.5723	8.3377	2.8463	6.6600	16.31	55.24	6.298E-15	-14.201
380.0	990.7	6.8722	5.4242	8.2633	2.6615	6.6412	16.21	55.91	5.61E-15	-14.279
390.0	991.7	6.7430	5.2767	8.1894	2.4775	6.6226	16.11	56.53	4.404E-15	-14.356
400.0	992.6	6.6144	5.1299	8.1158	2.2943	6.6040	16.02	57.12	3.693E-15	-14.433

Table 6 (Cont.)

EXOSPHERIC TEMPERATURE = 1000 DEGREES

HEIGHT KM	TEMP DEG K	LOG N(N2) /CM3	LOG N(O2) /CM3	LOG N(O) /CM3	LOG N(A) /CM3	LOG N(H) /CM3	LOG N(H) /CM3	MEAN MOL WT	DENSITY HT KM	SCALE HT KM	DENSITY GM/CM3	LOG DEN GM/CM3
420.0	994.1	6.3588	4.8380	7.9695	1.9301	6.5672	15.84	58.20	2.611E-15	-14.583		
440.0	995.2	6.1052	4.5484	7.8245	1.5686	6.5307	15.65	59.18	1.857E-15	-14.731		
460.0	996.1	5.8535	4.2609	7.6805	1.2097	6.4946	15.44	60.10	1.328E-15	-14.877		
480.0	996.8	5.6034	3.9753	7.5376	0.8533	6.4587	15.21	60.98	9.543E-16	-15.020		
500.0	997.3	5.3551	3.6917	7.3956	0.4993	6.4231	4.4375	14.94	61.85	6.891E-16	-15.162	
520.0	997.7	5.1083	3.4099	7.2546	0.1475	6.3878	4.4285	14.63	62.75	4.999E-16	-15.301	
540.0	998.1	4.8631	3.1298	7.1145	0.3527	6.3527	4.4195	14.27	63.71	3.643E-16	-15.439	
560.0	998.4	4.6195	2.8515	6.9753	0.3178	6.4106	13.86	64.75	2.668E-16	-15.574		
580.0	998.6	4.3773	2.5749	6.8370	0.2831	6.4018	13.38	65.91	1.964E-16	-15.707		
600.0	998.8	4.1366	2.2999	6.6994	0.2487	6.3931	12.85	67.23	1.454E-16	-15.837		
620.0	998.9	3.8973	2.0266	6.5627	0.2145	6.3844	12.26	68.76	1.084E-16	-15.965		
640.0	999.1	3.6595	1.7549	6.4269	0.1805	6.3758	11.62	70.55	8.131E-17	-16.090		
660.0	999.2	3.4230	1.4848	6.2918	0.1466	6.3672	10.94	72.68	6.149E-17	-16.211		
680.0	999.3	3.1879	1.2163	6.1575	0.1130	6.3587	10.24	75.20	4.691E-17	-16.329		
700.0	999.4	2.9542	0.9493	6.0240	0.0796	6.3503	9.54	78.21	3.614E-17	-16.442		
720.0	999.4	2.7218	0.6838	5.8912	0.0464	6.3419	8.85	81.79	2.814E-17	-16.551		
740.0	999.5	2.4907	0.4199	5.7593	0.0134	6.3335	8.20	86.04	2.217E-17	-16.654		
760.0	999.5	2.2609	0.1575	5.6280	0.9805	6.3253	7.59	91.06	1.768E-17	-16.753		
780.0	999.6	2.0325	0.4976	5.4979	0.3170	7.04	96.93	1.429E-17	-16.845			
800.0	999.6	1.8053	5.3678	5.9154	0.3088	6.55	103.78	1.170E-17	-16.932			
820.0	999.7	1.5795	5.2388	5.8831	0.3007	6.11	111.59	9.717E-18	-17.012			
840.0	999.7	1.3549	5.1105	5.8510	0.2926	5.74	120.41	8.177E-18	-17.087			
860.0	999.7	1.1315	4.9829	5.8191	0.2845	5.42	130.22	8.969E-18	-17.157			
880.0	999.8	0.9094	4.8561	5.7874	0.2765	5.15	140.93	6.013E-18	-17.221			
900.0	999.8	0.6885	4.7299	5.7558	0.2686	4.92	152.38	5.245E-18	-17.280			
920.0	999.8	0.4688	4.6044	5.7244	0.2607	4.73	164.37	4.623E-18	-17.335			
940.0	999.8	0.2503	4.4797	5.6932	0.2528	4.57	176.68	4.0111E-18	-17.386			
960.0	999.8	0.0331	4.3556	5.6622	0.2450	4.44	189.03	3.6885E-18	-17.434			
980.0	999.8	0.0000	4.2321	5.6313	0.2372	4.33	201.18	3.3266E-18	-17.478			
1000.0	999.9	0.0000	4.1094	5.6006	0.2295	4.24	212.90	3.019E-18	-17.520			
1050.0	999.9	3.8055	5.5245	4.2103	4.08	239.22	2.421E-18	-17.616				
1100.0	999.9	3.5056	5.4495	4.1914	3.98	260.46	1.982E-18	-17.703				
1150.0	999.9	3.2098	5.3755	4.1728	3.90	276.79	1.646E-18	-17.784				
1200.0	999.9	2.9179	5.3025	4.1544	3.85	289.21	1.379E-18	-17.860				
1250.0	999.9	2.6298	5.2304	4.1362	3.81	298.96	1.164E-18	-17.934				
1300.0	999.9	2.3454	5.1593	4.1183	3.77	306.93	9.869E-19	-18.006				
1350.0	1000.0	2.0648	5.0891	4.1006	3.73	313.78	8.400E-19	-18.076				
1400.0	1000.0	1.7878	5.0198	4.0831	3.70	319.95	7.174E-19	-18.144				
1450.0	1000.0	1.5143	4.9513	4.0659	3.66	325.81	6.145E-19	-18.211				
1500.0	1000.0	1.2444	4.8038	4.0489	3.62	331.51	5.278E-19	-18.278				
1600.0	1000.0	0.7146	4.7513	4.0155	3.54	342.80	3.923E-19	-18.406				
1700.0	1000.0	0.1980	4.6220	3.9830	3.44	354.61	2.945E-19	-18.531				
1800.0	1000.0	0.04959	4.4959	3.9512	3.34	367.06	2.232E-19	-18.651				
1900.0	1000.0	0.0000	4.3729	3.9203	3.22	380.56	1.708E-19	-18.768				
2000.0	1000.0	0.0000	4.2528	3.8900	3.10	395.21	1.320E-19	-18.880				
2100.0	1000.0	0.0000	4.1356	3.8605	2.96	411.14	1.030E-19	-18.987				
2200.0	1000.0	0.0000	4.0211	3.8317	2.83	428.74	8.113E-20	-19.091				
2300.0	1000.0	0.0000	3.9093	3.8035	2.69	448.16	6.458E-20	-19.190				
2400.0	1000.0	0.0000	3.8000	3.7760	2.55	469.53	5.192E-20	-19.285				
2500.0	1000.0	0.0000	3.6932	3.7491	2.41	493.39	4.218E-20	-19.355				

Table 6 (Cont.)

EXOSPHERIC TEMPERATURE = 1100 DEGREES

HEIGHT KM	TEMP DEG K	LOG N(N2) /CM3	LOG N(O2) /CM3	LOG N(O) /CM3	LOG N(A) /CM3	LOG N(He) /CM3	MEAN MOL WT	DENSITY SCALE HT KM	DENSITY GM/CM3	LOG DEN GM/CM3
90.0	183.0	13.7498	13.1687	11.8225	11.8276	8.6457	28.83	5.46	3.460E-09	-8.461
92.0	183.3	13.5899	12.9943	12.0534	11.6677	8.4859	28.63	5.41	2.395E-09	-8.621
94.0	184.3	13.64291	12.8126	12.1518	11.5068	8.3250	28.37	5.39	1.653E-09	-8.782
96.0	186.4	13.2682	12.6274	12.1670	11.3460	8.1642	28.09	5.41	1.142E-09	-8.962
98.0	189.9	13.1085	12.4443	12.1224	11.1863	8.0045	27.84	5.47	7.904E-10	-9.102
100.0	194.8	12.9509	12.2671	12.0383	11.0287	7.8468	27.64	5.54	5.498E-10	-9.260
102.0	201.5	12.7958	12.0921	11.9435	10.8138	7.8177	27.44	5.61	3.840E-10	-9.416
104.0	210.0	12.6427	11.9197	11.8483	10.6030	7.7873	27.23	5.73	2.699E-10	-9.569
106.0	220.4	12.4925	11.7512	11.3978	10.3978	7.7558	27.01	5.89	1.913E-10	-9.718
108.0	232.7	12.3463	11.5874	11.6599	10.1993	7.7237	26.79	6.10	1.370E-10	-9.863
110.0	246.9	12.2047	11.4294	11.5680	10.0084	7.6911	26.57	6.35	9.930E-11	-10.003
115.0	290.4	11.8750	11.0628	11.3495	9.5682	7.6104	26.02	7.16	4.720E-11	-10.326
120.0	343.2	11.5831	10.7397	11.1517	9.1829	7.5341	25.49	8.25	2.460E-11	-10.609
125.0	401.4	11.3290	10.4591	10.9773	8.8495	7.4653	25.00	9.62	1.402E-11	-10.853
130.0	460.4	11.1092	10.2166	10.8263	8.5615	7.4055	24.55	11.21	8.661E-12	-11.062
135.0	517.5	10.9775	10.0048	10.6950	8.3098	7.3539	24.13	12.90	5.714E-12	-11.243
140.0	571.3	10.7483	9.8176	10.5800	8.0868	7.3092	23.75	14.66	3.973E-12	-11.401
145.0	620.8	10.5970	9.6500	10.4781	7.8864	7.2704	23.39	16.48	2.880E-12	-11.541
150.0	665.8	10.4601	9.4979	10.3868	7.7042	7.2363	23.05	18.30	2.160E-12	-11.666
155.0	706.3	10.3348	9.3584	10.3043	7.5363	7.2062	22.73	20.10	1.664E-12	-11.779
160.0	742.5	10.2188	9.2290	10.2287	7.3801	7.1792	22.43	21.85	1.311E-12	-11.882
170.0	803.9	10.0081	8.9933	10.0936	7.0944	7.1327	21.86	25.6	8.567E-13	-12.067
180.0	853.4	9.8183	8.7801	9.9740	6.8348	7.0932	21.34	28.21	5.889E-13	-12.230
190.0	893.7	9.6432	8.5830	9.8655	6.5937	7.0586	20.86	31.01	4.201E-13	-12.377
200.0	926.9	9.4791	8.3977	9.7649	6.3663	7.0276	20.41	33.62	3.089E-13	-12.511
210.0	954.5	9.3232	8.2215	9.6705	6.1495	6.9992	20.00	36.01	2.313E-13	-12.636
220.0	977.4	9.1739	8.0525	9.5808	5.9410	6.9730	19.62	38.29	1.767E-13	-12.753
230.0	996.6	9.0299	7.8892	9.4949	5.7393	6.9484	19.27	40.42	1.371E-13	-12.863
240.0	1012.6	8.8902	7.7306	9.4121	5.5430	6.9251	18.95	42.44	1.077E-13	-12.968
250.0	1026.0	8.7540	7.5758	9.3319	5.3512	6.9029	18.65	44.33	8.551E-14	-13.068
260.0	1037.2	8.6207	7.4242	9.2538	5.1631	6.8817	18.38	46.11	6.855E-14	-13.164
270.0	1046.5	8.4899	7.2754	9.1774	4.9783	6.8611	18.13	47.77	5.540E-14	-13.257
280.0	1054.3	8.3612	7.1288	9.1025	4.7961	6.8412	17.91	49.34	4.509E-14	-13.346
290.0	1060.8	8.2342	6.9842	9.0288	4.6162	6.8218	17.70	50.80	3.692E-14	-13.433
300.0	1066.3	8.1088	6.8412	8.9562	4.4382	6.8028	17.51	52.17	3.041E-14	-13.517
310.0	1070.9	7.9847	6.6997	8.8845	4.2620	6.7841	17.33	53.44	2.516E-14	-13.599
320.0	1074.8	7.8617	6.5594	8.8136	4.0873	6.7658	17.17	54.63	2.091E-14	-13.680
330.0	1078.1	7.7397	6.4203	8.7434	3.9139	6.7478	17.03	55.74	1.744E-14	-13.758
340.0	1080.9	7.6186	6.2821	8.6737	3.7417	6.7299	16.89	56.78	1.460E-14	-13.836
350.0	1083.2	7.4984	6.1449	8.6047	3.5706	6.7123	16.77	57.74	1.226E-14	-13.911
360.0	1085.3	7.3789	6.0085	8.5360	3.4005	6.6948	16.65	58.64	1.033E-14	-13.986
370.0	1087.0	7.2600	5.8728	8.4679	3.2313	6.6775	16.55	59.49	8.719E-15	-14.060
380.0	1088.5	7.0418	5.6741	8.0401	3.0630	6.6603	16.44	60.28	7.378E-15	-14.132
390.0	1089.8	7.0421	5.6035	8.3327	2.8955	6.6433	16.35	61.02	6.257E-15	-14.204
400.0	1090.9	6.9070	5.4698	8.2656	2.7287	6.6263	16.26	61.72	5.316E-15	-14.274

Table 6 (Cont.)

EXOSPHERIC TEMPERATURE = 1100 DEGREES

HEIGHT KM	TEMP DEG K	LOG N(N2) /CM3	LOG N(O2) /CM3	LOG N(O) /CM3	LOG N(A) /CM3	LOG N(HE) /CM3	LOG N(H) /CM3	MEAN MOL WT	DENSITY GM/CM3	SCALE HT KM	DENSITY GM/CM3	LOG DEN GM/CM3
420.0	1092.7	6.6743	5.2041	8.1324	2.3971	6.5927	16.08	62.99	3.858E-15	-14.414		
440.0	1094.1	6.4435	4.9406	8.092	2.0682	6.595	15.92	64.19	2.816E-15	-14.550		
460.0	1095.1	6.2144	4.6789	7.8693	1.7417	6.5266	15.74	65.19	2.067E-15	-14.685		
480.0	1096.0	5.9870	4.4192	7.7392	1.4175	6.4939	15.57	66.18	1.525E-15	-14.817		
500.0	1096.6	5.7610	4.1612	7.6101	1.0954	6.4615	15.37	67.10	1.129E-15	-14.947		
520.0	1097.2	5.5366	3.9048	7.4818	7.755	6.4293	6.1741	68.02	8.400E-16	-15.076		
540.0	1097.6	5.3136	3.6501	7.3546	6.576	6.3974	6.1659	64.91	6.894	6.272E-16	-15.203	
560.0	1098.0	5.0920	3.3970	7.2278	6.1416	6.3657	6.1578	64.63	69.88	4.702E-16	-15.328	
580.0	1098.2	4.8718	3.1455	7.1020	6.3341	6.3341	6.1498	64.31	70.87	3.539E-16	-15.451	
600.0	1098.5	4.6529	2.8955	6.9769	6.3028	6.1418	6.1418	63.94	71.94	2.674E-16	-15.573	
620.0	1098.7	4.4354	2.6470	6.8526	6.2717	6.1339	13.53	73.10	2.029E-16	-15.693		
640.0	1098.8	4.2191	2.3999	6.7291	6.2408	6.1261	13.07	74.41	1.547E-16	-15.810		
660.0	1099.0	4.0041	2.1544	6.6062	6.2100	6.1183	12.56	75.88	1.186E-16	-15.926		
680.0	1099.1	3.7903	1.9102	6.4841	6.1795	6.106	12.01	77.57	9.135E-17	-16.039		
700.0	1099.2	3.5778	1.6674	6.3627	6.1491	6.1029	11.43	79.52	7.081E-17	-16.150		
720.0	1099.3	3.3665	1.4261	6.2421	6.1189	6.0952	10.82	81.78	5.525E-17	-16.253		
740.0	1099.4	3.1564	1.1861	6.1221	6.0888	6.0876	10.20	84.42	4.343E-17	-16.362		
760.0	1099.4	2.9476	9.475	6.0028	6.0590	6.0801	9.57	87.49	3.441E-17	-16.463		
780.0	1099.5	2.7399	7.103	5.8841	6.0293	6.0726	8.96	91.08	2.750E-17	-16.561		
800.0	1099.5	2.5333	4.744	5.7662	5.9998	6.0652	8.38	95.27	2.218E-17	-16.654		
820.0	1099.6	2.3280	2.1238	5.2399	5.6489	5.9704	4.0577	7.82	100.11	1.807E-17	-16.743	
840.0	1099.6	2.066	5.532	5.4163	5.9412	5.904	7.31	105.69	1.488E-17	-16.827		
860.0	1099.7	1.9207	1.9207	5.3009	5.9122	5.0431	6.85	112.09	1.238E-17	-16.907		
880.0	1099.7	1.7188	1.7188	5.1862	5.8834	4.0358	6.43	119.35	1.041E-17	-16.982		
900.0	1099.7	1.5180	5.0721	5.0214	5.8547	4.0286	6.06	127.51	8.854E-18	-17.053		
920.0	1099.7	1.3182	4.9587	5.0721	5.8261	4.0214	5.74	136.51	7.608E-18	-17.119		
940.0	1099.8	1.1196	4.8459	5.0721	5.7977	4.0142	5.46	146.51	6.605E-18	-17.180		
960.0	1099.8	9.9221	4.7337	5.0721	5.7695	4.0071	5.22	157.23	5.789E-18	-17.237		
980.0	1099.8	7.257	4.6221	5.0721	5.7414	4.0000	5.01	168.63	5.120E-18	-17.291		
1000.0	1099.8	5.503	4.6221	5.0721	5.7135	3.9930	4.83	180.55	4.566E-18	-17.340		
1050.0	1099.8	0.465	4.3458	2.399	5.6489	5.9756	4.51	211.38	3.535E-18	-17.452		
1100.0	1099.9	1.0662	4.0732	5.0066	5.5762	5.9584	4.29	241.29	2.834E-18	-17.548		
1150.0	1099.9	3.8042	3.8042	5.5089	5.5089	5.9414	4.15	267.81	2.329E-18	-17.633		
1200.0	1099.9	3.5388	5.4225	5.4225	5.4227	5.9247	4.06	289.79	1.947E-18	-17.711		
1250.0	1099.9	3.2769	5.3185	5.3185	5.3770	5.9082	4.00	307.38	1.647E-18	-17.783		
1300.0	1099.9	3.0185	5.2133	5.2133	5.3123	5.8919	3.95	321.26	1.405E-18	-17.852		
1350.0	1099.9	2.8000	2.7634	5.1855	5.2485	5.8758	3.92	332.33	1.206E-18	-17.919		
1400.0	1100.0	2.5115	2.5115	5.1855	5.18600	5.8600	3.89	341.38	1.039E-18	-17.983		
1450.0	1100.0	2.2629	2.2629	5.1233	5.1233	5.8443	3.87	349.13	8.994E-19	-18.046		
1500.0	1100.0	2.0175	2.0175	5.0619	5.0619	5.8288	3.85	356.01	7.805E-19	-18.108		
1600.0	1100.0	1.5359	1.5359	4.9414	4.9414	5.7985	3.81	368.21	5.922E-19	-18.228		
1700.0	1100.0	1.0662	4.8239	3.7689	3.7689	5.7689	3.76	379.68	4.532E-19	-18.344		
1800.0	1100.0	6081	4.7093	3.7400	3.7400	5.7400	3.71	390.94	3.496E-19	-18.456		
1900.0	1100.0	1610	4.5975	3.7119	3.7119	5.6844	3.66	414.43	2.127E-19	-18.566		
2000.0	1100.0	1100	4.4983	3.6883	3.6883	5.6844	3.60	446.2	1.127E-19	-18.672		
2100.0	1100.0	1100	4.3817	3.6575	3.6575	5.6575	3.53	462.77	1.677E-19	-18.776		
2200.0	1100.0	1100	4.2776	3.6313	3.6313	5.6313	3.45	479.87	1.331E-19	-18.876		
2300.0	1100.0	1100	4.1760	3.6057	3.6057	5.6057	3.37	493.67	1.331E-19	-18.973		
2400.0	1100.0	1100	4.0766	3.5807	3.5807	5.5807	3.28	498.18	8.565E-20	-19.067		
2500.0	1100.0	1100	3.9795	3.5562	3.5562	3.5562	3.18	483.73	6.942E-20	-19.159		

Table 6 (Cont.)

EXOSPHERIC TEMPERATURE = 1200 DEGREES

HEIGHT KM	TEMP DEG K	LOG N(N2) /CM3	LOG N(O2) /CM3	LOG N(O) /CM3	LOG N(A) /CM3	LOG N(H) /CM3	MEAN MOL WT	DENSITY SCALE HT KM	DENSITY GM/CM3	LOG DEN GM/CM3	
90.0	183.0	13.7498	13.1687	11.8225	8.6457	28.83	5.46	3.460E-09	-8.461		
92.0	183.3	13.5899	12.9943	12.0533	11.6677	8.4859	5.41	2.394E-09	-8.621		
94.0	184.4	13.4289	12.8125	12.1517	11.5067	8.3249	5.39	1.653E-09	-8.782		
96.0	186.6	13.2679	12.6271	12.1668	11.3457	8.1639	5.39	1.141E-09	-8.943		
98.0	190.2	13.1081	12.4438	12.1219	11.1859	8.0046	5.47	7.896E-10	-9.103		
100.0	195.4	12.9502	12.2665	12.0377	11.0280	7.8462	5.64	5.490E-10	-9.260		
102.0	202.4	12.7950	12.0914	11.9425	10.8132	7.8167	5.61	3.833E-10	-9.416		
104.0	211.3	12.6449	11.9190	11.8470	10.6027	7.7859	5.73	2.693E-10	-9.570		
106.0	222.2	12.4918	11.7519	10.3980	7.7541	5.90	1.909E-10	-9.719			
108.0	235.1	12.3457	11.5874	11.6580	10.2002	7.7215	6.02	1.368E-10	-9.864		
110.0	250.0	12.2045	11.4299	11.5659	10.0102	7.6886	6.37	9.924E-11	-10.003		
115.0	295.5	11.3764	9.0654	11.3473	5.5732	7.6071	7.20	4.735E-11	-10.325		
120.0	350.9	11.5868	10.7452	11.1499	9.1920	7.5301	8.32	2.477E-11	-10.606		
125.0	411.9	11.3355	10.4681	10.9765	8.8634	7.4610	25.05	9.73	1.420E-11	-10.848	
130.0	473.8	11.1188	10.2292	10.8267	8.5803	7.4010	24.61	11.35	8.824E-12	-11.054	
135.0	533.9	10.9302	10.0211	10.6967	8.3333	7.3493	24.21	13.07	5.854E-12	-11.233	
140.0	591.1	10.7638	9.8373	10.5827	8.1149	7.3044	23.84	14.87	4.090E-12	-11.388	
145.0	644.3	10.6152	9.6729	10.4818	7.9189	7.2653	23.50	16.71	2.979E-12	-11.526	
150.0	693.3	10.4809	9.5241	10.3915	7.7410	7.2310	23.17	18.58	2.243E-12	-11.649	
155.0	737.9	10.3582	9.3678	10.3098	7.5776	7.2005	22.87	20.43	1.736E-12	-11.760	
160.0	778.3	10.2450	9.2617	10.2352	7.4259	7.1733	22.57	22.25	1.373E-12	-11.862	
170.0	847.9	10.0402	9.0331	10.1023	7.1498	7.1263	22.03	25.75	9.049E-13	-12.043	
180.0	905.0	9.8570	8.8279	9.9855	6.9006	7.0866	21.54	29.01	6.279E-13	-12.202	
190.0	952.2	9.6891	8.6392	9.8801	6.6705	7.0521	21.08	32.04	4.525E-13	-12.344	
200.0	991.4	9.5326	8.4630	9.7832	6.4549	7.0214	20.65	34.88	3.355E-13	-12.474	
210.0	1024.3	9.3849	8.2962	9.6928	6.2503	6.9935	20.26	37.50	2.545E-13	-12.594	
220.0	1051.8	9.2441	8.1370	9.6074	6.0543	6.9679	19.89	39.99	1.966E-13	-12.706	
230.0	1074.8	9.1088	8.9780	9.5262	5.8655	6.9441	19.56	42.34	1.542E-13	-12.812	
240.0	1094.1	8.9780	7.8356	9.4477	5.6823	6.9217	19.24	44.55	1.225E-13	-12.912	
250.0	1110.3	8.8510	7.6914	9.3729	5.5038	6.9005	18.95	46.63	9.838E-14	-13.007	
260.0	1123.8	8.7270	7.5505	9.2998	5.3293	6.8803	18.68	48.59	7.974E-14	-13.098	
270.0	1135.1	8.6056	7.4124	9.2286	5.1580	6.8609	18.43	50.42	6.516E-14	-13.186	
280.0	1144.5	8.4863	7.2767	9.1589	4.9894	6.8421	18.20	52.15	5.362E-14	-13.271	
290.0	1152.5	8.3689	7.1430	9.0906	4.8232	6.8239	17.99	53.76	4.439E-14	-13.353	
300.0	1159.1	8.2530	7.0110	9.0233	4.6591	6.8061	17.79	55.27	3.695E-14	-13.432	
310.0	1164.7	8.1385	6.8805	8.9570	4.4966	6.7888	17.61	56.69	3.091E-14	-13.510	
320.0	1169.4	8.0251	6.7512	8.8915	4.3357	6.7718	17.44	58.02	2.596E-14	-13.586	
330.0	1173.4	7.9128	6.6231	8.8267	4.1761	6.7550	17.29	59.26	2.189E-14	-13.660	
340.0	1176.8	7.8013	6.4960	8.725	4.0177	6.7385	17.14	60.43	1.852E-14	-13.732	
350.0	1179.6	7.6907	6.3697	8.6989	3.8604	6.7222	17.01	61.52	1.572E-14	-13.803	
360.0	1182.1	7.5808	6.2443	8.6357	3.7041	6.7060	16.89	62.56	1.338E-14	-13.873	
370.0	1184.2	7.4716	6.1197	8.5730	3.5486	6.6901	16.78	63.53	1.142E-14	-13.942	
380.0	1186.0	7.3629	5.9957	8.5107	3.3940	6.6742	16.67	64.44	9.767E-15	-14.010	
390.0	1187.6	7.2548	5.8723	8.4487	3.2401	6.6585	16.57	65.30	8.371E-15	-14.077	
400.0	1188.9	7.1473	5.7495	8.3871	3.0870	6.6495	16.47	66.10	7.190E-15	-14.143	

Table 6 (Cont.)

EXOSPHERIC TEMPERATURE = 1200 DEGREES

HEIGHT KM	TEMP DEG K	LOG N(N2) /CM3	LOG N(O2) /CM3	LOG N(O) /CM3	LOG N(A) /CM3	LOG N(HE) /CM3	LOG N(H) /CM3	MEAN MOL WT	DENSITY HT KM	SCALE HT KM	DENSITY GM/CM3	LOG DEN GM/CM3	
420.0	1191.1	6.9337	5.5056	8.2647	2.7827	6.6120	16.30	16.59	5.331E-15	-14.273			
440.0	1192.8	6.9219	5.2638	8.4809	6.814	16.14	16.93	3.977E-15	-14.525				
460.0	1194.1	6.5117	5.0237	2.1813	6.5512	15.98	70.14	2.983E-15	-14.648				
480.0	1195.1	6.3030	4.7854	7.9039	1.8839	6.5212	15.83	7.126	2.248E-15	-14.769			
500.0	1195.9	6.0958	4.5488	7.7854	1.5885	6.4914	3.9659	15.67	72.30	1.701E-15	-14.889		
520.0	1196.6	5.8999	4.3137	7.6678	1.2951	6.4619	3.9583	15.50	7.329	1.293E-15	-15.006		
540.0	1197.1	5.6854	4.0880	7.5509	1.0036	6.4326	3.9507	15.31	7.426	9.857E-16	-15.122		
560.0	1197.5	5.5822	3.8480	7.4348	*7.139	6.4035	3.9433	15.11	75.21	7.542E-16	-15.237		
580.0	1197.9	5.2803	3.6174	7.3194	*4260	6.3746	3.9359	14.88	76.16	5.791E-16	-15.351		
600.0	1198.2	5.0796	3.3881	7.2047	*1398	6.3459	3.9286	14.63	77.14	4.461E-16			
620.0	1198.4	4.8801	3.1603	7.0907		6.3173	3.9213	14.34	78.17	3.448E-16	-15.462		
640.0	1198.6	4.6818	2.9338	6.9774		6.2889	3.9141	14.01	79.27	2.674E-16	-15.573		
660.0	1198.8	4.4847	2.7086	6.8648		6.2608	3.9069	13.65	80.45	2.082E-16	-15.682		
680.0	1198.9	4.2887	2.4848	6.7529		6.2227	3.8998	13.24	81.75	1.627E-16	-15.789		
700.0	1199.0	4.0939	2.2622	6.6416		6.2049	3.8928	12.80	83.00	1.276E-16	-15.894		
720.0	1199.1	3.9002	2.0410	6.5309		6.1772	3.8858	12.33	84.82	1.006E-16	-15.997		
740.0	1199.2	3.7076	1.88210	6.4209		6.1496	3.8788	11.82	86.65	7.966E-17	-16.099		
760.0	1199.3	3.5161	1.6023	6.3116		6.1223	3.8719	11.28	86.73	6.341E-17	-16.198		
780.0	1199.4	3.3257	1.3848	6.2028		6.0950	3.8650	10.73	91.11	5.076E-17	-16.294		
800.0	1199.4	3.1364	1.1685	6.0947		6.0680	3.8582	10.17	93.85	4.088E-17	-16.388		
820.0	1199.5	2.9482	9535	5.9871		6.0411	3.8514	9.61	96.97	3.315E-17	-16.480		
840.0	1199.5	2.7610	7397	5.8802		6.0143	3.8446	9.06	100.56	2.707E-17	-16.568		
860.0	1199.6	2.5748	5270	5.7739		5.9877	3.8379	8.53	104.67	2.227E-17	-16.652		
880.0	1199.6	2.3897	3156	5.6682		5.9613	3.8313	8.02	109.37	1.847E-17	-16.733		
900.0	1199.7	2.2056	1053	5.5630		5.9350	3.8246	7.55	114.72	1.545E-17	-16.811		
920.0	1199.7	2.0225		5.4584		5.9088	3.8180	7.11	120.77	1.304E-17	-16.885		
940.0	1199.7	1.8404		5.3544		5.8828	3.8115	6.71	127.59	1.110E-17	-16.955		
960.0	1199.7	1.6593		5.2510		5.8569	3.8049	6.35	135.20	9.528E-18	-17.021		
980.0	1199.8	1.4793		5.1482		5.8312	3.7984	6.03	143.62	8.254E-18	-17.083		
1000.0	1199.8	1.3002		5.0459		5.8056	3.7920	5.74	152.84	7.211E-18	-17.142		
1050.0	1199.8	8567	47926	5.7422		5.7760	5.17	179.14	5.329E-18	-17.273			
1100.0	1199.8	4192	45427	56797		5.7603	4.78	208.96	4.115E-18	-17.386			
1150.0	1199.9		42962	56180		5.7447	4.50	240.98	3.292E-18	-17.482			
1200.0	1199.9		40529	55571		5.7294	4.32	270.05	2.706E-18	-17.568			
1250.0	1199.9		38128	54971		5.7143	4.19	297.03	2.269E-18	-17.644			
1300.0	1199.9		35758	54378		5.6993	4.11	320.06	1.930E-18	-17.715			
1350.0	1199.9		33420	53793		5.6846	4.05	339.05	1.658E-18	-17.780			
1400.0	1199.9		31111	53215		5.6701	4.01	354.46	1.436E-18	-17.843			
1450.0	1199.9		28832	52645		5.6557	3.98	367.12	1.250E-18	-17.903			
1500.0	1200.0		26583	52082		5.6415	3.96	377.65	1.093E-18	-17.961			
1600.0	1200.0		22168	50978		5.6137	3.92	394.45	8.437E-19	-18.074			
1700.0	1200.0		17863	49901		5.5866	3.90	408.28	6.577E-19	-18.182			
1800.0	1200.0		13663	48850		5.5601	3.87	420.65	5.167E-19	-18.287			
1900.0	1200.0		1200.0	45566		5.5343	3.84	432.00	4.087E-19	-18.389			
2000.0	1200.0		11660	48825		5.6824	3.82	444.46	3.254E-19	-18.488			
2100.0	1200.0		11660	45847		5.4845	3.78	456.31	2.606E-19	-18.584			
2200.0	1200.0		11660	44893		5.4605	3.75	468.54	2.099E-19	-18.678			
2300.0	1200.0		11660	43961		5.4370	3.71	480.09	1.700E-19	-18.769			
2400.0	1200.0		11660	43050		5.4141	3.66	493.90	1.385E-19	-18.859			
2500.0	1200.0		11660	42160		5.3916	3.61	507.25	1.134E-19	-18.945			

Table 6 (Cont.)

EXOSPHERIC TEMPERATURE = 1300 DEGREES

HEIGHT KM	TEMP DEG K	LOG N(N2) /CM3	LOG N(O2) /CM3	LOG N(O) /CM3	LOG N(H) /CM3	MEAN MOL WT	DENSITY SCALE HT KM	DENSITY GM/CM3	LOG DEN GM/CM3
90.0	183.0	13.7498	13.1687	11.8225	8.6457	28.83	5.46	3.460E-09	-8.461
92.0	183.3	13.5899	12.9942	12.0533	11.6677	28.63	5.41	2.394E-09	-8.621
94.0	184.4	13.4288	12.8124	12.1516	11.5066	28.37	5.39	1.653E-09	-8.782
96.0	186.7	13.2677	12.6269	11.3455	8.1637	28.09	5.40	1.40E-09	-8.943
98.0	190.5	13.1077	12.4435	12.1215	11.1855	27.84	5.46	7.889E-10	-9.103
100.0	195.9	12.9497	12.2659	12.0371	11.0275	27.64	5.53	5.483E-10	-9.261
102.0	203.2	12.7944	12.0907	11.9416	10.8127	27.44	5.61	3.827E-10	-9.417
104.0	212.4	12.6411	11.9185	11.8458	10.6025	27.23	5.73	2.689E-10	-9.570
106.0	223.8	12.4911	11.7503	11.7504	10.3981	27.02	5.90	1.906E-10	-9.720
108.0	237.2	12.3552	11.5873	11.6562	10.2009	26.80	6.12	1.366E-10	-9.864
110.0	252.7	12.2043	11.4303	11.5640	10.0117	26.59	6.38	9.919E-11	-10.004
115.0	300.2	11.8776	11.0676	11.3453	9.5775	26.05	7.24	4.743E-11	-10.324
120.0	357.8	11.5900	10.7500	11.1484	9.2000	25.55	8.38	2.493E-11	-10.603
125.0	421.4	11.3412	10.4559	10.9758	8.8754	25.09	9.82	1.436E-11	-10.843
130.0	485.8	11.1271	10.2402	10.8270	8.5965	24.66	11.48	8.967E-12	-11.047
135.0	548.8	10.9410	10.0351	10.6980	8.3537	24.28	13.23	5.978E-12	-11.223
140.0	608.9	10.7770	9.8542	10.5850	8.1390	23.92	15.05	4.195E-12	-11.377
145.0	665.5	10.6307	9.6926	10.4849	7.9468	23.59	16.92	3.067E-12	-11.513
150.0	718.1	10.4986	9.5664	10.3953	7.7725	23.27	18.82	2.317E-12	-11.635
155.0	766.6	10.3781	9.4128	10.3143	7.6128	22.98	20.71	1.799E-12	-11.745
160.0	811.0	10.2671	9.2894	10.2404	7.4648	22.70	22.59	1.428E-12	-11.845
170.0	888.6	10.0671	9.0666	10.1091	7.1965	22.18	26.23	9.474E-13	-12.023
180.0	953.3	9.8890	8.8676	9.9944	6.9556	21.71	29.67	6.623E-13	-12.179
190.0	1027.5	9.7269	8.8558	9.8944	6.7346	21.27	32.91	4.811E-13	-12.318
200.0	1053.0	9.5766	8.5169	9.7974	6.5285	20.87	35.98	3.598E-13	-12.444
210.0	1091.4	9.3555	8.3579	9.7101	6.3340	20.49	38.83	2.754E-13	-12.560
220.0	1123.8	9.3017	8.2068	9.6282	6.1485	20.13	41.55	2.097E-13	-12.668
230.0	1151.0	9.1736	8.0620	9.5506	5.9703	19.81	44.11	1.700E-13	-12.769
240.0	1173.9	9.0503	7.9224	9.4766	5.7981	19.50	46.53	1.364E-13	-12.865
250.0	1193.0	8.9309	7.7870	9.4053	5.6308	19.21	48.80	1.106E-13	-12.956
260.0	1209.1	8.8146	7.6550	9.3365	5.4675	18.95	50.95	9.047E-14	-13.043
270.0	1222.6	8.7011	7.5260	9.2695	5.3076	18.70	52.95	7.463E-14	-13.127
280.0	1233.8	8.5898	7.3994	9.2042	5.1506	18.47	54.84	6.199E-14	-13.208
290.0	1243.3	8.4803	7.2749	9.1403	4.9959	18.25	56.60	5.181E-14	-13.286
300.0	1251.2	8.3725	7.1521	9.0776	4.8434	18.05	58.26	4.353E-14	-13.361
310.0	1257.9	8.2661	7.0309	9.0158	4.6925	17.87	59.80	3.675E-14	-13.435
320.0	1263.5	8.1608	6.9109	8.9584	4.5433	17.70	61.27	3.115E-14	-13.507
330.0	1268.2	8.0566	6.7921	8.8946	4.3953	17.54	62.64	2.651E-14	-13.577
340.0	1272.3	7.9533	6.6743	8.8350	4.2486	17.39	63.94	2.263E-14	-13.645
350.0	1275.7	7.8508	6.5573	8.7760	4.1029	17.25	65.15	1.939E-14	-13.713
360.0	1278.6	7.7490	6.4412	8.7174	3.9582	17.12	66.30	1.665E-14	-13.779
370.0	1281.1	7.6479	6.3258	8.6593	3.8143	17.00	67.39	1.434E-14	-13.844
380.0	1283.3	7.5473	6.2111	8.6016	3.6713	16.89	68.41	1.237E-14	-13.908
390.0	1285.2	7.4474	6.0970	8.5442	3.5290	16.78	69.38	1.070E-14	-13.971
400.0	1286.8	7.3479	5.9835	8.4874	3.3874	16.68	70.29	9.274E-15	-14.033

Table 6 (Cont.)

EXOSPHERIC TEMPERATURE = 1300 DEGREES

HEIGHT KM	TEMP DEG K	LOG N(N2) /CM3	LOG N(O2) /CM3	LOG N(O) /CM3	LOG N(A) /CM3	LOG N(He) /CM3	LOG N(H) /CM3	MEAN MOL WT	DENSITY SCALE HT KM	DENSITY GM/CM3	LOG DEN GM/CM3
420.0	1289.4	7.1504	5.7580	8.3740	3.1062	6.6266	16.50	11.98	7.001E-15	-14.155	
440.0	1291.4	6.9546	5.5345	8.2619	2.8273	6.5983	16.34	7.352	5.319E-15	-14.274	
460.0	1293.0	6.7604	5.3127	8.1507	2.5505	6.5703	16.18	74.91	4.062E-15	-14.391	
480.0	1294.2	6.5676	5.0926	8.0404	2.2758	6.5426	16.04	76.8	3.117E-15	-14.506	
500.0	1295.1	6.3762	4.8740	7.9310	2.0051	6.5151	3.7806	15.89	77.37	2.403E-15	-14.619
520.0	1295.9	6.1861	4.6568	7.8223	1.7320	6.4878	3.7735	15.75	78.48	1.859E-15	-14.731
540.0	1296.5	5.9973	4.4412	7.7144	1.4628	6.4607	3.7665	15.60	79.53	1.443E-15	-14.841
560.0	1297.0	5.8096	4.2269	7.6071	1.1953	6.4338	3.7596	15.44	80.55	1.124E-15	-14.949
580.0	1297.5	5.6232	4.0139	7.5006	9.9294	6.4071	3.7527	15.26	81.55	8.782E-16	-15.056
600.0	1297.8	5.4379	3.8022	7.3947	6.6652	6.3806	3.7459	15.07	82.54	6.882E-16	-15.162
620.0	1298.1	5.2537	3.5919	7.2894	4.026	6.3542	3.7392	14.86	83.53	5.409E-16	-15.267
640.0	1298.3	5.0706	3.3827	7.1848	1.1416	6.3280	3.7326	14.62	84.55	4.264E-16	-15.370
660.0	1298.5	4.8886	3.1749	7.0809	6.3020	3.7259	14.36	85.62	3.370E-16	-15.472	
680.0	1298.7	4.7075	2.9682	6.9775	6.2761	3.7194	14.07	86.75	2.672E-16	-15.573	
700.0	1298.9	4.5278	2.7628	6.8748	6.2504	3.7129	13.74	87.96	2.125E-16	-15.673	
720.0	1299.0	4.3490	2.5585	6.7726	6.2248	3.7064	13.39	89.26	1.696E-16	-15.771	
740.0	1299.1	4.1712	2.3554	6.6711	6.1994	3.6999	13.00	90.69	1.358E-16	-15.867	
760.0	1299.2	4.0944	2.1535	6.5701	6.1741	3.6935	12.58	92.26	1.091E-16	-15.962	
780.0	1299.3	3.8187	1.9527	6.4697	6.1490	3.6872	12.13	94.01	8.803E-17	-16.055	
800.0	1299.3	3.6439	1.7531	6.3698	6.1240	3.6809	11.66	95.99	7.131E-17	-16.147	
820.0	1299.4	3.4701	1.5546	6.2706	6.0991	3.6746	11.17	98.18	5.803E-17	-16.236	
840.0	1299.5	3.2973	1.3572	6.1719	6.0744	3.6684	10.67	100.66	4.746E-17	-16.324	
860.0	1299.5	3.1255	1.1609	6.0737	6.0499	3.6622	10.16	103.46	3.901E-17	-16.419	
880.0	1299.6	2.9546	9.657	5.9761	6.0255	3.6560	9.65	106.63	3.224E-17	-16.492	
900.0	1299.6	2.7846	7.716	5.8791	6.012	3.6499	9.15	110.21	2.681E-17	-16.572	
920.0	1299.6	2.6156	5.7825	5.7716	5.9770	3.6438	8.66	114.27	2.243E-17	-16.649	
940.0	1299.7	2.4475	3.866	5.6865	5.9530	3.6377	8.20	118.84	1.889E-17	-16.724	
960.0	1299.7	2.2804	1.956	5.5911	5.9291	3.6317	7.76	123.99	1.602E-17	-16.795	
980.0	1299.7	2.1142	0.0058	5.4961	5.9054	3.6257	7.35	129.76	1.368E-17	-16.864	
1000.0	1299.7	1.9489	5.4017	5.4017	5.8817	3.6198	6.96	136.19	1.177E-17	-16.929	
1050.0	1299.8	1.5395	1.5167	5.1679	5.8232	3.6050	6.15	155.37	8.343E-18	-17.079	
1100.0	1299.8	1.1356	4.9372	4.9372	5.7655	3.5905	5.53	179.12	6.179E-18	-17.209	
1150.0	1299.8	0.7371	4.7096	4.7096	5.7086	3.5761	5.07	206.92	4.765E-18	-17.322	
1200.0	1299.9	0.3439	4.4851	4.4851	5.6524	3.5620	4.74	237.42	3.803E-18	-17.420	
1250.0	1299.9	0.0234	4.2634	4.2634	5.5970	3.5480	4.50	268.80	3.121E-18	-17.506	
1300.0	1299.9	0.4047	4.0447	4.0447	5.5422	3.5342	4.34	299.07	2.617E-18	-17.582	
1350.0	1299.9	3.8289	3.8289	3.8289	5.4882	3.5206	4.23	326.68	2.230E-18	-17.652	
1400.0	1299.9	3.6158	3.6158	3.6158	5.4349	3.5072	4.15	350.77	1.924E-18	-17.716	
1450.0	1299.9	3.4054	3.4054	3.4054	5.3823	3.4939	4.09	371.28	1.675E-18	-17.776	
1500.0	1299.9	3.1977	3.1977	3.1977	5.3303	3.4808	4.05	388.46	1.469E-18	-17.833	
1600.0	1300.0	1.0000	2.7902	2.7902	5.2284	3.4552	4.00	414.87	1.146E-18	-17.941	
1700.0	1300.0	1.0000	2.3928	2.3928	5.1290	3.4301	3.97	434.51	9.055E-19	-18.043	
1800.0	1300.0	1.0000	2.0051	2.0051	5.0320	3.4057	3.94	450.28	7.223E-19	-18.141	
1900.0	1300.0	1.0000	1.6269	1.6269	4.9373	3.3819	3.93	464.27	5.805E-19	-18.236	
2000.0	1300.0	1.0000	1.2577	1.2577	4.8450	3.3586	3.91	477.37	4.694E-19	-18.328	
2100.0	1300.0	1.0000	0.8972	0.8972	4.7548	3.3359	3.89	490.00	3.817E-19	-18.418	
2200.0	1300.0	1.0000	0.5451	0.5451	4.6667	3.3137	3.88	502.67	3.121E-19	-18.506	
2300.0	1300.0	1.0000	0.2013	0.2013	4.5807	3.2921	3.86	515.43	2.564E-19	-18.591	
2400.0	1300.0	1.0000	0.4966	0.4966	4.4966	3.2709	3.83	528.20	2.117E-19	-18.674	
2500.0	1300.0	1.0000	0.4144	0.4144	4.4144	3.2502	3.81	541.35	1.756E-19	-18.756	

Table 6 (Cont.)

EXOSPHERIC TEMPERATURE = 1400 DEGREES

HEIGHT KM	TEMP DEG K	LOG N(N2) /CM3	LOG N(O2) /CM3	LOG N(O) /CM3	LOG N(A) /CM3	LOG N(HE) /CM3	MEAN MOL WT	DENSITY SCALE HT KM	DENSITY GM/CM3	LOG DEN GM/CN3
90.0	183.0	13.7498	13.1687	11.8225	11.8276	8.6457	28.83	5.46	3.460E-09	-8.461
92.0	183.3	13.5888	12.9942	12.0533	11.6676	8.4858	28.63	5.41	2.394E-09	-8.621
94.0	184.5	13.4287	12.8123	12.1515	11.5065	8.3247	28.37	5.38	1.652E-09	-8.782
96.0	186.9	13.2675	12.6267	12.1663	11.3453	8.1634	28.09	5.40	1.140E-09	-8.943
98.0	190.8	13.1073	12.4431	12.1212	11.1851	8.0033	27.84	5.46	7.882E-10	-9.103
100.0	196.4	12.9492	12.2654	12.0366	11.0270	7.8451	27.64	5.52	5.476E-10	-9.262
102.0	204.9	12.7937	12.0902	11.9408	10.8123	7.8151	27.44	5.60	3.822E-10	-9.418
104.0	213.5	12.6645	11.9179	11.8447	10.6022	7.7837	27.23	5.73	2.685E-10	-9.571
106.0	225.3	12.4405	11.7499	11.7490	10.3982	7.7512	27.02	5.91	1.903E-10	-9.720
108.0	239.2	12.3448	11.5872	11.6547	10.2016	7.7179	26.81	6.13	1.365E-10	-9.865
110.0	255.3	12.2042	11.4306	11.5622	10.0131	7.6843	26.59	6.40	9.913E-11	-10.004
115.0	304.4	11.8886	10.696	11.3435	9.5814	7.6013	26.07	7.27	4.752E-11	-10.323
120.0	364.1	11.5929	10.7563	11.1470	9.2071	7.5234	25.57	8.44	2.507E-11	-10.601
125.0	430.0	11.3462	10.4828	10.9751	8.8861	7.4537	25.12	9.91	1.450E-11	-10.839
130.0	496.8	11.1344	10.2498	10.8272	8.6108	7.3935	24.71	11.60	9.095E-12	-11.041
135.0	562.3	10.906	10.0475	10.6999	8.3715	7.3416	24.33	13.37	6.088E-12	-11.216
140.0	625.2	10.7886	9.8690	10.5869	8.1602	7.2965	23.99	15.21	4.288E-12	-11.368
145.0	684.9	10.6643	9.7097	10.4875	7.9712	7.2569	23.67	17.10	3.145E-12	-11.502
150.0	740.8	10.5140	9.5658	10.3985	7.8000	7.2221	23.36	19.02	2.384E-12	-11.623
155.0	792.8	10.3953	9.4344	10.3181	7.6433	7.1911	23.08	20.95	1.856E-12	-11.731
160.0	841.0	10.2861	9.3133	10.2447	7.4984	7.1632	22.81	22.87	1.477E-12	-11.831
170.0	926.2	10.0899	9.0952	10.1147	7.2366	7.1152	22.31	26.63	9.855E-13	-12.006
180.0	998.5	9.9161	8.9014	10.0014	7.0027	7.0748	21.86	30.24	6.931E-13	-12.159
190.0	1059.9	10.7587	8.7252	9.9004	6.7891	7.0399	21.44	33.67	5.067E-13	-12.295
200.0	1111.9	9.6135	8.5623	9.8085	6.5910	7.0093	21.05	36.95	3.817E-13	-12.418
210.0	1156.2	9.4779	8.4098	9.7238	6.4048	6.9818	20.69	40.01	2.943E-13	-12.531
220.0	1193.6	9.3498	8.2054	9.6447	6.2280	6.9569	20.35	42.96	2.633E-13	-12.636
230.0	1225.3	9.2278	8.1277	9.5702	6.0589	6.9340	20.03	45.74	1.846E-13	-12.734
240.0	1252.0	9.1107	7.9953	9.4993	5.8959	6.9128	19.73	48.38	1.492E-13	-12.826
250.0	1274.4	8.9977	7.8673	9.4314	5.7380	6.8930	19.45	50.85	1.220E-13	-12.914
260.0	1293.2	8.8880	7.7429	9.3661	5.5844	6.8743	19.19	53.19	1.007E-13	-12.997
270.0	1309.0	8.811	7.6216	9.3028	5.4342	6.8565	18.95	55.37	8.373E-14	-13.077
280.0	1322.2	8.6766	7.5028	9.2412	5.2869	6.8395	18.72	57.42	7.013E-14	-13.154
290.0	1333.3	8.5740	7.3861	9.1810	5.1422	6.8231	18.50	59.33	5.909E-14	-13.228
300.0	1342.6	8.4730	7.2712	9.1221	4.9995	6.8072	18.30	61.13	5.005E-14	-13.301
310.0	1350.4	8.3734	7.1578	9.0641	4.8586	6.7918	18.12	62.81	4.259E-14	-13.371
320.0	1357.1	8.2751	7.0458	9.0070	4.7192	6.7768	17.94	64.40	3.640E-14	-13.439
330.0	1362.6	8.1778	6.9349	8.9507	4.5813	6.7620	17.78	65.90	3.122E-14	-13.506
340.0	1367.4	8.0815	6.8251	8.8950	4.4445	6.7475	17.62	67.31	2.687E-14	-13.571
350.0	1371.4	7.9859	6.7161	8.8399	4.3088	6.7332	17.48	68.63	2.319E-14	-13.635
360.0	1374.9	7.8911	6.6079	8.7853	4.1740	6.7192	17.34	69.89	2.007E-14	-13.697
370.0	1377.8	7.7969	6.5005	8.7311	4.0401	6.7053	17.22	71.09	1.742E-14	-13.759
380.0	1380.4	7.7033	6.3337	8.6773	3.9070	6.6915	17.10	72.22	1.515E-14	-13.820
390.0	1382.5	7.6103	6.2875	8.6239	3.7746	6.6779	16.99	73.29	1.320E-14	-13.879
400.0	1384.0	7.5178	6.1819	8.5708	3.6429	6.6644	16.89	74.31	1.153E-14	-13.938

Table 6 (Cont.)

EXOSPHERIC TEMPERATURE = 1400 DEGREES

HEIGHT KM	TEMP DEG K	LOG N(N2) /CM3	LOG N(O2) /CM3	LOG NO /CM3	LOG N(A) /CM3	LOG N(He) /CM3	LOG NH /CM3	MEAN MOL WT	DENSITY HT KM	SCALE HT KM	DENSITY GM/CM3	LOG DEN GM/CM3
420.0	1387.5	7.3340	5.9722	8.4654	3.3814	6.6377	1.6.70	7.6.21	8.841E-15	-14.054		
440.0	1389.9	7.1520	5.7644	8.3611	3.2221	6.6113	1.6.53	7.7.93	6.020E-15	-14.16		
460.0	1391.7	6.9715	5.5583	8.2574	2.8649	6.5853	1.6.37	7.9.50	5.290E-15	-14.277		
480.0	1393.1	6.7923	5.3537	8.1553	2.6096	6.5594	1.6.23	8.0.95	4.123E-15	-14.385		
500.0	1394.3	6.6145	5.1506	8.0536	2.3561	6.5339	3.6208	8.2.29	3.227E-15	-14.491		
520.0	1395.2	6.4379	4.9489	7.9526	2.1044	6.5085	1.6.09	8.3.53	3.227E-15	-14.59		
540.0	1395.9	6.2624	4.7485	7.8523	1.8543	6.4833	3.6076	8.4.70	1.999E-15	-14.69		
560.0	1396.5	6.0881	4.5494	7.7526	1.6058	6.4583	3.6012	15.68	85.82	1.581E-15	-14.801	
580.0	1397.0	5.9149	4.3516	7.6536	1.3589	6.4335	3.5948	15.54	86.90	1.254E-15	-14.902	
600.0	1397.4	5.7428	4.1550	7.5553	1.1135	6.4089	3.5885	15.39	87.95	9.977E-16	-15.001	
620.0	1397.8	5.5717	3.9596	7.4575	.8696	6.3864	3.5822	15.22	88.97	7.958E-16	-15.099	
640.0	1398.0	5.4017	3.7654	7.3604	.6272	6.3600	3.5760	15.04	90.00	6.364E-16	-15.196	
660.0	1398.3	5.2327	3.5724	7.2638	.3862	6.3358	3.5698	14.84	91.04	5.102E-16	-15.292	
680.0	1398.5	5.0646	3.3804	7.1678	.1466	6.3118	3.5637	14.62	92.11	4.101E-16	-15.387	
700.0	1398.7	4.8976	3.1896	7.0724		6.2879	3.5537	14.38	93.21	3.305E-16	-15.481	
720.0	1398.8	4.7315	3.0000	6.9775		6.2642	3.5516	14.12	94.38	2.670E-16	-15.573	
740.0	1398.9	4.5664	2.8114	6.8832		6.2405	3.5457	13.83	95.61	2.163E-16	-15.665	
760.0	1399.0	4.4023	2.6238	6.7894		6.2171	3.5397	13.51	96.93	1.575E-16	-15.755	
780.0	1399.1	4.2390	2.4374	6.6962		6.1937	3.5338	13.16	98.35	1.432E-16	-15.844	
800.0	1399.2	4.0767	2.2520	6.6035		6.1705	3.5280	12.79	99.91	1.170E-16	-15.932	
820.0	1399.3	3.9154	2.0677	6.5113		6.1475	3.5221	12.40	101.60	9.595E-17	-16.018	
840.0	1399.4	3.7549	1.8844	6.4197		6.1245	3.5163	11.98	103.47	7.895E-17	-16.103	
860.0	1399.4	3.5953	1.7021	6.3285		6.1017	3.5106	11.54	105.53	6.519E-17	-16.186	
880.0	1399.5	3.4366	1.5208	6.2379		6.0790	3.5049	11.09	107.83	5.405E-17	-16.267	
900.0	1399.5	3.2788	1.3406	6.1477		6.0565	3.4992	10.63	11.040	4.499E-17	-16.347	
920.0	1399.6	3.1218	1.1613	6.0581		6.0341	3.4935	10.16	113.27	3.762E-17	-16.425	
940.0	1399.6	2.9658	9830	5.9689		6.0118	3.4879	9.70	116.47	3.161E-17	-16.500	
960.0	1399.6	2.8106	8057	5.8803		5.9896	3.4823	9.24	120.05	2.6669E-17	-16.574	
980.0	1399.7	2.6562	6294	5.7921		5.9675	3.4767	8.80	124.05	2.265E-17	-16.645	
1000.0	1399.7	2.5027	4541	5.7044		5.9456	3.4712	8.37	128.51	1.933E-17	-16.714	
1050.0	1399.7	2.1225	.0198	5.4873		5.8913	3.4575	7.38	141.95	1.334E-17	-16.875	
1100.0	1399.8	1.7475	5.2731	5.2731		5.8377	3.4440	6.56	159.17	9.563E-18	-17.019	
1150.0	1399.8	1.3775	5.0618	5.0618		5.7848	3.4307	5.89	180.54	7.017E-18	-17.148	
1200.0	1399.8	1.0124	4.8533	4.8533		5.7326	3.4175	5.38	205.95	5.490E-18	-17.260	
1250.0	1399.9	.6520	4.6475	4.6475		5.6811	3.4045	5.00	234.82	4.373E-18	-17.359	
1300.0	1399.9	.2965	4.4444	4.4444		5.6303	3.3917	4.72	265.89	3.580E-18	-17.446	
1350.0	1399.9		4.2439	4.2439		5.5802	3.3791	4.51	297.54	2.998E-18	-17.523	
1400.0	1399.9		4.0460	4.0460		5.5307	3.3666	4.36	328.14	2.555E-18	-17.593	
1450.0	1399.9		3.8507	3.8507		5.4888	3.3543	4.25	356.50	2.208E-18	-17.656	
1500.0	1399.9		3.6579	3.6579		5.4335	3.3422	4.18	381.83	1.928E-18	-17.715	
1600.0	1399.9		3.2794	3.2794		5.3389	3.3183	4.08	422.69	1.504E-18	-17.823	
1700.0	1400.0		2.9104	2.9104		5.2465	3.2951	4.02	452.78	1.197E-18	-17.922	
1800.0	1400.0		2.5505	2.5505		5.1565	3.2724	3.99	475.43	9.655E-19	-18.015	
1900.0	1400.0		2.1992	2.1992		5.0886	3.2503	3.97	493.79	7.855E-19	-18.105	
2000.0	1400.0		1.8564	1.8564		4.9829	3.2287	3.96	509.70	6.436E-19	-18.191	
2100.0	1400.0		1.5216	1.5216		4.8991	3.2076	3.95	524.18	5.304E-19	-18.275	
2200.0	1400.0		1.1947	1.1947		4.8173	3.1870	3.94	538.18	4.394E-19	-18.357	
2300.0	1400.0		1.0460	1.0460		4.7374	3.1669	3.93	551.90	3.657E-19	-18.437	
2400.0	1400.0		1.0000	1.0000		4.6594	3.1472	3.91	565.41	3.058E-19	-18.515	
2500.0	1400.0		1.0000	1.0000		4.5831	3.1280	3.90	579.15	2.568E-19	-18.590	

Table 6 (Cont.)

EXOSPHERIC TEMPERATURE = 1500 DEGREES

HEIGHT KM	TEMP DEG K	LOG N(N2) /CM3	LOG N(O2) /CM3	LOG N(O) /CM3	LOG N(A) /CM3	LOG N(HE) /CM3	MEAN MOL WT		DENSITY SCALE HT KM	DENSITY GM/CM3	LOG DEN GM/CM3
							DENSITY	MOL WT			
90.0	183.0	13.7498	13.1687	11.8225	11.8276	8.6457	28.83	5.46	3.460E-09	-8.461	
92.0	183.3	13.5898	12.9942	12.0533	11.6676	8.4858	28.63	5.41	2.394E-09	-8.621	
94.0	184.5	13.4287	12.8122	12.1514	11.5065	8.3246	28.37	5.38	1.652E-09	-8.782	
96.0	187.0	13.2673	12.6265	12.1661	11.3451	8.1632	28.09	5.39	1.139E-09	-8.943	
98.0	191.0	13.1070	12.4428	12.1208	11.1848	8.0029	27.84	5.45	7.816E-10	-9.104	
100.0	196.8	12.9487	12.2649	12.0361	11.0265	7.8447	27.64	5.52	5.470E-10	-9.262	
102.0	204.6	12.7932	12.0897	11.9401	10.8119	7.8144	27.44	5.60	3.817E-10	-9.418	
104.0	214.5	12.6399	11.9175	11.8437	10.6220	7.7827	27.24	5.73	2.681E-10	-9.572	
106.0	226.6	12.4899	11.7496	11.7478	10.3983	7.7499	27.03	5.91	1.901E-10	-9.721	
108.0	241.0	12.3444	11.5871	11.6532	10.2021	7.7163	26.81	6.14	1.339E-10	-9.865	
110.0	257.6	12.2040	11.4309	11.5607	10.0144	7.66825	26.60	6.41	9.908E-11	-10.004	
115.0	308.3	11.8796	11.0714	11.3419	9.5849	7.5989	26.08	7.30	4.760E-11	-10.322	
120.0	370.0	11.5954	10.7581	11.1457	9.2135	7.5205	25.60	8.49	2.59E-11	-10.599	
125.0	438.0	11.3507	10.4890	10.9744	8.8956	7.4506	25.15	9.99	1.462E-11	-10.835	
130.0	507.0	11.1409	10.2584	10.8274	8.6236	7.3903	24.75	11.70	9.211E-12	-11.036	
135.0	574.7	10.9590	10.0584	10.7001	8.3074	7.3383	24.39	13.50	6.189E-12	-11.208	
140.0	640.2	10.7989	9.8822	10.5886	8.1791	7.2931	24.05	15.35	4.313E-12	-11.359	
145.0	702.7	10.6562	9.7250	10.4898	7.9928	7.2534	23.74	17.26	3.217E-12	-11.493	
150.0	761.7	10.5276	9.5830	10.4013	7.8243	7.283	23.44	19.20	2.45E-12	-11.612	
155.0	817.1	10.4104	9.4535	10.3213	7.6702	7.1870	23.17	21.16	1.998E-12	-11.719	
160.0	868.7	10.3028	9.3343	10.2484	7.5280	7.1589	22.91	23.11	1.522E-12	-11.818	
170.0	961.4	10.1098	9.1202	10.1193	7.2716	7.1104	22.43	26.97	1.020E-12	-11.991	
180.0	1041.1	9.9395	8.9306	10.0072	7.0435	7.0695	21.99	30.71	7.09E-13	-12.142	
190.0	1109.6	9.7590	8.7590	9.9076	6.8363	7.034	21.59	34.32	5.299E-13	-12.276	
200.0	1168.3	9.6450	8.6012	9.8175	6.6448	7.0035	21.21	37.79	4.055E-13	-12.396	
210.0	1218.6	9.5139	8.4541	9.7348	6.4657	6.9761	20.86	41.07	3.115E-13	-12.507	
220.0	1261.4	9.3906	8.3155	9.6580	6.2963	6.9513	20.54	44.23	2.45E-13	-12.608	
230.0	1297.8	9.2737	8.1837	9.5859	6.1348	6.9288	20.23	47.24	1.980E-13	-12.703	
240.0	1328.5	9.1620	8.0575	9.5177	5.9198	6.9019	19.94	50.10	1.62E-13	-12.793	
250.0	1354.4	9.0544	7.9358	9.4527	5.8300	6.8886	19.67	52.78	1.327E-13	-12.877	
260.0	1376.2	8.9504	7.8179	9.3903	5.6846	6.8704	19.42	55.31	1.103E-13	-12.957	
270.0	1394.4	8.8492	7.7032	9.3301	5.5427	6.8532	19.18	57.68	9.223E-14	-13.034	
280.0	1409.7	8.7504	7.5910	9.2716	5.4039	6.8368	18.95	59.90	7.797E-14	-13.108	
290.0	1422.6	8.6537	7.4811	9.2147	5.2676	6.8211	18.74	61.97	6.617E-14	-13.179	
300.0	1433.4	8.5586	7.3730	9.1590	5.1335	6.8050	18.54	63.91	5.665E-14	-13.248	
310.0	1442.5	8.4650	7.2665	9.1043	5.0012	6.7913	18.35	65.73	4.838E-14	-13.315	
320.0	1450.1	8.3727	7.1613	9.0506	4.8704	6.7770	18.17	67.45	4.163E-14	-13.381	
330.0	1456.6	8.2814	7.0573	8.9976	4.7411	6.7630	18.00	69.05	3.596E-14	-13.444	
340.0	1462.1	8.1910	6.9543	8.9453	4.6129	6.7493	17.85	70.58	3.166E-14	-13.506	
350.0	1466.8	8.1015	6.8522	8.8936	4.4858	6.7359	17.70	72.01	2.708E-14	-13.567	
360.0	1470.8	8.0127	6.7509	8.8423	4.3597	6.7226	17.56	73.38	2.360E-14	-13.627	
370.0	1474.2	7.9245	6.6504	8.7916	4.2344	6.7055	17.43	74.67	2.022E-14	-13.686	
380.0	1477.2	7.8369	6.5504	8.7412	4.1099	6.6966	17.31	75.89	1.866E-14	-13.743	
390.0	1479.7	7.7499	6.4511	8.6911	3.9861	6.6838	17.19	77.07	1.564E-14	-13.800	
400.0	1481.9	7.6633	6.3524	8.6414	3.8629	6.6711	17.09	78.19	1.393E-14	-13.856	

Table 6 (Cont.)

EXOSPHERIC TEMPERATURE = 1500 DEGREES

HEIGHT KM	TEMP DEG K	LOG N(N2) /CM3	LOG N(O2) /CM3	LOG N(O) /CM3	LOG N(A) /CM3	LOG N(He) /CM3	LOG N(H) /CM3	MEAN MOL WT	DENSITY HT KM	DENSITY SCALE	DENSITY GM/CM3	LOG DEN GM/CM3
420.0	1485.5	7.4916	6.1563	8.5429	3.6185	6.6461	16.89	80.28	1.082E-14	-13.966		
440.0	1488.3	7.3215	5.9621	8.4454	3.3762	6.6214	16.71	82.18	8.460E-15	-14.073		
460.0	1490.4	7.1528	5.7695	8.3488	3.1359	6.5970	16.55	83.93	6.650E-15	-14.177		
480.0	1492.0	6.9854	5.5784	8.2530	2.8975	6.5729	16.40	85.54	4.252E-15	-14.280		
500.0	1493.4	6.8193	5.3888	8.1580	2.6608	6.5490	16.26	87.04	4.165E-15	-14.380		
520.0	1494.4	6.6544	5.2004	8.0636	2.4257	6.5253	16.13	88.43	3.316E-15	-14.479		
540.0	1495.3	6.4906	5.0133	7.9700	2.1922	6.5017	16.01	89.75	2.650E-15	-14.577		
560.0	1496.0	6.3278	4.8274	7.8769	1.9602	6.4784	15.88	90.99	2.124E-15	-14.673		
580.0	1496.5	6.1661	4.6427	7.7845	1.7297	6.552	15.76	92.15	1.707E-15	-14.768		
600.0	1497.0	6.0054	4.4592	7.6927	1.5006	6.4322	15.62	93.29	1.376E-15	-14.861		
620.0	1497.4	5.8457	4.2768	7.6014	1.2729	6.4093	15.49	94.40	1.112E-15	-14.954		
640.0	1497.7	5.6870	4.0955	7.5107	1.0465	6.3866	15.34	95.48	9.005E-16	-15.046		
660.0	1498.0	5.5292	3.9153	7.4206	0.8216	6.3640	15.19	96.54	7.312E-16	-15.136		
680.0	1498.2	5.3724	3.7361	7.3309	0.5979	6.3415	15.02	97.61	5.951E-16	-15.225		
700.0	1498.4	5.2164	3.5580	7.2419	0.3756	6.3192	14.83	98.70	4.854E-16	-15.314		
720.0	1498.6	5.0614	3.3810	7.1533	0.1546	6.2971	14.63	99.81	3.926E-16	-15.401		
740.0	1498.8	4.9073	3.2049	7.0653	0.0250	6.2750	14.41	100.96	3.021E-16	-15.488		
760.0	1498.9	4.7540	3.0299	6.9777	0.0253	6.2531	14.16	102.16	2.670E-16	-15.574		
780.0	1499.0	4.6017	2.8559	6.8907	0.0233	6.2313	13.90	103.41	2.198E-16	-15.658		
800.0	1499.1	4.4502	2.6828	6.8042	0.0207	6.2097	13.61	104.77	1.813E-16	-15.741		
820.0	1499.2	4.2996	2.5108	6.7181	0.0181	6.1881	13.31	106.18	1.500E-16	-15.824		
840.0	1499.3	4.1498	2.3397	6.6326	0.0167	6.1667	12.97	107.71	1.244E-16	-15.905		
860.0	1499.3	4.0009	2.1695	6.5475	0.0154	6.1454	12.62	109.36	1.035E-16	-15.985		
880.0	1499.4	3.8527	2.0003	6.4629	0.0143	6.1243	12.25	111.17	8.632E-17	-16.064		
900.0	1499.4	3.7054	1.8321	6.3788	0.0132	6.1032	11.86	113.15	7.222E-17	-16.141		
920.0	1499.5	3.5589	1.6648	6.2951	0.0123	6.0823	11.45	115.32	6.062E-17	-16.217		
940.0	1499.5	3.4133	1.4984	6.2119	0.0114	6.0614	11.04	117.71	5.105E-17	-16.292		
960.0	1499.6	3.2684	1.3329	6.1291	0.0107	6.0407	10.61	120.35	4.316E-17	-16.365		
980.0	1499.6	3.1243	1.1683	6.0468	0.0202	6.0202	10.19	123.27	3.662E-17	-16.436		
1000.0	1499.6	2.9810	1.0046	5.9650	0.0046	5.9997	9.76	126.49	3.120E-17	-16.506		
1050.0	1499.7	3.7016	2.6262	5.994	5.7624	5.9490	8.73	136.11	2.130E-17	-16.672		
1100.0	1499.7	3.3572	2.3762	5.995	5.5624	5.8989	3.3169	7.78	148.45	1.498E-17	-16.825	
1150.0	1499.8	3.0213	1.9308	5.952	5.1705	5.8496	3.3045	6.95	164.04	1.087E-17	-16.964	
1200.0	1499.8	1.5900	1.4998	5.950	4.9785	5.7528	3.2902	6.27	183.27	8.141E-18	-17.089	
1250.0	1499.8	1.2537	1.2537	5.9889	4.7889	5.054	3.2801	5.72	206.37	6.294E-18	-17.201	
1300.0	1499.9	9218	9218	5.9889	4.6018	5.054	3.2682	5.29	233.10	5.010E-18	-17.300	
1350.0	1499.9	5943	5943	5.9889	4.4171	5.054	3.2564	4.96	262.74	4.093E-18	-17.388	
1400.0	1499.9	2709	2709	5.9889	4.2348	5.0568	3.2447	4.71	294.17	3.420E-18	-17.466	
1450.0	1499.9	4.0548	4.0548	5.9889	3.7219	5.0528	3.2332	4.52	326.13	2.910E-18	-17.536	
1500.0	1499.9	•8819	•8819	5.9889	4.0548	5.0528	3.2219	4.38	357.24	2.514E-18	-17.600	
1600.0	1499.9	3.7016	3.7016	5.9889	3.1996	5.04334	3.3295	4.20	412.87	1.939E-18	-17.712	
1700.0	1500.0	1500.0	1500.0	5.9889	3.3572	5.03472	3.1779	4.10	457.20	1.541E-18	-17.812	
1800.0	1500.0	1500.0	1500.0	5.9889	3.0213	5.02632	3.1568	4.05	490.89	1.249E-18	-17.904	
1900.0	1500.0	1500.0	1500.0	5.9889	2.6934	5.01812	3.1361	4.01	517.05	1.024E-18	-17.990	
2000.0	1500.0	1500.0	1500.0	5.9889	2.3734	5.0101	3.1160	3.99	538.23	8.473E-19	-18.072	
2100.0	1500.0	1500.0	1500.0	5.9889	2.0610	5.00230	3.0963	3.98	556.29	7.058E-19	-18.151	
2200.0	1500.0	1500.0	1500.0	5.9889	1.7559	4.9666	3.0771	3.97	572.77	5.913E-19	-18.228	
2300.0	1500.0	1500.0	1500.0	5.9889	1.4579	4.8721	3.0583	3.96	588.30	4.977E-19	-18.303	
2400.0	1500.0	1500.0	1500.0	5.9889	1.1666	4.7992	3.0399	3.95	603.18	4.208E-19	-18.376	
2500.0	1500.0	1500.0	1500.0	5.9889	•8819	4.7280	3.0220	3.95	618.02	3.572E-19	-18.447	

Table 6 (Cont.)

EXOSPHERIC TEMPERATURE = 1600 DEGREES

HEIGHT KM	TEMP DEG K	LOG N(N2) /CM3	LOG N(O2) /CM3	LOG N(O) /CM3	LOG N(H) /CM3	MEAN MOL WT	DENSITY HT KM	DENSITY HT CM3	LOG DEN GM/CM3
90.0	183.0	13.7498	13.1687	11.8225	8.6457	28.83	5.46	3.460E-09	-8.461
92.0	183.3	13.5898	12.9942	12.0533	11.6676	28.63	5.40	2.394E-09	-8.621
94.0	184.6	13.4286	12.8121	12.1513	11.5064	28.37	5.38	1.652E-09	-8.782
96.0	187.1	13.2671	12.6263	11.3449	8.1631	28.09	5.39	1.139E-09	-8.944
98.0	191.2	13.1067	12.4424	12.1205	11.1845	8.0026	5.44	7.870E-10	-9.104
100.0	197.2	12.9483	12.2645	12.0357	11.0261	7.8442	5.64	5.465E-10	-9.262
102.0	205.2	12.7926	12.0892	11.9394	10.8115	7.8137	5.60	3.812E-10	-9.419
104.0	215.4	12.6393	11.9170	11.8428	10.6018	7.7818	5.24	2.677E-10	-9.572
106.0	222.9	12.4894	11.7493	11.7467	10.3984	7.7487	5.03	5.91	1.899E-10
108.0	242.7	12.3440	11.6519	10.2027	7.7149	26.82	6.14	1.362E-10	-9.866
110.0	259.8	12.2039	11.4312	11.5592	10.0155	7.6808	6.42	9.903E-11	-10.004
115.0	312.0	11.8804	11.0731	11.3404	9.5881	7.5966	26.09	7.33	4.768E-11
120.0	375.4	11.5977	10.7616	11.1444	9.2193	7.5179	25.62	8.53	2.530E-11
125.0	445.4	11.3577	10.4945	10.9738	8.9043	7.4477	25.18	10.06	1.474E-11
130.0	516.4	11.1468	10.2662	10.8275	8.6352	7.3873	24.79	11.80	9.317E-12
135.0	586.3	10.9667	10.0683	10.7010	8.4018	7.3353	24.43	13.61	6.281E-12
140.0	654.1	10.8082	9.8941	10.5901	8.1961	7.2900	24.10	15.49	4.451E-12
145.0	719.2	10.6670	9.7387	10.4918	8.0123	7.2502	23.80	17.41	3.283E-12
150.0	781.1	10.5398	9.5984	10.4037	7.8462	7.2149	23.51	19.36	2.501E-12
155.0	839.6	10.4240	9.4706	10.3242	7.6944	7.1834	23.25	21.34	1.956E-12
160.0	894.6	10.3177	9.3531	10.2516	7.5545	7.1550	23.00	23.32	1.563E-12
170.0	994.3	10.1274	9.1423	10.1233	7.3028	7.1060	22.53	27.26	1.052E-12
180.0	1081.3	9.9601	8.9563	10.0121	7.0797	7.0647	22.11	31.12	7.464E-13
190.0	1151.9	9.8097	7.7887	9.9136	6.8777	7.0292	21.72	34.87	5.511E-13
200.0	1222.4	9.6723	8.6352	9.8249	6.6919	6.9981	21.36	38.52	4.195E-13
210.0	1228.9	9.5450	8.4926	9.7438	6.5188	6.9706	21.02	42.01	3.272E-13
220.0	1327.2	9.4259	8.3588	9.6688	6.3558	6.9459	20.71	45.39	2.603E-13
230.0	1368.5	9.3133	8.2321	9.5988	6.2010	6.9234	20.41	48.62	2.104E-13
240.0	1403.5	9.2061	8.1112	9.5329	6.0527	6.9029	20.13	51.70	1.724E-13
250.0	1433.1	9.1033	7.9950	9.4703	5.9099	6.8839	19.87	54.60	1.428E-13
260.0	1457.9	9.0041	7.8828	9.4104	5.7716	6.8661	19.62	57.33	1.194E-13
270.0	1478.8	8.9078	7.7737	9.3528	5.6371	6.8494	19.38	59.88	1.007E-13
280.0	1496.4	8.8141	7.6674	9.2971	5.5056	6.8336	19.16	62.28	8.550E-14
290.0	1511.1	8.7224	7.5633	9.2429	5.3767	6.8185	18.95	64.51	7.303E-14
300.0	1523.5	8.6325	7.4611	9.1900	5.2500	6.8039	18.75	66.61	6.207E-14
310.0	1533.9	8.5441	7.3605	9.1383	5.1251	6.7899	18.55	68.56	5.407E-14
320.0	1542.7	8.4570	7.2613	9.0874	5.0019	6.7763	18.39	70.40	4.683E-14
330.0	1550.2	8.3709	7.1633	9.0374	4.8801	6.7630	18.22	72.12	4.070E-14
340.0	1556.5	8.2818	7.0663	8.9880	4.7594	6.7500	18.06	73.76	3.548E-14
350.0	1561.9	8.2015	6.9702	8.9392	4.6399	6.7372	17.91	75.30	3.103E-14
400.0	1579.2	7.7836	6.5004	8.7019	4.0545	6.6761	17.28	-	-13.508

Table 6 (Cont.)

EXOSPHERIC TEMPERATURE = 1600 DEGREES

HEIGHT KM	TEMP DEG K	LOG N(N2) /CM3	LOG N(O2) /CM3	LOG N(O) /CM3	LOG N(A) /CM3	LOG N(HE) /CM3	LOG N(H) /CM3	MEAN MOL WT	DENSITY HT KM	DENSITY SCALE HT KM	DENSITY GM/CM3	LOG DEN GM/CM3
420.0	1583.4	7.6283	6.3164	8.6093	3.8250	6.6525	6.6292	17.07	84.21	1.292E-14	-13.839	
440.0	1586.5	7.4686	6.1340	8.5177	3.5976	6.6292	6.6292	16.89	86.28	1.022E-14	-13.991	
460.0	1588.9	7.3103	5.9533	8.4270	3.3722	6.6063	6.6063	16.72	88.21	8.126E-15	-14.090	
480.0	1590.9	7.1532	5.7740	8.3371	3.1484	6.5836	6.5836	16.57	89.99	6.492E-15	-14.188	
500.0	1592.4	6.9974	5.5961	8.2479	2.9264	6.5611	6.5611	16.43	91.63	5.209E-15	-14.283	
520.0	1593.6	6.8427	5.4194	8.1594	2.7059	6.5389	6.5389	16.30	93.18	4.195E-15	-14.377	
540.0	1594.6	6.6890	5.2439	8.0715	2.4869	6.5168	6.5168	16.17	94.64	3.391E-15	-14.470	
560.0	1595.4	6.5364	5.0696	7.9842	2.2693	6.4949	6.4949	16.05	96.01	2.749E-15	-14.561	
580.0	1596.0	6.3867	4.8964	7.8976	2.0531	6.4731	6.4731	15.94	97.30	2.235E-15	-14.651	
600.0	1596.5	6.2340	4.7243	7.8114	1.8383	6.4515	6.4515	15.82	98.54	1.822E-15	-14.739	
620.0	1597.0	6.0843	4.5532	7.7258	1.6248	6.4301	6.4301	15.70	99.74	1.489E-15	-14.827	
640.0	1597.4	5.9354	4.3832	7.6408	1.4126	6.4088	6.4088	15.57	100.90	1.220E-15	-14.914	
660.0	1597.7	5.7875	4.2142	7.5582	1.2016	6.3876	6.3876	15.44	102.04	1.002E-15	-14.999	
680.0	1598.0	5.6404	4.0462	7.4722	9.919	6.3665	6.3665	15.31	103.15	8.244E-16	-15.084	
700.0	1598.2	5.4942	3.8792	7.3887	7.835	6.3456	6.3456	15.16	104.26	6.798E-16	-15.168	
720.0	1598.4	5.3489	3.7132	7.3057	5.762	6.3248	6.3248	15.00	105.37	6.617E-16	-15.250	
740.0	1598.6	5.2044	3.5482	7.2231	3.702	6.3041	6.3041	14.82	106.50	6.651E-16	-15.332	
760.0	1598.7	5.0607	3.3840	7.1410	1.653	6.2834	6.2834	14.64	107.65	3.858E-16	-15.414	
780.0	1598.9	4.9178	3.2209	7.0594	6.2632	6.2632	6.2632	14.43	108.84	3.207E-16	-15.494	
800.0	1599.0	4.7758	3.0587	6.9783	6.2429	6.2429	6.2429	14.21	110.09	2.672E-16	-15.573	
820.0	1599.1	4.6346	2.8974	6.8976	6.2227	6.2227	6.2227	13.97	111.36	2.230E-16	-15.652	
840.0	1599.1	4.4941	2.7369	6.8174	6.2026	6.2026	6.2026	13.71	112.71	1.866E-16	-15.729	
860.0	1599.2	4.3545	2.5774	6.7377	6.1826	6.2646	6.2646	13.43	114.14	1.564E-16	-15.806	
880.0	1599.3	4.2156	2.4188	6.6583	6.1628	6.2595	6.2595	13.13	115.67	1.314E-16	-15.881	
900.0	1599.4	4.0775	2.2611	6.5794	6.1431	6.2546	6.2546	12.82	117.31	1.107E-16	-15.956	
920.0	1599.4	3.9402	2.1042	6.5010	6.1234	6.2496	6.2496	12.48	119.08	9.345E-17	-16.029	
940.0	1599.5	3.8036	1.9482	6.4230	6.1039	6.2447	6.2447	12.13	120.99	7.910E-17	-16.102	
960.0	1599.5	3.6678	1.7930	6.3454	6.0845	6.2398	6.2398	11.77	123.07	6.714E-17	-16.173	
980.0	1599.5	3.5327	1.6387	6.2883	6.0652	6.2349	6.2349	11.39	125.33	5.716E-17	-16.243	
1000.0	1599.6	3.3984	1.4853	6.1915	6.0460	6.2300	6.2300	11.01	127.80	4.880E-17	-16.312	
1050.0	1599.7	3.0658	1.1053	6.0016	5.9984	3.2181	10.03	135.02	3.334E-17	-16.477		
1100.0	1599.7	2.7376	7305	5.8141	5.9515	2.2062	9.06	144.11	2.329E-17	-16.633		
1150.0	1599.8	2.4138	3606	5.6292	5.9053	3.1946	8.15	155.54	1.667E-17	-16.778		
1200.0	1599.8	2.0943	54467	5.4467	5.8596	3.1831	7.34	169.74	1.225E-17	-16.912		
1250.0	1599.8	1.7790	5.2666	5.8146	3.1717	6.64	1.87	171.19	9.250E-18	-17.034		
1300.0	1599.8	1.4679	5.0889	5.7701	3.1695	6.06	2.08	179.14	7.179E-18	-17.144		
1350.0	1599.8	1.1608	4.9135	5.7262	3.1495	5.59	2.32	170.90	5.718E-18	-17.243		
1400.0	1599.9	.8576	4.7404	5.6829	3.1385	5.22	2.60	172.55	4.666E-18	-17.331		
1450.0	1599.9	.5583	4.5695	5.6401	3.1278	4.93	2.90	174.50	3.890E-18	-17.400		
1500.0	1599.9	.2629	4.4007	5.5979	3.1171	4.71	3.22	176.34	3.304E-18	-17.481		
1600.0	1599.9	4.0696	5.151	3.0963	4.41	386.19	2.490E-18					
1700.0	1599.9	3.7467	5.4343	3.0759	4.23	443.96	1.957E-18					
1800.0	1600.0	3.4317	5.3555	3.0561	4.13	491.47	1.581E-18					
1900.0	1600.0	3.1244	5.2786	3.0367	4.07	529.14	1.300E-18					
2000.0	1600.0	2.8244	5.2036	3.0178	4.03	558.96	1.082E-18					
2100.0	1600.0	2.5315	5.1303	2.9994	4.01	583.18	9.079E-19					
2200.0	1600.0	2.2455	5.0587	2.9813	4.00	604.02	7.671E-19					
2300.0	1600.0	1.9661	4.9888	2.9637	3.99	622.67	6.518E-19					
2400.0	1600.0	1.6930	4.9205	2.9465	3.98	639.85	5.563E-19					
2500.0	1600.0	1.4261	4.8538	2.9297	3.97	656.47	4.767E-19					

Table 6 (Cont.)

EXOSS-4 ERIC TEMPERATURE = 1700 DEGREES

HEIGHT KM	TEMP DEG K	LOG N(2)			LOG N(0)			LOG N(A)			LOG N(HE)			MEAN MOL WT	DENSITY HT KM	DENSITY GM/CM ³	LOG DEN GM/CM ³
		LOG N/CM ³	/CM ³	/CM ³	LOG N/CM ³	/CM ³	/CM ³	LOG N/CM ³	/CM ³	/CM ³	LOG N/CM ³	/CM ³	/CM ³				
90.0	163.0	13.7498	13.1687	11.8225	11.8276	8.6457	28.83	5.46	3.460E-09	-8.461							
92.0	183.3	13.5898	12.9942	12.0532	11.6676	8.4857	28.63	5.40	2.394E-09	-8.621							
94.0	184.6	13.4285	12.8121	12.1512	11.5063	8.3245	28.37	5.37	1.651E-09	-8.782							
96.0	167.2	13.2669	12.6261	12.1658	11.1347	8.1629	28.09	5.39	1.138E-09	-8.944							
98.0	191.5	13.1064	12.4421	12.1202	11.1842	8.0023	27.84	5.44	7.865E-10	-9.104							
100.0	197.6	12.9478	12.2641	12.0353	11.0256	7.8438	27.64	5.51	5.460E-10	-9.263							
102.0	205.8	12.7921	12.0887	11.9387	10.8111	7.8131	27.44	5.60	3.808E-10	-9.419							
104.0	216.3	12.6387	11.9166	11.8419	10.6016	7.7809	27.24	5.73	2.674E-10	-9.573							
106.0	229.1	12.4889	11.7490	11.7456	10.3985	7.7476	27.03	5.92	1.896E-10	-9.722							
108.0	244.3	12.3436	11.5870	11.6507	10.2032	7.7135	26.82	6.15	1.361E-10	-9.866							
110.0	261.8	12.2037	11.4315	11.5578	10.0166	7.6792	26.61	6.43	9.899E-11	-10.004							
115.0	315.4	11.8812	11.0146	11.3389	9.5911	7.5945	26.10	7.36	4.775E-11	-10.321							
120.0	380.5	11.5998	10.7648	11.1433	9.2246	7.5154	25.63	8.58	2.541E-11	-10.595							
125.0	452.4	11.3584	10.4996	10.972	8.9122	7.4451	25.21	10.12	1.485E-11	-10.828							
130.0	525.3	11.1521	10.2733	10.8275	8.6458	7.3846	24.83	11.89	9.414E-12	-11.026							
135.0	597.2	10.9736	10.0773	10.7017	8.4150	7.3325	24.48	13.72	6.366E-12	-11.196							
140.0	667.2	10.8167	9.9049	10.5914	8.2117	7.2871	24.15	15.61	4.524E-12	-11.344							
145.0	734.7	10.6769	9.7511	10.4936	8.0301	7.2472	23.86	17.54	3.345E-12	-11.476							
150.0	799.3	10.5509	9.6125	10.4060	7.8661	7.2117	23.58	19.51	2.553E-12	-11.593							
155.0	860.7	10.4363	9.4862	10.3268	7.7164	7.1800	23.32	21.51	2.000E-12	-11.699							
160.0	918.8	10.3312	9.3701	10.2545	7.5785	7.1515	23.08	23.51	1.602E-12	-11.795							
170.0	1025.3	10.1433	9.1623	10.1268	7.3309	7.1019	22.62	27.51	1.081E-12	-11.966							
180.0	1119.3	9.9785	8.9794	10.0163	7.1121	7.0602	22.21	31.47	7.701E-13	-12.113							
190.0	1202.1	9.8308	8.8151	9.9187	6.9143	7.0423	21.84	35.35	5.707E-13	-12.244							
200.0	1274.3	9.6964	8.6652	9.8311	6.7338	6.9930	21.49	39.16	4.362E-13	-12.360							
210.0	1337.2	9.5724	8.5265	9.7513	6.5659	6.9653	21.17	42.84	3.418E-13	-12.466							
220.0	1391.3	9.4568	8.3969	9.6779	6.4084	6.9406	20.86	46.43	2.732E-13	-12.564							
230.0	1437.6	9.3479	8.2146	9.6096	6.2592	6.9182	20.57	49.88	2.219E-13	-12.654							
240.0	1477.1	9.2446	8.1583	9.5456	6.1169	6.8979	20.30	53.18	1.828E-13	-12.738							
250.0	1510.5	9.1459	8.0469	9.4850	5.9802	6.8791	20.05	56.30	1.523E-13	-12.817							
260.0	1538.6	9.0509	7.9395	9.4273	5.8482	6.8617	19.81	59.25	1.281E-13	-12.893							
270.0	1562.3	8.9590	7.8355	9.3719	5.7199	6.8454	19.58	62.00	1.086E-13	-12.964							
280.0	1582.3	8.8696	7.7342	9.3186	5.5949	6.8300	19.36	64.58	9.272E-14	-13.033							
290.0	1599.0	8.7824	7.6352	9.2668	5.4725	6.8154	19.15	66.97	7.965E-14	-13.099							
300.0	1613.0	8.6970	7.5382	9.2164	5.3523	6.8014	18.96	69.22	6.877E-14	-13.163							
310.0	1624.9	8.6132	7.4429	9.1671	5.2341	6.7879	18.77	71.31	5.965E-14	-13.224							
320.0	1634.9	8.5306	7.3489	9.1188	5.1174	6.7748	18.59	73.28	5.194E-14	-13.284							
330.0	1643.4	8.4491	7.2562	9.0713	5.0022	6.7621	18.43	75.12	4.539E-14	-13.333							
340.0	1650.5	8.3686	7.1645	9.0245	4.8882	6.7497	18.27	76.86	3.980E-14	-13.400							
350.0	1656.6	8.2889	7.0737	8.9783	4.7753	6.7375	18.12	78.50	3.4999E-14	-13.456							
360.0	1661.9	8.2100	6.9837	8.9327	4.6633	6.7256	17.97	80.06	3.084E-14	-13.511							
370.0	1666.3	8.1317	6.8995	8.8875	4.5522	6.7139	17.84	81.55	2.725E-14	-13.565							
380.0	1670.2	8.0540	6.8059	8.8427	4.4418	6.7023	17.71	82.93	2.413E-14	-13.617							
390.0	1673.5	6.9768	6.7217	8.7982	4.3321	6.6908	17.59	84.30	2.141E-14	-13.669							
400.0	1676.4	7.3001	6.6330	8.7541	4.2231	6.6795	17.47	85.59	1.904E-14	-13.720							

Table 6 (Cont.)

EXOZOETRIC TEMPERATURE = 1700 DEGREES

HIGHT KM	TEMP DEG K	LOG N(N2) /CM3	LOG N(O2) /CM3	LOG N(O) /CM3	LOG N(A) /CM3	LOG N(HE) /CM3	LOG N(H) /CM3	MEAN MUL WT	DENSITY HT KM	DENSITY SCALE	DENSITY GM/CM3	LOG DEN GM/CM3
420.0	1681.1	7.7481	6.4568	8.6667	4.0067	6.6572	17.26	88.02	1.512E-14	-13.820		
440.0	1684.7	7.5975	6.2850	8.5803	3.7924	6.6353	17.07	90.26	1.208E-14	-13.918		
460.0	1687.4	7.4484	6.1147	8.4949	3.5800	6.6136	16.89	92.34	9.705E-15	-14.013		
480.0	1689.6	7.3034	5.9458	8.4101	3.3693	6.5922	16.73	94.28	7.833E-15	-14.106		
500.0	1691.3	7.1537	5.7782	8.3261	3.1602	6.5710	3.2558	16.59	96.09	6.348E-15	-14.197	
520.0	1692.7	7.0080	5.6118	8.2427	2.9526	6.5500	3.2502	16.46	97.78	5.165E-15	-14.287	
540.0	1693.8	6.8633	5.4466	8.1600	2.7464	6.5292	3.2448	16.33	99.38	4.217E-15	-14.375	
560.0	1694.7	6.7195	5.2825	8.0778	2.5415	6.5086	3.2394	16.21	100.89	3.453E-15	-14.462	
580.0	1695.5	6.5768	5.1194	7.9962	2.3380	6.4881	3.2341	16.10	102.32	2.836E-15	-14.547	
600.0	1696.1	6.4349	4.9574	7.9151	2.1357	6.4677	3.2288	15.99	103.68	2.336E-15	-14.632	
620.0	1696.6	6.2939	4.7963	7.8345	1.9347	6.4475	3.2236	15.88	104.98	1.928E-15	-14.715	
640.0	1697.0	6.1538	4.6363	7.7544	1.7350	6.4275	3.2185	15.76	106.23	1.596E-15	-14.797	
660.0	1697.4	6.0145	4.4772	7.6748	1.5364	6.4075	3.2134	15.65	107.45	1.323E-15	-14.878	
680.0	1697.7	5.8761	4.3191	7.5957	1.3390	6.3877	3.2083	15.53	108.64	1.100E-15	-14.959	
700.0	1698.0	5.7384	4.1619	7.5171	1.1428	6.3680	3.033	15.41	109.81	9.156E-16	-15.038	
720.0	1698.2	5.6016	4.0056	7.4389	0.9477	6.3484	3.1983	15.27	110.97	7.638E-16	-15.117	
740.0	1698.4	5.4656	3.8503	7.3612	0.7538	6.3290	3.1933	15.13	112.12	6.385E-16	-15.195	
760.0	1698.5	5.3034	3.6958	7.2840	0.5609	6.3096	3.1884	14.98	113.27	5.346E-16	-15.272	
780.0	1698.7	5.1959	3.5422	7.2072	0.3692	6.2904	3.1836	14.82	114.44	4.485E-16	-15.348	
800.0	1698.8	5.0622	3.3895	7.1308	0.1786	6.2713	3.1787	14.64	115.67	3.769E-16	-15.424	
820.0	1698.9	4.9293	3.2377	7.0549	0.2523	6.2523	3.1739	14.46	116.88	3.174E-16	-15.498	
840.0	1699.0	4.7971	3.0867	6.9794	0.2334	6.2334	3.1691	14.25	118.14	2.677E-16	-15.572	
860.0	1699.1	4.6657	2.9366	6.9043	0.2146	6.2146	3.1644	14.03	119.45	2.262E-16	-15.645	
880.0	1699.2	4.5350	2.7873	6.8296	0.1959	6.1959	3.1597	13.79	120.82	1.915E-16	-15.718	
900.0	1699.3	4.4050	2.6388	6.7554	0.1773	6.1773	3.1550	13.54	122.27	1.625E-16	-15.789	
920.0	1699.3	4.2757	2.4912	6.6815	0.1588	6.1588	3.1503	13.27	123.81	1.381E-16	-15.860	
940.0	1699.4	4.1472	2.3443	6.6081	0.1405	6.1405	3.1457	12.99	125.44	1.176E-16	-15.930	
960.0	1699.4	4.0194	2.1983	6.5351	0.1222	6.1222	3.1410	12.69	127.18	1.004E-16	-15.998	
980.0	1699.5	3.8922	2.0531	6.4625	0.1040	6.1040	3.1365	12.37	129.05	8.587E-17	-16.066	
1000.0	1699.5	3.7658	1.9087	6.3903	0.0860	6.0860	3.1319	12.04	131.05	7.363E-17	-16.133	
1050.0	1699.6	3.4527	1.5510	6.2115	0.0412	6.0412	3.1206	11.17	136.78	5.067E-17	-16.295	
1100.0	1699.7	3.1438	1.0982	6.0350	0.0971	5.9971	3.1095	10.27	143.80	3.547E-17	-16.450	
1150.0	1699.7	2.8391	0.8501	5.8610	0.9535	5.9535	3.0985	9.37	152.46	2.530E-17	-16.597	
1200.0	1699.8	2.5384	0.5067	5.6892	0.9106	5.9106	3.0877	8.50	163.10	1.842E-17	-16.735	
1250.0	1699.8	2.2416	0.1677	5.5198	0.8682	5.8682	3.0770	7.71	176.20	1.371E-17	-16.863	
1300.0	1699.8	1.9488	0.9488	5.3525	0.8263	5.8263	3.0665	7.01	192.11	1.044E-17	-16.981	
1350.0	1699.9	1.6598	0.5184	5.1874	0.7850	5.7850	3.0560	6.42	211.14	8.145E-18	-17.089	
1400.0	1699.9	1.3744	0.2044	5.0244	0.7442	5.7442	3.0458	5.92	233.43	6.501E-18	-17.187	
1450.0	1699.9	1.0928	0.0928	4.8636	0.7040	5.7040	3.0356	5.51	258.99	5.304E-18	-17.275	
1500.0	1699.9	0.8147	0.8147	4.7048	0.6643	5.6643	3.0256	5.18	287.43	4.416E-18	-17.355	
1600.0	1699.9	0.2690	0.2690	4.3931	0.3060	5.5863	3.0060	4.72	350.22	3.222E-18	-17.492	
1700.0	1699.9	0.1700	0.1700	4.0892	2.9868	5.5103	2.9868	4.43	415.00	2.480E-18	-17.606	
1800.0	1699.9	0.1700	0.1700	3.7928	2.9682	5.4361	2.9682	4.26	474.65	1.981E-18	-17.703	
1900.0	1699.9	0.1700	0.1700	3.5035	2.9321	5.3637	2.9321	4.15	525.78	1.622E-18	-17.790	
2000.0	1699.9	0.1700	0.1700	3.2212	2.9148	5.2931	2.9148	4.09	567.16	1.351E-18	-17.869	
2100.0	1699.9	0.1700	0.1700	2.9455	2.8978	5.2241	2.9148	4.05	600.72	1.138E-18	-17.944	
2200.0	1699.9	0.1700	0.1700	2.6763	2.8978	5.1568	2.8978	4.03	628.57	9.675E-19	-18.014	
2300.0	1699.9	0.1700	0.1700	2.4133	2.8812	5.0910	2.8812	4.01	652.38	8.277E-19	-18.082	
2400.0	1699.9	0.1700	0.1700	2.1563	2.8650	5.0267	2.8650	4.00	673.36	7.118E-19	-18.148	
2500.0	1699.9	0.1700	0.1700	1.9051	2.8492	4.9639	2.8492	3.99	692.84	6.148E-19	-18.211	

Table 6 (Cont.)

EXOSPHERIC TEMPERATURE = 1800 DEGREES

HEIGHT KM	TEMP DEG K	LOG N(42) /CM ³	LOG N(72) /CM ³	LOG N(0) /CM ³	LOG N(A) /CM ³	LOG N(HE) /CM ³	MEAN MOL WT	DENSITY SCALE HT KM	DENSITY GM/CM ³	LOG DEN GM/CM ³	
90.0	183.0	13.7498	13.1687	11.8225	8.6457	28.83	5.46	3.460E-09	-8.461		
92.0	183.3	13.5898	12.9941	12.0532	8.4857	28.63	5.40	2.394E-09	-6.621		
94.0	184.7	13.4284	12.8120	12.1512	8.3244	28.37	5.37	1.651E-09	-8.782		
96.0	187.3	13.2668	12.6259	12.1656	8.1627	28.09	5.38	1.138E-09	-8.944		
98.0	191.7	13.1061	12.4419	12.1200	8.0021	27.84	5.44	7.860E-10	-9.105		
100.0	197.9	12.9475	12.2637	12.0349	7.8434	27.64	5.51	5.455E-10	-9.263		
102.0	206.4	12.7917	12.0883	11.9381	7.8108	27.44	5.59	3.803E-10	-9.420		
104.0	217.1	12.6382	11.9162	11.8411	10.6014	27.24	5.73	2.671E-10	-9.573		
106.0	230.2	12.4884	11.7487	11.7446	10.3986	27.03	5.92	1.899E-10	-9.723		
108.0	245.8	12.3433	11.5869	11.6495	10.2037	26.82	6.16	1.360E-10	-9.867		
110.0	263.8	12.2036	11.4317	11.5566	10.0176	26.62	6.44	9.895E-11	-10.005		
115.0	318.7	11.8819	11.0760	11.3376	9.5938	26.11	7.38	4.781E-11	-10.320		
120.0	385.4	11.6018	10.7677	11.1422	9.2296	7.5131	8.62	2.551E-11	-10.593		
125.0	459.0	11.3618	10.5044	10.7726	8.9196	7.4426	10.23	1.495E-11	-10.825		
130.0	533.8	11.1571	10.2799	10.8275	8.6556	7.3820	11.97	9.500E-12	-11.022		
135.0	607.6	10.9800	10.0857	10.7023	8.4271	7.3299	14.51	6.446E-12	-11.191		
140.0	679.7	10.8245	9.9149	10.5926	8.2260	7.2845	15.20	15.73	4.593E-12	-11.338	
145.0	749.4	10.6859	9.7627	10.4953	8.0666	7.2444	17.91	17.67	3.403E-12	-11.468	
150.0	816.5	10.5612	9.6254	10.4080	7.8845	7.2088	23.64	19.66	2.603E-12	-11.585	
155.0	880.6	10.4477	9.5005	10.3291	7.7366	7.1770	23.39	21.66	2.043E-12	-11.690	
160.0	941.7	10.3436	9.3857	10.2572	7.6006	7.1482	23.15	23.68	1.638E-12	-11.786	
170.0	1054.6	10.1578	9.1805	10.1300	7.3566	7.0982	22.71	27.73	1.109E-12	-11.955	
180.0	1155.6	9.9951	9.0003	10.0201	7.1415	7.0560	22.31	31.77	7.923E-13	-12.101	
190.0	1245.3	9.8498	8.8389	9.9232	6.9481	7.0197	21.95	35.77	5.890E-13	-12.230	
200.0	1324.4	9.7179	8.6921	9.8364	6.7715	6.9881	21.61	39.72	4.518E-13	-12.345	
210.0	1393.6	9.5967	8.5569	9.7577	6.6681	6.9603	21.30	43.58	3.553E-13	-12.449	
220.0	1453.6	9.4842	8.4308	9.6855	6.4554	6.9354	21.00	47.37	2.852E-13	-12.545	
230.0	1505.2	9.3786	8.3124	9.6187	6.3112	6.9131	20.73	51.04	2.327E-13	-12.633	
240.0	1549.3	9.2787	8.2001	9.553	6.1741	6.8929	20.46	54.56	1.936E-13	-12.715	
250.0	1586.7	9.1835	8.0928	9.4975	6.0428	6.8743	20.22	57.90	1.612E-13	-12.793	
260.0	1618.3	9.0922	7.9897	9.4416	5.9162	6.8572	19.98	61.06	1.362E-13	-12.866	
270.0	1644.9	9.0040	7.8901	9.3883	5.7936	6.8416	19.76	64.01	1.161E-13	-12.935	
280.0	1667.3	8.9186	7.7933	9.3369	5.6442	6.8262	19.54	66.78	9.955E-14	-13.002	
290.0	1686.2	8.8353	7.6989	9.2873	5.5576	6.8120	19.34	69.35	8.603E-14	-13.065	
300.0	1702.0	8.7539	7.6065	9.2391	5.4432	6.7984	19.15	71.76	7.467E-14	-13.127	
310.0	1715.3	8.6741	7.5157	9.1920	5.3208	6.7854	18.96	73.99	6.509E-14	-13.186	
320.0	1726.6	8.5955	7.4264	9.1459	5.2200	6.7728	18.79	76.09	5.637E-14	-13.244	
330.0	1736.1	8.5181	7.3384	9.1007	5.1016	6.7606	18.62	78.03	5.004E-14	-13.301	
340.0	1744.2	8.4417	7.2514	9.0562	5.0025	6.7487	18.46	79.89	4.409E-14	-13.356	
350.0	1751.1	8.3661	7.1653	9.0123	4.8855	6.7371	18.31	81.63	3.895E-14	-13.409	
360.0	1757.0	8.2913	7.0800	8.9689	4.7894	6.7257	18.17	83.29	3.450E-14	-13.462	
370.0	1762.1	8.2171	6.9954	8.9260	4.6841	6.7145	18.03	84.87	3.064E-14	-13.514	
380.0	1766.4	8.1435	6.9115	8.8835	4.5796	6.7035	17.90	86.36	2.726E-14	-13.565	
390.0	1770.2	8.0704	6.8282	8.8414	4.4758	6.6926	17.78	87.79	2.430E-14	-13.614	
400.0	1773.4	7.9979	6.7454	8.7996	4.3726	6.6819	17.66	89.16	2.170E-14	-13.663	

Table 6 (Cont.)

EXOSPHERIC TEMPERATURE = 1600 DEGREES

HEIGHT KM	TEMP DEG K	LOG N(N2) /CM3	LOG N(O2) /CM3	LOG N(O) /CM3	LOG N(A) /CM3	LOG N(HE) /CM3	LOG N(+) /CM3	MEAN MOL WT	DENSITY HT KM	DENSITY SCALE HT KM	DENSITY GM/CM3	LOG DEN GM/CM3
420.0	1778.7	7.8540	6.5812	8.7169	4.1680	6.6607	17.44	91.74	1.740E-14	-13.759		
440.0	1782.7	7.7116	6.4187	8.6351	3.9654	6.6399	17.24	94.13	1.403E-14	-13.853		
460.0	1785.8	7.5706	6.2577	8.5543	3.7646	6.6194	17.06	96.36	1.137E-14	-13.944		
480.0	1788.3	7.4307	6.0981	8.4741	3.5654	6.5991	16.90	98.45	9.262E-15	-14.033		
500.0	1790.2	7.2920	5.9397	8.3947	3.3678	6.5791	16.75	100.40	7.575E-15	-14.121		
520.0	1791.8	7.1543	5.7824	8.3159	3.1716	6.5592	16.59	102.25	6.218E-15	-14.206		
540.0	1793.0	7.0176	5.6263	8.2377	2.9768	6.5395	16.48	103.98	5.122E-15	-14.291		
560.0	1794.0	6.8818	5.4712	8.1600	2.7832	6.5200	16.36	105.63	4.232E-15	-14.373		
580.0	1794.9	6.7469	5.3172	8.0829	2.5909	6.5006	16.25	107.19	3.507E-15	-14.455		
600.0	1795.6	6.6128	5.1641	8.0062	2.3999	6.4814	16.14	108.67	2.914E-15	-14.536		
620.0	1796.2	6.4797	5.0120	7.9301	2.2100	6.4623	16.03	110.10	2.427E-15	-14.615		
640.0	1796.6	6.3473	4.8608	7.8545	2.0213	6.4433	15.93	111.47	2.026E-15	-14.693		
660.0	1797.0	6.2157	4.7105	7.7793	1.8337	6.4245	15.82	112.77	1.695E-15	-14.771		
680.0	1797.4	6.0850	4.5612	7.7046	1.6473	6.4058	15.72	114.04	1.421E-15	-14.847		
700.0	1797.7	5.9550	4.4127	7.6303	1.4619	6.3872	15.61	115.29	1.194E-15	-14.923		
720.0	1797.9	5.8257	4.2651	7.5565	1.2977	6.3687	15.49	116.52	0.004E-15	-14.998		
740.0	1798.2	5.6973	4.1184	7.4831	1.0945	6.3503	15.040	117.72	8.467E-16	-15.072		
760.0	1798.4	5.5695	3.9725	7.4101	• 9124	6.3320	15.25	118.92	7.150E-16	-15.146		
780.0	1798.5	5.4425	3.8274	7.3375	• 7313	6.3139	15.12	120.12	6.048E-16	-15.218		
800.0	1798.7	5.3163	3.6832	7.2654	• 5512	6.2958	14.97	121.34	5.125E-16	-15.290		
820.0	1798.8	5.1907	3.5398	7.1937	• 3722	6.2778	14.82	122.54	4.350E-16	-15.362		
840.0	1798.9	5.0659	3.3971	7.1224	• 1942	6.2600	14.66	123.77	3.698E-16	-15.432		
860.0	1799.0	4.9417	3.2553	7.0515	• 0172	6.2422	14.50	125.03	3.149E-16	-15.502		
880.0	1799.1	4.8183	3.1143	6.9809	6.2246	3.0721	14.29	126.34	2.685E-16	-15.571		
900.0	1799.2	4.6955	2.9741	6.9108	6.2070	3.0677	14.09	127.69	2.294E-16	-15.639		
920.0	1799.2	4.5734	2.8346	6.8411	6.1896	3.0633	13.87	129.09	1.963E-16	-15.707		
940.0	1799.3	4.4520	2.6960	6.7717	6.1722	3.0589	13.64	130.56	1.633E-16	-15.774		
960.0	1799.4	4.3313	2.5581	6.7028	6.1550	3.0545	13.40	132.11	1.445E-16	-15.846		
980.0	1799.4	4.2112	2.4209	6.6342	6.1378	3.0502	13.14	133.74	1.243E-16	-15.905		
1000.0	1799.5	4.0918	2.2845	6.5660	6.1207	3.0459	12.87	135.46	1.072E-16	-15.970		
1050.0	1799.6	3.7961	1.9468	6.3971	6.0785	3.0352	12.13	140.25	7.455E-17	-16.128		
1100.0	1799.6	3.5044	1.6135	6.2305	6.0368	3.0247	11.33	145.96	5.255E-17	-16.279		
1150.0	1799.7	3.2165	1.2848	6.0661	5.9957	3.0143	10.50	152.81	3.759E-17	-16.425		
1200.0	1799.7	2.9326	0.9604	5.9039	5.9551	3.0041	9.65	161.07	2.733E-17	-16.563		
1250.0	1799.8	2.6523	0.6402	5.7438	5.9150	2.9940	8.83	171.12	2.021E-17	-16.694		
1300.0	1799.8	2.3757	0.3243	5.5858	5.8755	2.9841	8.07	183.29	1.524E-17	-16.817		
1350.0	1799.8	2.1027	0.0125	5.4299	5.8365	2.9742	7.38	197.90	1.172E-17	-16.931		
1400.0	1799.9	1.8332	5.2760	5.1241	5.7980	2.9645	6.77	215.25	9.194E-18	-17.036		
1450.0	1799.9	1.5672	4.9741	5.0918	5.7600	2.9550	6.25	235.62	7.363E-18	-17.133		
1500.0	1799.9	1.3046	4.9741	5.0918	5.7225	2.9455	5.81	259.05	6.013E-18	-17.221		
1600.0	1799.9	0.7893	4.6798	4.3927	5.6488	2.9269	5.16	314.37	4.233E-18	-17.313		
1700.0	1799.9	0.2867	4.1128	4.0812	5.5770	2.9089	4.73	377.85	3.167E-18	-17.499		
1800.0	1799.9	0.0000	1.8000	1.8000	5.5070	2.8912	4.46	443.35	2.481E-18	-17.605		
1900.0	1800.0	0.0000	1.8000	1.8000	5.4386	2.8740	4.29	505.11	2.010E-18	-17.697		
2000.0	1800.0	0.0000	1.8000	1.8000	5.3719	2.8572	4.18	559.25	1.665E-18	-17.778		
2100.0	1800.0	0.0000	1.8000	1.8000	5.3068	2.8408	4.11	604.62	1.403E-18	-17.853		
2200.0	1800.0	0.0000	1.8000	1.8000	5.2432	2.8248	4.07	642.36	1.195E-18	-17.923		
2300.0	1800.0	0.0000	1.8000	1.8000	5.1810	2.8091	4.04	673.95	1.027E-18	-17.989		
2400.0	1800.0	0.0000	1.8000	1.8000	5.1203	2.7938	4.02	700.85	8.876E-19	-18.052		
2500.0	1800.0	0.0000	1.8000	1.8000	5.0610	2.7789	4.01	724.85	7.714E-19	-18.113		

Table 6 (Cont.)

EXOSPHERIC TEMPERATURE = 1900 DEGREES

HEIGHT KM	TEMP DEG K	LOG N(12) /CM ³	LOG N(20) /CM ³	LOG N(10) /CM ³	LOG N(A) /CM ³	LOG N(HE) /CM ³	MEAN MUL WT	DENSITY HT KM	SCALE HT KM	DENSITY GM/CM ³	LOG DEN GM/CM ³
90.0	183.0	13.7498	13.1687	11.8225	11.8276	8.6457	28.83	5.46	3.460E-09	-8.461	
92.0	183.4	13.5898	12.9941	12.0532	11.6675	8.4857	28.63	5.40	2.394E-09	-8.621	
94.0	184.7	13.4284	12.8119	12.1511	11.5061	8.3243	28.37	5.37	1.651E-09	-8.782	
96.0	187.4	13.2666	12.6258	12.1654	11.4444	8.1626	28.09	5.38	1.137E-09	-8.944	
98.0	191.9	13.1058	12.4416	12.1197	11.1836	8.0018	27.84	5.43	7.855E-10	-9.105	
100.0	198.3	12.9471	12.2633	12.0345	11.0449	7.8430	27.64	5.50	5.450E-10	-9.264	
102.0	206.9	12.7912	12.0879	11.9375	10.8104	7.8120	27.44	5.59	3.799E-10	-9.420	
104.0	217.9	12.6378	11.9158	11.8403	10.6012	7.7793	27.24	5.73	2.668E-10	-9.574	
106.0	231.3	12.4880	11.7484	11.7436	10.3987	7.7455	27.03	5.92	1.892E-10	-9.723	
108.0	247.2	12.3429	11.5868	11.6484	10.2041	7.7110	26.83	6.16	1.35E-10	-9.867	
110.0	265.6	12.2034	11.4319	11.5553	10.0185	7.6762	26.62	6.45	9.890E-11	-10.005	
115.0	321.8	11.8826	11.0773	11.3663	9.5964	7.5109	26.12	7.40	4.787E-11	-10.320	
120.0	390.1	11.6036	10.7705	11.1412	9.2342	7.5109	25.67	8.66	2.56E-11	-10.592	
125.0	465.4	11.3649	10.5088	10.9720	8.8265	7.4402	25.26	10.24	1.504E-11	-10.823	
130.0	541.9	11.1617	10.2860	10.8275	8.6648	7.3796	24.89	12.05	9.594E-12	-11.018	
135.0	617.5	10.9860	10.0934	10.7029	8.4285	7.3275	24.55	13.92	6.522E-12	-11.186	
140.0	691.5	10.8317	9.9242	10.5937	8.2394	7.2820	24.24	15.84	4.658E-12	-11.332	
145.0	763.4	10.6944	9.7734	10.4968	8.0619	7.2418	23.96	17.80	3.458E-12	-11.461	
150.0	832.9	10.5707	9.6375	10.4100	7.9016	7.2061	23.69	19.79	2.650E-12	-11.577	
155.0	899.6	10.4582	9.5138	10.3314	7.5554	7.1741	23.45	21.81	2.093E-12	-11.681	
160.0	963.4	10.3551	9.4002	10.2597	7.3810	7.1451	23.21	23.84	1.673E-12	-11.777	
170.0	1082.5	10.1712	9.1973	10.1329	7.3804	7.0947	22.79	27.93	1.136E-12	-11.945	
180.0	1190.1	10.0104	9.0195	10.0235	7.0686	7.0521	22.40	32.04	8.34E-13	-12.090	
190.0	1286.7	9.8671	8.9671	9.9271	6.9187	7.0155	22.05	36.13	6.064E-13	-12.217	
200.0	1372.6	9.7375	8.7166	8.8410	6.8059	6.9836	21.72	40.21	4.665E-13	-12.331	
210.0	1448.4	9.6187	8.5843	9.7632	6.6664	6.9555	21.42	44.24	3.681E-13	-12.434	
220.0	1514.3	9.5087	8.4614	9.6921	6.4978	6.9305	21.13	48.23	2.965E-13	-12.528	
230.0	1571.4	9.4060	8.3463	9.6265	6.3581	6.9082	20.86	52.10	2.429E-13	-12.615	
240.0	1620.3	9.3091	8.2375	9.5655	6.2256	6.8880	20.61	55.84	2.018E-13	-12.695	
250.0	1661.8	9.2170	8.1339	9.5082	6.0990	6.8696	20.37	59.40	1.696E-13	-12.770	
260.0	1697.0	9.1290	8.0346	9.4540	5.9773	6.8526	20.14	62.78	1.440E-13	-12.842	
270.0	1726.7	9.0442	7.9389	9.4023	5.8597	6.8369	19.92	65.94	1.233E-13	-12.909	
280.0	1751.7	8.9622	7.8461	9.3528	5.7453	6.8222	19.72	68.90	1.063E-13	-12.973	
290.0	1772.7	8.8824	7.7557	9.3050	5.6338	6.8084	19.52	71.64	9.220E-14	-13.035	
300.0	1790.4	8.8045	7.6674	9.2587	5.5246	6.7952	19.33	74.22	8.039E-14	-13.095	
310.0	1805.3	8.7223	7.5808	9.2136	5.4174	6.7826	19.15	76.60	7.040E-14	-13.152	
320.0	1817.9	8.6534	7.4956	9.1695	5.3118	6.7704	18.97	78.83	6.190E-14	-13.208	
330.0	1828.6	8.5796	7.4117	9.1263	5.2077	6.7587	18.81	80.90	5.662E-14	-13.263	
340.0	1837.6	8.5068	7.3289	9.0838	5.048	6.7473	18.65	82.86	4.334E-14	-13.316	
350.0	1845.3	8.4349	7.2470	9.0419	5.0031	6.7361	18.50	84.70	4.290E-14	-13.368	
360.0	1851.9	8.3637	7.1659	9.0006	4.9022	6.7252	18.35	86.45	3.817E-14	-13.418	
370.0	1857.6	8.2932	7.0856	8.9598	4.8022	6.7145	18.22	88.12	3.044E-14	-13.468	
380.0	1862.4	8.2233	7.0059	8.9194	4.7030	6.7040	18.08	89.69	3.042E-14	-13.517	
390.0	1866.6	8.1539	6.9267	8.8793	4.6045	6.6936	17.96	91.20	2.723E-14	-13.565	
400.0	1870.2	8.0850	6.8481	8.8396	4.5065	6.6833	17.84	92.65	2.443E-14	-13.612	

Table 6 (Cont.)

EXOSPHERIC TEMPERATURE = 1900 DEGREES

HEIGHT K	TEMP DEG K	LOG N(N2) /CM3	LOG N(O2) /CM3	LOG N(O) /CM3	LOG N(A) /CM3	LOG N(HE) /CM3	LOG N(H) /CM3	MEAN MOL WT	DENSITY GM/CM3	SCALE HT KM	DENSITY GM/CM3	LOG DEN GM/CM3
420.0	1876.1	7.9484	6.6923	8.7610	4.3124	6.6632	17.62	95.38	1.975E-14	-13.705		
440.0	1880.7	7.8133	6.5382	8.6834	4.1202	6.6434	17.41	97.90	1.606E-14	-13.794		
460.0	1884.1	7.6795	6.3855	8.6067	3.9298	6.6239	17.23	100.28	1.312E-14	-13.882		
480.0	1886.9	7.5469	6.2341	8.507	3.7409	6.6046	17.06	102.51	1.077E-14	-13.968		
500.0	1889.1	7.4154	6.0839	8.4553	3.5536	6.5856	16.90	104.60	8.881E-15	-14.052		
520.0	1890.8	7.2849	5.9349	8.3806	3.3676	6.5668	16.76	106.58	7.348E-15	-14.134		
540.0	1892.2	7.1553	5.7869	8.3065	3.1829	6.5481	16.63	108.46	6.101E-15	-14.215		
560.0	1893.3	7.0266	5.6399	8.2328	2.9995	6.5296	16.51	110.24	5.081E-15	-14.294		
580.0	1894.3	6.8987	5.4939	8.1597	2.8173	6.5112	16.39	111.92	4.244E-15	-14.372		
600.0	1895.0	6.7717	5.3489	8.0871	2.6363	6.4930	16.28	113.54	3.554E-15	-14.449		
620.0	1895.7	6.6455	5.2047	8.0150	2.4563	6.4749	16.18	115.09	2.984E-15	-14.525		
640.0	1896.2	6.5201	5.0615	7.9433	2.2775	6.4569	16.08	116.57	2.511E-15	-14.600		
660.0	1896.7	6.3954	4.9191	7.8720	2.0998	6.4390	15.98	117.98	2.117E-15	-14.674		
680.0	1897.1	6.2715	4.7776	7.8012	1.9231	6.4213	15.88	119.35	1.789E-15	-14.747		
700.0	1897.4	6.1483	4.6369	7.7308	1.7475	6.4036	15.78	120.69	1.514E-15	-14.820		
720.0	1897.7	6.0259	4.4970	7.6609	1.5729	6.3861	15.68	121.99	1.284E-15	-14.891		
740.0	1898.0	5.9042	4.3580	7.5913	1.3994	6.3687	15.57	123.27	1.091E-15	-14.962		
760.0	1898.2	5.7632	4.2197	7.5222	1.2268	6.3514	15.46	124.53	9.282E-16	-15.032		
780.0	1898.4	5.6628	4.0823	7.4535	1.0552	6.3342	15.35	125.78	7.911E-16	-15.102		
800.0	1898.5	5.5432	3.9457	7.3851	0.8847	6.3171	15.23	127.04	6.753E-16	-15.170		
820.0	1898.7	5.4242	3.8098	7.3172	7.151	6.3000	15.10	128.27	5.774E-16	-15.239		
840.0	1898.8	5.3060	3.6747	7.2496	5.464	6.2831	15.00	129.50	4.944E-16	-15.306		
860.0	1898.9	5.1883	3.5403	7.1824	3.787	6.2663	14.92	130.76	4.240E-16	-15.373		
880.0	1899.0	5.0714	3.4067	7.1156	2.1119	6.2496	14.82	132.04	3.641E-16	-15.439		
900.0	1899.1	4.9551	3.2739	7.0492	0.0460	6.2330	14.71	133.35	3.132E-16	-15.504		
920.0	1899.2	4.8394	3.1418	6.9174	6.2164	6.2986	14.63	134.69	2.697E-16	-15.569		
940.0	1899.2	4.7244	3.0104	6.9174	6.2000	6.2982	14.54	136.08	2.327E-16	-15.633		
960.0	1899.3	4.6100	2.8797	6.8521	6.1836	6.2978	13.95	137.51	2.010E-16	-15.697		
980.0	1899.3	4.4962	2.7498	6.7871	6.1674	6.2974	13.74	139.01	1.740E-16	-15.760		
1000.0	1899.4	4.3831	2.6205	6.7225	6.1512	6.2903	13.51	140.57	1.508E-16	-15.822		
1050.0	1899.5	4.1030	2.3006	6.5625	6.1112	2.9602	12.90	144.79	1.062E-16	-15.974		
1100.0	1899.6	3.8266	1.9849	6.4046	6.0717	2.9503	12.22	149.66	7.560E-17	-16.121		
1150.0	1899.7	3.5539	1.6734	6.2489	6.0327	2.9405	11.48	155.34	5.445E-17	-16.284		
1200.0	1899.7	3.2849	1.3661	6.0952	5.9943	2.9308	10.71	162.02	3.973E-17	-16.401		
1250.0	1899.7	3.0193	1.0628	5.9435	5.9563	2.9212	9.92	170.00	2.939E-17	-16.532		
1300.0	1899.8	2.7573	0.7635	5.7939	5.9189	2.9118	9.15	179.53	2.207E-17	-16.666		
1350.0	1899.8	2.4987	4.681	5.6462	5.8454	2.9024	8.41	190.89	1.684E-17	-16.774		
1400.0	1899.8	2.2434	0.1765	5.5004	5.8094	2.8933	7.73	204.39	1.307E-17	-16.884		
1450.0	1899.9	1.9914	5.3564	5.2143	5.7739	2.8752	7.13	220.35	1.033E-17	-16.986		
1500.0	1899.9	1.7426	4.9355	4.2046	5.7041	2.8577	6.59	238.99	8.304E-18	-17.081		
1600.0	1899.9	1.2544	4.6636	4.0327	5.6361	2.8405	5.15	284.70	5.654E-18	-17.248		
1700.0	1899.9	0.7783	3.139	4.3983	5.5697	2.8238	4.75	405.05	4.101E-18	-17.387		
1800.0	1899.9	0.3139	4.1395	4.1395	5.5050	2.8075	4.49	471.48	3.134E-18	-17.504		
1900.0	1899.9	0.1899	2.9341	2.9341	5.4418	2.7916	4.32	535.10	2.044E-18	-17.603		
2000.0	1900.0	0.1900	2.7094	3.8669	5.3801	2.7760	4.21	592.14	1.712E-18	-17.690		
2100.0	1900.0	0.1900	3.6402	3.6402	5.3198	2.7609	4.14	641.51	1.456E-18	-17.767		
2200.0	1900.0	0.1900	3.3994	3.3994	5.2609	2.7461	4.09	683.39	1.252E-18	-17.837		
2300.0	1900.0	0.1900	2.9341	2.9341	5.2034	2.7316	4.06	718.80	1.085E-18	-17.94		
2400.0	1900.0	0.1900	2.7094	2.7094	5.1472	2.7174	4.04	749.53	9.472E-19	-18.024		

Table 7. Atmospheric density as a function of height and exospheric temperature (decimal logarithms, g cm⁻³).

SUMMARY OF LOG DENSITIES

	500	550	600	650	700	750	800	850	900	950
90	-8.461	-8.461	-8.461	-8.461	-8.461	-8.461	-8.461	-8.461	-8.461	-8.461
92	-8.621	-8.621	-8.621	-8.621	-8.621	-8.621	-8.621	-8.621	-8.621	-8.621
94	-8.780	-8.781	-8.781	-8.781	-8.781	-8.781	-8.781	-8.781	-8.781	-8.781
96	-8.940	-8.940	-8.941	-8.941	-8.941	-8.941	-8.941	-8.941	-8.942	-8.942
98	-9.098	-9.098	-9.099	-9.099	-9.100	-9.100	-9.100	-9.101	-9.101	-9.101
100	-9.254	-9.254	-9.255	-9.255	-9.256	-9.256	-9.257	-9.257	-9.258	-9.259
102	-9.408	-9.409	-9.410	-9.411	-9.411	-9.412	-9.412	-9.413	-9.414	-9.414
104	-9.561	-9.562	-9.563	-9.563	-9.564	-9.566	-9.566	-9.567	-9.567	-9.567
106	-9.711	-9.712	-9.713	-9.713	-9.714	-9.715	-9.715	-9.716	-9.717	-9.717
108	-9.858	-9.858	-9.859	-9.859	-9.860	-9.860	-9.861	-9.862	-9.862	-9.862
110	-10.001	-10.001	-10.001	-10.001	-10.002	-10.002	-10.002	-10.002	-10.002	-10.003
115	-10.340	-10.338	-10.336	-10.335	-10.333	-10.332	-10.331	-10.330	-10.329	-10.328
120	-10.648	-10.642	-10.637	-10.633	-10.629	-10.626	-10.622	-10.620	-10.617	-10.615
125	-10.924	-10.913	-10.904	-10.896	-10.889	-10.883	-10.877	-10.872	-10.868	-10.864
130	-11.168	-11.151	-11.138	-11.125	-11.115	-11.106	-11.097	-11.090	-11.083	-11.077
135	-11.383	-11.361	-11.342	-11.326	-11.312	-11.300	-11.289	-11.279	-11.270	-11.263
140	-11.574	-11.546	-11.522	-11.502	-11.485	-11.470	-11.456	-11.445	-11.434	-11.425
145	-11.746	-11.712	-11.684	-11.660	-11.639	-11.621	-11.605	-11.591	-11.579	-11.568
150	-11.903	-11.864	-11.830	-11.802	-11.778	-11.758	-11.739	-11.723	-11.709	-11.697
155	-12.049	-12.004	-11.966	-11.933	-11.906	-11.882	-11.862	-11.844	-11.828	-11.813
160	-12.187	-12.135	-12.092	-12.055	-12.024	-11.998	-11.974	-11.954	-11.936	-11.921
170	-12.440	-12.376	-12.323	-12.278	-12.240	-12.207	-12.179	-12.154	-12.132	-12.113
180	-12.672	-12.596	-12.534	-12.480	-12.435	-12.396	-12.362	-12.333	-12.307	-12.284
190	-12.887	-12.801	-12.728	-12.667	-12.614	-12.569	-12.530	-12.496	-12.466	-12.440
200	-13.090	-12.992	-12.911	-12.841	-12.782	-12.731	-12.686	-12.647	-12.613	-12.583
210	-13.282	-13.174	-13.083	-13.006	-13.022	-12.939	-12.882	-12.833	-12.789	-12.751
220	-13.466	-13.346	-13.247	-13.162	-13.089	-13.026	-12.971	-12.923	-12.881	-12.843
230	-13.642	-13.512	-13.403	-13.311	-13.232	-13.163	-13.103	-13.050	-13.004	-12.963
240	-13.813	-13.672	-13.554	-13.454	-13.368	-13.294	-13.229	-13.172	-13.121	-13.076
250	-13.980	-13.828	-13.701	-13.593	-13.500	-13.420	-13.350	-13.289	-13.234	-13.186
260	-14.143	-13.979	-13.843	-13.727	-13.628	-13.542	-13.467	-13.401	-13.343	-13.291
270	-14.302	-14.127	-13.982	-13.858	-13.752	-13.661	-13.580	-13.510	-13.448	-13.392
280	-14.459	-14.273	-14.117	-13.966	-13.873	-13.776	-13.691	-13.616	-13.549	-13.490
290	-14.613	-14.416	-14.251	-14.111	-13.992	-13.888	-13.798	-13.719	-13.648	-13.586
300	-14.764	-14.557	-14.382	-14.234	-14.108	-13.999	-13.903	-13.819	-13.745	-13.679
310	-14.914	-14.696	-14.511	-14.355	-14.222	-14.107	-14.006	-13.918	-13.840	-13.770
320	-15.061	-14.833	-14.639	-14.475	-14.335	-14.213	-14.108	-14.015	-13.932	-13.859
330	-15.205	-14.968	-14.765	-14.593	-14.446	-14.318	-14.207	-14.110	-14.023	-13.946
340	-15.346	-15.102	-14.890	-14.710	-14.555	-14.422	-14.306	-14.204	-14.113	-14.032
350	-15.483	-15.234	-15.013	-14.825	-14.664	-14.524	-14.403	-14.296	-14.201	-14.117
360	-15.617	-15.363	-15.135	-14.939	-14.771	-14.625	-14.499	-14.387	-14.288	-14.201
370	-15.745	-15.491	-15.256	-15.052	-14.877	-14.726	-14.593	-14.477	-14.375	-14.283
380	-15.868	-15.616	-15.375	-15.164	-14.982	-14.825	-14.687	-14.567	-14.460	-14.364
390	-15.984	-15.738	-15.493	-15.275	-15.087	-14.923	-14.780	-14.655	-14.544	-14.445
400	-16.092	-15.857	-15.355	-15.052	-14.797	-14.598	-14.387	-14.247	-14.142	-14.022

Table 7 (Cont.)

Spectral Log Densities

	500	550	600	650	700	750	800	850	900	950
420	-16.283	-16.084	-15.833	-15.600	-15.393	-15.213	-15.055	-14.915	-14.792	-14.682
440	-16.436	-16.290	-16.048	-15.809	-15.592	-15.402	-15.234	-14.954	-14.836	-14.754
460	-16.555	-16.472	-16.251	-16.010	-15.786	-15.487	-15.253	-15.113	-14.989	-14.836
480	-16.644	-16.628	-16.437	-16.202	-15.974	-15.767	-15.417	-15.270	-15.139	-15.139
500	-16.712	-16.756	-16.605	-16.363	-16.155	-15.943	-15.751	-15.579	-15.425	-15.286
520	-16.765	-16.860	-16.752	-16.550	-16.327	-16.113	-15.916	-15.737	-15.577	-15.432
540	-16.808	-16.943	-16.878	-16.701	-16.489	-16.276	-16.076	-15.892	-15.726	-15.575
560	-16.845	-16.984	-17.011	-16.837	-16.639	-16.431	-16.230	-16.043	-15.871	-15.715
580	-16.878	-17.067	-17.074	-16.955	-16.776	-16.576	-16.378	-16.189	-16.014	-15.853
600	-16.926	-17.116	-17.150	-17.058	-16.899	-16.711	-16.518	-16.329	-16.152	-15.988
620	-16.936	-17.159	-17.215	-17.147	-17.009	-16.835	-16.649	-16.463	-16.286	-16.119
640	-16.962	-17.197	-17.272	-17.225	-17.105	-16.947	-16.771	-16.591	-16.414	-16.247
660	-16.987	-17.233	-17.323	-17.293	-17.191	-17.048	-16.884	-16.710	-16.537	-16.369
680	-17.011	-17.266	-17.369	-17.353	-17.266	-17.138	-16.986	-16.821	-16.653	-16.487
700	-17.034	-17.298	-17.412	-17.408	-17.334	-17.219	-17.079	-16.924	-16.762	-16.600
720	-17.057	-17.327	-17.452	-17.459	-17.394	-17.291	-17.163	-17.018	-16.864	-16.706
740	-17.079	-17.356	-17.491	-17.506	-17.450	-17.356	-17.238	-17.104	-16.958	-16.807
760	-17.100	-17.383	-17.527	-17.551	-17.502	-17.415	-17.307	-17.182	-17.045	-16.904
780	-17.120	-17.409	-17.562	-17.593	-17.550	-17.470	-17.370	-17.253	-17.125	-16.987
800	-17.140	-17.434	-17.595	-17.634	-17.596	-17.520	-17.426	-17.317	-17.198	-17.068
820	-17.160	-17.458	-17.627	-17.673	-17.640	-17.568	-17.478	-17.376	-17.264	-17.142
840	-17.179	-17.481	-17.658	-17.711	-17.682	-17.614	-17.528	-17.431	-17.325	-17.210
860	-17.197	-17.504	-17.687	-17.747	-17.723	-17.657	-17.574	-17.482	-17.381	-17.273
880	-17.226	-17.525	-17.716	-17.783	-17.763	-17.700	-17.618	-17.529	-17.433	-17.331
900	-17.234	-17.546	-17.743	-17.817	-17.802	-17.740	-17.661	-17.574	-17.482	-17.384
920	-17.251	-17.567	-17.770	-17.851	-17.840	-17.780	-17.702	-17.616	-17.527	-17.434
940	-17.269	-17.586	-17.795	-17.883	-17.877	-17.819	-17.742	-17.657	-17.570	-17.480
960	-17.286	-17.606	-17.820	-17.915	-17.913	-17.857	-17.780	-17.697	-17.611	-17.524
980	-17.303	-17.624	-17.844	-17.946	-17.948	-17.895	-17.818	-17.735	-17.651	-17.565
1000	-17.320	-17.642	-17.867	-17.975	-17.983	-17.931	-17.855	-17.772	-17.689	-17.605
109										
1050	-17.361	-17.686	-17.921	-18.046	-18.066	-18.021	-17.946	-17.863	-17.779	-17.697
1100	-17.400	-17.727	-17.972	-18.111	-18.145	-18.106	-18.033	-17.949	-17.864	-17.782
1150	-17.439	-17.667	-18.018	-18.171	-18.219	-18.188	-18.118	-18.033	-17.946	-17.863
1200	-17.477	-17.805	-18.062	-18.227	-18.289	-18.267	-18.200	-18.114	-18.026	-17.941
1250	-17.514	-17.841	-18.102	-18.278	-18.354	-18.342	-18.279	-18.194	-18.104	-18.017
1300	-17.551	-17.876	-18.141	-18.326	-18.415	-18.414	-18.356	-18.271	-18.180	-18.090
1350	-17.587	-17.911	-18.177	-18.371	-18.472	-18.483	-18.430	-18.347	-18.254	-18.163
1400	-17.622	-17.944	-18.212	-18.413	-18.526	-18.547	-18.502	-18.420	-18.327	-18.234
1450	-17.657	-17.977	-18.246	-18.452	-18.576	-18.609	-18.570	-18.492	-18.399	-18.303
1500	-17.691	-18.009	-18.278	-18.489	-18.622	-18.667	-18.637	-18.562	-18.468	-18.371
1600	-17.758	-18.071	-18.339	-18.557	-18.706	-18.761	-18.695	-18.603	-18.504	-18.504
1700	-17.823	-18.132	-18.398	-18.618	-18.781	-18.867	-18.874	-18.819	-18.732	-18.632
1800	-17.887	-18.190	-18.453	-18.676	-18.847	-18.950	-18.976	-18.935	-18.854	-18.755
1900	-17.949	-18.247	-18.507	-18.729	-18.907	-19.025	-19.068	-19.043	-18.969	-18.872
2000	-18.010	-18.302	-18.558	-18.780	-18.962	-19.091	-19.151	-19.141	-19.078	-18.984
2100	-18.069	-18.356	-18.609	-18.829	-19.013	-19.150	-19.225	-19.231	-19.179	-19.091
2200	-18.126	-18.409	-18.657	-18.875	-19.061	-19.205	-19.292	-19.313	-19.274	-19.193
2300	-18.183	-18.460	-18.705	-18.920	-19.106	-19.254	-19.353	-19.388	-19.361	-19.288
2400	-18.238	-18.510	-18.751	-18.964	-19.149	-19.407	-19.456	-19.442	-19.379	-19.379
2500	-18.292	-18.559	-18.796	-19.006	-19.344	-19.517	-19.545	-19.518	-19.463	-19.463

Table 7 (Cont.)

SUMMARY OF LOG DENSITIES

	1000	1050	1100	1150	1200	1250	1300	1350	1400	1450
90	-8.461	-8.461	-8.461	-8.461	-8.461	-8.461	-8.461	-8.461	-8.461	-8.461
92	-8.621	-8.621	-8.621	-8.621	-8.621	-8.621	-8.621	-8.621	-8.621	-8.621
94	-8.782	-8.782	-8.782	-8.782	-8.782	-8.782	-8.782	-8.782	-8.782	-8.782
96	-8.942	-8.942	-8.942	-8.942	-8.942	-8.942	-8.942	-8.942	-8.942	-8.942
98	-9.102	-9.102	-9.102	-9.102	-9.102	-9.102	-9.102	-9.102	-9.102	-9.102
100	-9.259	-9.259	-9.260	-9.260	-9.260	-9.260	-9.260	-9.260	-9.260	-9.260
102	-9.415	-9.415	-9.416	-9.416	-9.416	-9.416	-9.416	-9.416	-9.416	-9.416
104	-9.568	-9.568	-9.569	-9.569	-9.569	-9.570	-9.570	-9.570	-9.571	-9.571
106	-9.718	-9.718	-9.718	-9.718	-9.719	-9.720	-9.720	-9.720	-9.720	-9.721
108	-9.863	-9.863	-9.863	-9.863	-9.864	-9.864	-9.864	-9.865	-9.865	-9.865
110	-10.003	-10.003	-10.003	-10.003	-10.003	-10.003	-10.003	-10.004	-10.004	-10.004
115	-10.327	-10.327	-10.326	-10.325	-10.325	-10.324	-10.324	-10.324	-10.323	-10.323
120	-10.613	-10.613	-10.609	-10.608	-10.608	-10.605	-10.603	-10.602	-10.601	-10.600
125	-10.860	-10.860	-10.856	-10.853	-10.850	-10.848	-10.845	-10.843	-10.841	-10.837
130	-11.072	-11.067	-11.062	-11.058	-11.054	-11.051	-11.047	-11.044	-11.041	-11.038
135	-11.255	-11.249	-11.243	-11.238	-11.233	-11.228	-11.223	-11.219	-11.216	-11.212
140	-11.416	-11.408	-11.401	-11.394	-11.388	-11.383	-11.377	-11.372	-11.368	-11.363
145	-11.558	-11.549	-11.541	-11.533	-11.526	-11.519	-11.513	-11.508	-11.502	-11.497
150	-11.685	-11.675	-11.666	-11.657	-11.649	-11.642	-11.635	-11.629	-11.623	-11.617
155	-11.801	-11.789	-11.779	-11.769	-11.760	-11.752	-11.745	-11.738	-11.731	-11.725
160	-11.906	-11.894	-11.882	-11.872	-11.862	-11.853	-11.845	-11.838	-11.831	-11.824
170	-12.096	-12.081	-12.067	-12.055	-12.043	-12.033	-12.023	-12.015	-12.006	-11.999
180	-12.264	-12.246	-12.230	-12.215	-12.202	-12.190	-12.179	-12.169	-12.159	-12.150
190	-12.416	-12.395	-12.377	-12.360	-12.344	-12.330	-12.318	-12.306	-12.295	-12.285
200	-12.556	-12.532	-12.511	-12.492	-12.474	-12.458	-12.444	-12.431	-12.418	-12.407
210	-12.687	-12.660	-12.636	-12.614	-12.594	-12.576	-12.560	-12.545	-12.531	-12.518
220	-12.810	-12.780	-12.753	-12.728	-12.706	-12.686	-12.668	-12.651	-12.636	-12.622
230	-12.926	-12.893	-12.863	-12.836	-12.812	-12.790	-12.769	-12.751	-12.734	-12.718
240	-13.036	-13.000	-12.968	-12.939	-12.912	-12.888	-12.865	-12.845	-12.826	-12.809
250	-13.142	-13.103	-13.068	-13.036	-13.007	-12.981	-12.956	-12.934	-12.914	-12.895
260	-13.244	-13.202	-13.164	-13.130	-13.098	-13.070	-13.043	-13.019	-12.997	-12.976
270	-13.342	-13.297	-13.257	-13.220	-13.186	-13.155	-13.127	-13.101	-13.077	-13.055
280	-13.437	-13.389	-13.346	-13.307	-13.271	-13.238	-13.208	-13.180	-13.154	-13.130
290	-13.529	-13.479	-13.433	-13.391	-13.353	-13.318	-13.286	-13.256	-13.228	-13.203
300	-13.619	-13.566	-13.517	-13.473	-13.432	-13.395	-13.361	-13.330	-13.301	-13.274
310	-13.707	-13.651	-13.599	-13.553	-13.510	-13.471	-13.435	-13.401	-13.371	-13.342
320	-13.793	-13.734	-13.680	-13.631	-13.586	-13.544	-13.507	-13.471	-13.439	-13.409
330	-13.877	-13.815	-13.758	-13.707	-13.660	-13.616	-13.577	-13.540	-13.506	-13.474
340	-13.960	-13.895	-13.836	-13.782	-13.732	-13.687	-13.645	-13.607	-13.571	-13.537
350	-14.041	-13.973	-13.911	-13.855	-13.803	-13.756	-13.713	-13.672	-13.635	-13.600
360	-14.122	-14.051	-13.986	-13.927	-13.873	-13.824	-13.779	-13.736	-13.697	-13.661
370	-14.201	-14.127	-14.060	-13.998	-13.942	-13.891	-13.844	-13.800	-13.759	-13.721
380	-14.279	-14.202	-14.132	-14.068	-14.010	-13.968	-13.927	-13.862	-13.820	-13.780
390	-14.356	-14.276	-14.204	-14.138	-14.077	-14.022	-13.971	-13.923	-13.879	-13.838
400	-14.433	-14.350	-14.274	-14.206	-14.143	-14.086	-14.033	-13.984	-13.938	-13.896

Table 7 (Cont.)

SUMMARY OF LOG DENSITIES

	1000	1050	1100	1150	1200	1250	1300	1350	1400	1450
420	-14.583	-14.494	-14.414	-14.340	-14.273	-14.212	-14.155	-14.102	-14.054	-14.008
440	-14.731	-14.636	-14.550	-14.472	-14.400	-14.335	-14.274	-14.218	-14.166	-14.118
460	-14.877	-14.776	-14.685	-14.601	-14.525	-14.456	-14.391	-14.332	-14.277	-14.225
480	-15.020	-14.914	-14.817	-14.729	-14.648	-14.574	-14.506	-14.443	-14.385	-14.330
500	-15.162	-15.049	-14.947	-14.854	-14.769	-14.691	-14.619	-14.553	-14.491	-14.434
520	-15.301	-15.183	-15.076	-14.978	-14.889	-14.806	-14.731	-14.661	-14.596	-14.536
540	-15.439	-15.315	-15.203	-15.100	-15.006	-14.920	-14.841	-14.767	-14.699	-14.636
560	-15.574	-15.445	-15.328	-15.221	-15.122	-15.032	-14.949	-14.872	-14.801	-14.735
580	-15.707	-15.573	-15.451	-15.340	-15.237	-15.143	-15.056	-14.976	-14.902	-14.832
600	-15.837	-15.699	-15.573	-15.457	-15.351	-15.253	-15.162	-15.079	-15.001	-14.929
620	-15.965	-15.823	-15.693	-15.573	-15.462	-15.361	-15.267	-15.180	-15.099	-15.024
640	-16.090	-15.945	-15.810	-15.687	-15.573	-15.468	-15.370	-15.280	-15.196	-15.118
660	-16.211	-16.063	-15.926	-15.799	-15.682	-15.573	-15.472	-15.379	-15.292	-15.211
680	-16.329	-16.179	-16.039	-15.909	-15.789	-15.677	-15.573	-15.477	-15.387	-15.304
700	-16.442	-16.292	-16.150	-16.017	-15.894	-15.779	-15.673	-15.573	-15.481	-15.395
720	-16.551	-16.400	-16.258	-16.123	-15.997	-15.880	-15.771	-15.669	-15.573	-15.485
740	-16.654	-16.505	-16.362	-16.227	-16.099	-15.979	-15.867	-15.763	-15.655	-15.574
760	-16.753	-16.606	-16.463	-16.327	-16.198	-16.076	-15.952	-15.855	-15.755	-15.661
780	-16.845	-16.702	-16.561	-16.424	-16.294	-16.171	-16.055	-15.946	-15.844	-15.748
800	-16.932	-16.793	-16.654	-16.519	-16.388	-16.264	-16.147	-16.036	-15.932	-15.834
820	-17.012	-16.878	-16.743	-16.609	-16.480	-16.355	-16.236	-16.124	-16.018	-15.918
840	-17.087	-16.959	-16.827	-16.696	-16.568	-16.433	-16.324	-16.210	-16.103	-16.001
860	-17.157	-17.034	-16.907	-16.779	-16.652	-16.528	-16.409	-16.295	-16.186	-16.083
880	-17.221	-17.104	-16.982	-16.858	-16.733	-16.611	-16.492	-16.377	-16.267	-16.163
900	-17.280	-17.169	-17.053	-16.933	-16.811	-16.690	-16.572	-16.457	-16.347	-16.242
920	-17.335	-17.200	-17.003	-16.885	-16.766	-16.649	-16.535	-16.425	-16.319	-16.216
940	-17.386	-17.286	-17.180	-16.955	-16.839	-16.724	-16.610	-16.500	-16.394	-16.294
960	-17.434	-17.338	-17.237	-17.131	-17.021	-16.908	-16.795	-16.683	-16.574	-16.467
980	-17.478	-17.387	-17.291	-17.189	-17.083	-16.974	-16.864	-16.754	-16.645	-16.539
1000	-17.520	-17.432	-17.340	-17.244	-17.142	-17.037	-16.929	-16.821	-16.714	-16.608
1050	-17.616	-17.535	-17.452	-17.365	-17.273	-17.178	-17.079	-16.977	-16.875	-16.772
1100	-17.703	-17.625	-17.548	-17.468	-17.386	-17.299	-17.209	-17.115	-17.019	-16.922
1150	-17.784	-17.707	-17.633	-17.558	-17.482	-17.404	-17.322	-17.236	-17.148	-17.057
1200	-17.860	-17.784	-17.711	-17.639	-17.568	-17.495	-17.420	-17.342	-17.260	-17.176
1250	-17.934	-17.857	-17.783	-17.713	-17.644	-17.576	-17.506	-17.434	-17.359	-17.282
1300	-18.006	-17.927	-17.852	-17.782	-17.715	-17.648	-17.582	-17.515	-17.446	-17.374
1350	-18.076	-17.994	-17.919	-17.848	-17.780	-17.715	-17.652	-17.588	-17.523	-17.457
1400	-18.144	-18.061	-17.983	-17.911	-17.843	-17.778	-17.716	-17.654	-17.593	-17.530
1450	-18.211	-18.126	-18.046	-17.972	-17.903	-17.838	-17.776	-17.716	-17.656	-17.597
1500	-18.278	-18.189	-18.032	-18.032	-17.961	-17.895	-17.833	-17.773	-17.715	-17.657
1600	-18.406	-18.314	-18.228	-18.148	-18.074	-18.005	-17.941	-17.880	-17.823	-17.767
1700	-18.531	-18.434	-18.344	-18.260	-18.182	-18.110	-18.043	-17.981	-17.922	-17.866
1800	-18.651	-18.551	-18.456	-18.368	-18.287	-18.211	-18.141	-18.076	-18.015	-17.958
1900	-18.768	-18.664	-18.566	-18.474	-18.399	-18.309	-18.236	-18.168	-18.105	-18.046
2000	-18.880	-18.774	-18.672	-18.577	-18.498	-18.405	-18.328	-18.257	-18.191	-18.130
2100	-18.987	-18.880	-18.776	-18.677	-18.584	-18.498	-18.418	-18.344	-18.275	-18.211
2200	-19.091	-18.983	-18.876	-18.774	-18.678	-18.589	-18.506	-18.429	-18.357	-18.290
2300	-19.190	-19.082	-18.973	-18.868	-18.769	-18.677	-18.591	-18.511	-18.437	-18.368
2400	-19.285	-19.177	-19.067	-18.960	-18.859	-18.763	-18.674	-18.592	-18.515	-18.443
2500	-19.375	-19.269	-19.159	-19.050	-18.945	-18.847	-18.756	-18.670	-18.590	-18.516

Table 7 (Cont.)

SUMMARY OF LOG DENSITIES

	1500	1550	1600	1650	1700	1750	1800	1850	1900
90	-8.461	-8.461	-8.461	-8.461	-8.461	-8.461	-8.461	-8.461	-8.461
92	-8.621	-8.621	-8.621	-8.621	-8.621	-8.621	-8.621	-8.621	-8.621
94	-8.782	-8.782	-8.782	-8.782	-8.782	-8.782	-8.782	-8.782	-8.782
96	-8.943	-8.944	-8.944	-8.944	-8.944	-8.944	-8.944	-8.944	-8.944
98	-9.104	-9.104	-9.104	-9.104	-9.104	-9.104	-9.104	-9.105	-9.105
100	-9.262	-9.262	-9.262	-9.263	-9.263	-9.263	-9.263	-9.263	-9.264
102	-9.418	-9.419	-9.419	-9.419	-9.419	-9.419	-9.420	-9.420	-9.420
104	-9.572	-9.572	-9.572	-9.573	-9.573	-9.573	-9.573	-9.574	-9.574
106	-9.721	-9.721	-9.722	-9.722	-9.722	-9.722	-9.723	-9.723	-9.723
108	-9.865	-9.866	-9.866	-9.866	-9.866	-9.866	-9.866	-9.867	-9.867
110	-10.004	-10.004	-10.004	-10.004	-10.004	-10.004	-10.005	-10.005	-10.005
115	-10.322	-10.322	-10.322	-10.321	-10.321	-10.321	-10.320	-10.320	-10.320
120	-10.599	-10.598	-10.597	-10.596	-10.595	-10.594	-10.593	-10.593	-10.592
125	-10.835	-10.833	-10.832	-10.830	-10.828	-10.827	-10.825	-10.824	-10.823
130	-11.036	-11.033	-11.031	-11.028	-11.028	-11.026	-11.024	-11.024	-11.024
135	-11.208	-11.205	-11.202	-11.199	-11.196	-11.193	-11.191	-11.191	-11.191
140	-11.359	-11.355	-11.352	-11.348	-11.344	-11.341	-11.338	-11.335	-11.335
145	-11.493	-11.488	-11.484	-11.480	-11.476	-11.472	-11.468	-11.465	-11.461
150	-11.612	-11.607	-11.602	-11.597	-11.593	-11.589	-11.585	-11.581	-11.577
155	-11.719	-11.714	-11.709	-11.704	-11.699	-11.694	-11.690	-11.685	-11.681
160	-11.818	-11.812	-11.806	-11.801	-11.795	-11.790	-11.786	-11.781	-11.777
170	-11.991	-11.985	-11.978	-11.972	-11.966	-11.960	-11.955	-11.950	-11.945
180	-12.142	-12.134	-12.127	-12.120	-12.113	-12.107	-12.101	-12.095	-12.090
190	-12.276	-12.267	-12.259	-12.251	-12.244	-12.237	-12.230	-12.223	-12.217
200	-12.396	-12.386	-12.377	-12.369	-12.360	-12.352	-12.345	-12.338	-12.331
210	-12.507	-12.495	-12.485	-12.475	-12.466	-12.458	-12.449	-12.442	-12.434
220	-12.608	-12.596	-12.585	-12.574	-12.564	-12.554	-12.545	-12.536	-12.528
230	-12.703	-12.690	-12.677	-12.665	-12.654	-12.643	-12.633	-12.624	-12.615
240	-12.793	-12.778	-12.764	-12.750	-12.738	-12.726	-12.715	-12.705	-12.695
250	-12.877	-12.861	-12.845	-12.831	-12.817	-12.805	-12.793	-12.781	-12.770
260	-12.957	-12.939	-12.923	-12.907	-12.893	-12.879	-12.866	-12.853	-12.842
270	-13.034	-13.015	-12.997	-12.980	-12.964	-12.949	-12.935	-12.922	-12.909
280	-13.108	-13.087	-13.068	-13.050	-13.033	-13.017	-13.002	-12.987	-12.973
290	-13.179	-13.157	-13.137	-13.117	-13.099	-13.082	-13.065	-13.050	-13.035
300	-13.248	-13.225	-13.203	-13.182	-13.163	-13.144	-13.127	-13.110	-13.095
310	-13.315	-13.290	-13.267	-13.245	-13.224	-13.205	-13.186	-13.169	-13.152
320	-13.381	-13.354	-13.330	-13.306	-13.284	-13.264	-13.244	-13.226	-13.208
330	-13.444	-13.416	-13.390	-13.366	-13.343	-13.321	-13.301	-13.281	-13.263
340	-13.506	-13.477	-13.450	-13.424	-13.400	-13.377	-13.356	-13.335	-13.316
350	-13.567	-13.537	-13.508	-13.481	-13.456	-13.432	-13.409	-13.388	-13.368
360	-13.627	-13.595	-13.565	-13.537	-13.511	-13.486	-13.462	-13.440	-13.418
370	-13.686	-13.653	-13.621	-13.592	-13.565	-13.538	-13.514	-13.490	-13.468
380	-13.743	-13.709	-13.677	-13.646	-13.617	-13.590	-13.565	-13.540	-13.517
390	-13.800	-13.764	-13.731	-13.699	-13.669	-13.641	-13.614	-13.589	-13.565
400	-13.856	-13.819	-13.784	-13.751	-13.720	-13.691	-13.663	-13.637	-13.612

Table 7 (Cont.)

SUMMARY OF LOG DENSITIES

	1500	1550	1600	1650	1700	1750	1800	1850	1900
420	-13.926	-13.889	-13.854	-13.820	-13.789	-13.759	-13.731	-13.705	-13.705
440	-14.030	-13.953	-13.918	-13.885	-13.853	-13.823	-13.794	-13.794	-13.794
460	-14.132	-14.090	-14.050	-14.013	-13.978	-13.944	-13.912	-13.882	-13.882
480	-14.232	-14.188	-14.146	-14.106	-14.069	-14.033	-14.000	-13.968	-13.968
500	-14.330	-14.283	-14.239	-14.197	-14.158	-14.121	-14.085	-14.052	-14.052
520	-14.427	-14.377	-14.331	-14.287	-14.246	-14.206	-14.169	-14.134	-14.134
540	-14.522	-14.470	-14.421	-14.375	-14.332	-14.291	-14.252	-14.215	-14.215
560	-14.615	-14.561	-14.510	-14.462	-14.416	-14.373	-14.333	-14.294	-14.294
580	-14.707	-14.651	-14.597	-14.547	-14.500	-14.455	-14.413	-14.372	-14.372
600	-14.861	-14.798	-14.739	-14.684	-14.632	-14.582	-14.536	-14.491	-14.449
620	-14.954	-14.888	-14.827	-14.769	-14.715	-14.664	-14.615	-14.569	-14.525
640	-15.046	-14.977	-14.914	-14.854	-14.797	-14.744	-14.693	-14.646	-14.600
660	-15.136	-15.065	-14.999	-14.937	-14.878	-14.823	-14.771	-14.721	-14.674
680	-15.225	-15.152	-15.084	-15.019	-14.959	-14.902	-14.847	-14.796	-14.747
700	-15.314	-15.238	-15.168	-15.101	-15.038	-14.979	-14.923	-14.870	-14.820
720	-15.401	-15.324	-15.250	-15.182	-15.117	-15.056	-14.998	-14.943	-14.891
740	-15.488	-15.408	-15.332	-15.262	-15.195	-15.132	-15.072	-15.016	-14.962
760	-15.574	-15.491	-15.414	-15.341	-15.272	-15.207	-15.146	-15.088	-15.032
780	-15.658	-15.573	-15.494	-15.419	-15.348	-15.281	-15.218	-15.159	-15.102
800	-15.741	-15.655	-15.573	-15.496	-15.424	-15.355	-15.290	-15.229	-15.170
820	-15.824	-15.735	-15.652	-15.573	-15.498	-15.428	-15.362	-15.298	-15.239
840	-15.905	-15.815	-15.729	-15.649	-15.572	-15.500	-15.432	-15.367	-15.306
860	-15.985	-15.893	-15.806	-15.723	-15.645	-15.572	-15.502	-15.436	-15.373
880	-16.064	-15.970	-15.881	-15.797	-15.718	-15.642	-15.571	-15.503	-15.439
900	-16.141	-16.064	-15.956	-15.870	-15.789	-15.712	-15.639	-15.570	-15.504
920	-16.217	-16.121	-16.029	-15.942	-15.860	-15.781	-15.707	-15.636	-15.569
940	-16.292	-16.195	-16.102	-16.014	-15.930	-15.850	-15.774	-15.702	-15.633
960	-16.365	-16.267	-16.173	-16.084	-15.998	-15.917	-15.840	-15.767	-15.697
980	-16.436	-16.338	-16.243	-16.152	-16.066	-15.984	-15.905	-15.831	-15.760
1000	-16.506	-16.407	-16.312	-16.220	-16.133	-16.050	-15.970	-15.894	-15.822
1050	-16.672	-16.573	-16.477	-16.384	-16.295	-16.210	-16.128	-16.049	-15.974
1100	-16.825	-16.728	-16.633	-16.540	-16.450	-16.363	-16.279	-16.199	-16.121
1150	-16.964	-16.871	-16.778	-16.687	-16.597	-16.510	-16.425	-16.343	-16.264
1200	-17.089	-17.001	-16.912	-16.823	-16.735	-16.648	-16.563	-16.481	-16.401
1250	-17.201	-17.118	-17.034	-16.948	-16.863	-16.778	-16.694	-16.612	-16.532
1300	-17.300	-17.223	-17.144	-17.063	-16.981	-16.899	-16.817	-16.736	-16.656
1350	-17.388	-17.317	-17.243	-17.167	-17.089	-17.010	-16.931	-16.852	-16.774
1400	-17.466	-17.400	-17.331	-17.260	-17.187	-17.112	-17.036	-16.960	-16.884
1450	-17.536	-17.474	-17.410	-17.344	-17.275	-17.205	-17.133	-17.060	-16.986
1500	-17.630	-17.541	-17.481	-17.419	-17.355	-17.289	-17.221	-17.151	-17.081
1600	-17.712	-17.658	-17.604	-17.549	-17.492	-17.434	-17.373	-17.311	-17.248
1700	-17.812	-17.760	-17.708	-17.657	-17.606	-17.553	-17.499	-17.444	-17.387
1800	-17.904	-17.852	-17.801	-17.752	-17.703	-17.654	-17.605	-17.555	-17.504
1900	-17.990	-17.937	-17.886	-17.837	-17.790	-17.743	-17.697	-17.650	-17.603
2000	-18.072	-18.018	-17.966	-17.917	-17.869	-17.823	-17.778	-17.734	-17.690
2100	-18.151	-18.095	-18.042	-17.992	-17.944	-17.898	-17.853	-17.810	-17.767
2200	-18.228	-18.170	-18.115	-18.063	-18.014	-17.968	-17.923	-17.879	-17.837
2300	-18.303	-18.243	-18.186	-18.133	-18.082	-18.034	-17.989	-17.945	-17.902
2400	-18.376	-18.313	-18.255	-18.200	-18.148	-18.098	-18.052	-17.995	-17.964
2500	-18.447	-18.382	-18.322	-18.265	-18.211	-18.161	-18.113	-18.067	-18.024